Martina Marchetti-Deschmann

TECHNISCHE UNIVERSITÄT WIEN
Vienna University of Technology

Masterarbeit

Development of a quantitative proteomics method to study the adaption of fungi to extreme environments

Ausgeführt am

Institut für Chemische Technologie und Analytik

der Technischen Universität Wien

unter der Anleitung von

Assoc.-Prof. Mag.rer.nat. Dr.rer.nat. Martina Marchetti-Deschmann

durch

Sandra Stranzinger, BSc

Münzgrabenstraße 45/5/2, 8010 Graz

15.08.2013   Sandra Stranzinger, BSc

Abstract

Originally black fungi – also called dematiaceous fungi – were characterized as inhabitants of living and dead plant material. In the last 30 years they have been isolated from hypersaline waters, acidic environments, radioactive areas, as human pathogens or opportunists and as a dominant part of the epi- and endolithic microbial communities. Recent studies have shown that their stress resistance against solar radiation, radioactivity, desiccation and oligotrophic conditions even allows them to survive in space and under Martian conditions.

Due to all these facts this organism is of great interest for many studies to acquire knowledge about their biological behavior in extreme environments. Findings of the regulation of cell products will help to understand the enormous stress tolerance. For this a method for relative protein quantitation can be helpful to get deeper insight into biological functions.

To develop an appropriate method Bovine Serum Albumin (BSA) has been used to establish a quantitation method based on iTRAQ (isobaric Tags for Relative and Absolute Protein Quantitation) labeling. With molecular weight matched iTRAQ labels peptides in different samples were labeled and up to 4 samples were measured and relatively quantified in parallel by matrix-assisted laser desorption/ionization reflectron time-of-flight mass spectrometry (MALDI-RTOF-MS). Analytical parameters like reproducibility of peptide labeling, sample clean-up and relative quantities were gathered and the dynamic range for concentration differences for different samples was evaluated.

To adapt the established method to black fungi samples of the strain *Exophiala dermatitidis,* different clean-up steps necessary to remove interfering substances have been tested. The implementation of a suitable method proved to be difficult because of the high amount of disturbing buffer substances necessary for efficient protein extraction of *Exophiala dermatitidis* samples as well as the thick melanized cell walls. Nevertheless, the established iTRAQ based quantitation method gave insights into biological up- and down regulation of some peptides of *Exophiala dermatitidis* samples. Although the developed method still requires improvement, it has high potential for the final analysis.

To get deeper insights into biological functions of black fungi also protein identification of separated proteins is essential. Therefore protein identification after two dimensional (2D) gel electrophoresis was carried out. 25 spots of a 2D gel of an extract of microcolonial black fungi were cut out, trypsinized and measured by MALDI mass spectrometry. An online available gel of *Saccharomyces cerevisiae* was used as a reference gel to get a first idea of protein identity. Using this approach some proteins of the strain *Exophiala dermatitidis* could be identified with the demanded significance.

Danksagung

Während meiner Zeit an der Technischen Universität Wien durfte ich eine Vielzahl von Menschen kennenlernen. Hiermit möchte ich mich ganz besonders bei denen bedanken, die mich zu jeder Zeit unterstützten und die mein Leben während meiner Arbeit besonders bereichert haben.

Am Beginn möchte ich mich ganz herzlich bei Prof. Mag. rer.nat. Dr.rer. nat. Martina Marchetti-Deschmann für die Aufnahme in ihrer Arbeitsgruppe bedanken. Ich danke ihr für die tatkräftige Unterstützung während meiner Arbeit und dafür dass sie jederzeit ein offenes Ohr für etwaige Probleme und Fragestellungen hatte.

Ganz besonders möchte ich mich auch bei Prof. Dr. Katja Sterflinger bedanken, die es mir ermöglichte mit meiner Arbeit einen Teil zu ihrem vom FWF unterstützten Projekt beitragen zu können. Für die Probenvorbereitung sowie für die nette Unterstützung an der BOKU Wien darf ich mich ganz herzlich bei Donatella Tesei, MSc und Dipl.-Ing. Dr.nat.techn. Gorji Marzban bedanken.

Mein herzlicher Dank gilt der gesamten Arbeitsgruppe von Univ. Prof. Mag.pharm. Dr.rer.nat. Günter Allmaier. Ganz besonders möchte ich mich bei Bianca Bruckner, Michaela Helmel, Max Kosok, Nicole Engel und Sophie Fröhlich für die schönen Stunden in der Gruppe bedanken. Des Weiteren gebührt meinen Studienkollegen besonderer Dank, die mich während meines gesamten Studiums immer unterstützten. Hervorheben möchte ich Maximilian Bonta, der mich zu jeder Zeit bei meiner Arbeit unterstütze, mir Verbesserungsvorschläge und Tipps gegeben hat und nicht nur ein Kollege sondern ein ganz besonderer Freund geworden ist.

Schließlich möchte ich noch meiner Familie und meinen Freunden danken, dass sie zu jeder Zeit hinter mir standen und mir die Kraft gegeben haben, die für das Zustandekommen dieser Arbeit notwendig war. Mein größter Dank gilt meinem Freund Florian Beschliesser, der mich zu jeder Zeit unterstützte und mir auch in schwierigen Zeiten die notwendige Geduld und Verständnis entgegenbrachte.

Table of contents

Abbreviations

2-DE	Two-dimensional gel electrophoresis
2-D DIGE	Two-dimensional difference gel electrophoresis
CAD	Collisionally activated dissociation
CHAPS	3-[(3-cholamidopropyl)dimethylammonio]-1-propanesulfonate
CID	Collision induced dissociation
CFR	Curved field reflectron
Da	Dalton
EDTA	Ethylenediaminetetraacetic acid
ESI	Electrostray ionization
Fmol	femtomole
FTICR	Fourier transform ion cyclotron resonance
FWHM	Full width at half maximum
IR	Infrared
ICAT	Isotope-coded affinity tag
ICPL	Isotope-coded protein label
IEF	Isoelectric focusing
IPG	Immobilized pH gradient
iTRAQ	isobaric tags for relative and absolute quantitation
kV	Kilovolt
keV	Kiloelectronvolt
LC	Liquid chromatography
LID	Laser induced dissociation
MALDI	Matrix-assisted laser desorption/ionization
OGE	Off-gel electrophoresis
pmol	Picomole
ppm	parts per million

SDS	Sodium dodecyl sulfate
SILAC	Stable isotope labeling by amino acids in cell culture
SOP	Standard operation procedure
SPE	Solid phase extraction
TCEP	Tris(2-carboxyethyl)phosphine
TEAB	Triethylammonium bicarbonate
TFA	Trifluoroacetic acid
TMT	Tandem mass tag
TOF	Time-of-flight

CaCl2	Calcium chloride
CH_3COOH	Acetic acid
HCl	Hydrogen chloride
HCOOH	Formic acid
$K_3Fe(CN)_6$ (III)	Potassium hexacyanoferrate (III)
$Na_2S_2O_3$	Sodium thiosulfate
NH_4HCO_3	Ammonium bicarbonate

1   Introduction

1.1   Biological background

1.1.1   Black fungi

The term 'Black fungi' is used to group the two heterogeneous lineages of *Chaetothyriomycetidae* and *Dothideomycetidae* with melanised cell walls, including fungi with diverse ecology and different growth styles, such as black yeasts or meristematic black fungi. The word meristematic was originally introduced for black fungi by de Hoog and Hermandides-Nijhof (1977), describing non-disintegrating phenotypes which form aggregates of thick-walled, melanised cells. Black fungi are found in extreme environments and under poor nutrient conditions, where they often grow meristematically [1].

Originally black fungi – also called dematiaceous fungi – were characterized as inhabitants of living and dead plant material. In the last 30 years they have been isolated from hypersaline waters [2], acidic environments [3], radioactive areas [4], as human pathogens or opportunists [5] and as a dominant part of the epi- and endolithic microbial communities [6] [7] [8] [9] [10] [11]. To handle harsh conditions like osmotic stress, UV and oxidative stress and rapid variation of temperature, water supply, and nutrient availability [12] [13], organisms living in such environments need either permanently existing or exceptionally fast adaptive cellular or metabolic responses. The work of Urzi *et al.* (2000) describes some morphological and physiological characters as an obligate basis to tolerance of physical and chemical stress on rock and plant surfaces. Considered characteristics for adaptations to extreme environments are slow growth rates, an optimal surface/volume ratio of the cauliflower-like colonies, thick and strongly melanised cell walls, exopolysaccharide production, the high intracellular content of trehalose, and polyoles as well as lack of structures for sexual reproduction [14].

Cell composition

Cells of black micro-colonial fungi (MCF) consist majorly of lipids (e.g. mono-, di- and triacylglycerols, phosphotidilcholine, phosphatidylethanolamines, sterols, sterol ethers, phosphatidilethanolamines, and free fatty acids), pigments (e.g. melanins, carotenoids in colorless and brown-red formations) and a very complex and dense cell wall made of chitin, melanin and polysaccharides. All these components are involved in a machinery which allows black micro-colonial fungi to be the most

resistant eukaryotic organism on the Earth. These terrestrial organisms seem to be also able to survive the severe and hostile conditions in outer space over extended periods of time. Some of the previously mentioned features might also be responsible for the human pathogenicity of some black yeasts like e.g. *Exophiala dermatitidis.* Figure 1 shows colonies of *Exophiala dermatitidis* cultivated on solid media [15].
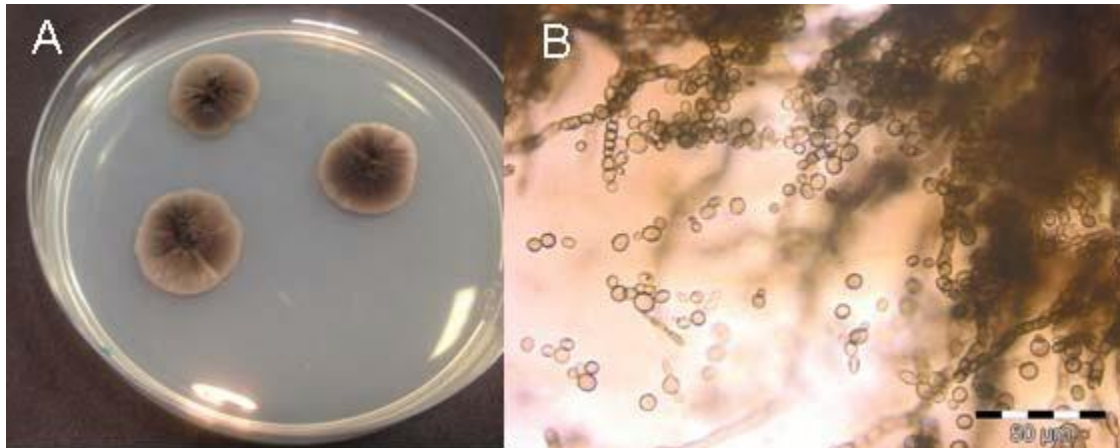
Figure 1: Colonies of *Exophiala dermatitidis* cultivated on solid media. Pictures taken by A) stereo microscope and B) optical microscope [15]

According to ecological and physiological data known by now, black fungi thrive in three main habitats which demand different degrees of specialization and allow different ecological amplitudes.

(1) Rock surfaces in hot deserts and moderate climates

Fungi within this group are thermotolerant but neither thermo- nor cryophilic and they thrive in moderate dry environments like low Alpine and Mediterranean areas, however with high UV radiation due to sun exposure.

Best known genera of this group are *Coniosporium, Sarcinomyces* and *Capnobotryella.* They are highly resistant against desiccation and withstand temperatures up to 130 °C in the dehydrated stage. However, their growth optimum is lower 30 °C, thus they must be regarded as thermotolerant but mesophilic.

(2) Cold deserts in Polar and high mountain regions

Fungi of this group are highly specialized to the cold extreme environments and are real extremophiles amongst the black fungi. The can be characterized as cryophilic with growth optima around -12 °C. As no change to mycelial growth has been observed in this group of fungi, a

microcolonial growth seems to be obligate for these fungi. The largest genera representing this group are *Cryomyces* and *Friedmanniomyces.*

<u>*(3) Human body and other animals*</u>

Human associated black fungi are represented by black yeasts that belong to the *genera Exophiala, Fonsecea, Capronia, Phaeococcomyces* and *Cladophialophora.* These genera are accumulated in the order of *Chaetothyriales.* Many of these fungi are associated with animals, humans – *Exophiala dermatitidis* - or human environments like bathrooms, sauna facilities or dishwashers.

Fungi belonging to this group are mesophilic but with a tendency to be moderate termophilic as a prerequisite for pathogenicity in humans [16].

As the extreme stress tolerance of black micro-colonial fungi is a virgin field of research, only some facts about these fungi like their phenotypes, a slow growth rate and a complex structural composition are known. Until now full genomic sequences of only two strains of black fungi – *Exophiala dermatitidis* and *Coniosporium apollinis* – are available in international databases. In general proteomic and genomic data for black micro-colonial fungi are rare, indicating major analytical and methodological challenges. Some features of black fungi, e.g. the rigid cell wall and the high melanin content, seems to pose major challenges in sample preparation prior to analysis which is going far beyond the routine efforts [15].

1.1.2   Aim of the study

The aim of the study was to get a deeper understanding of the ecology of black micro-colonial fungi and the underlying cellular mechanisms responsible for their enormous stress tolerance. For this a proteomic-based approach for relative protein quantitation had to be developed. Only the knowledge on protein regulation allows a deeper insight into biological functions. Gathered knowledge may then allow genetic engineering for targeted applications. Bovine serum albumin (BSA) was used to establish a robust analytical method. At first proteins were tryptic digested and the obtained peptides in different samples were labeled using differing, however isobaric, labels and could be measured in parallel and relatively quantified by mass spectrometry. Relative and absolute protein quantitation by mass spectrometry is usually based on labels attached to proteins or peptides. In this work a MS compatible labeling strategy on the peptide level, the so called iTRAQ (isobaric tags for multiplexed relative and absolute protein quantitation) strategy, was applied. The

molecular weight matched labels itself consists of a reporter group (m/z 114, 115, 116 or 117), a counteracting balance group (m/z 31, 30, 29 or 28) and an amino-reactive group which can covalently link to the N-terminus of the peptide. The established method is a basis for protein quantitation of black fungi samples of the strain *Exophiala dermatitidis.* The method helps to understand the response of this fungus against different environmental influences. In the future the knowledge can help to develop tools useful for waste management and to understand biological data collected during space programs.

1.2 Qualitative and quantitative proteome analysis

1.2.1 Proteome analysis

The word 'Proteome' was used first time by Marc Wilkins in 1995, defined as the 'protein complement to a genome' [17] [18]. 'Proteome' describes the protein expression of a cell, an organism or a complex body fluid at a given time and condition [18]. The systematic identification and quantification of proteins expressed in a biological system was popularized under the name proteomics [19].

A particular gene can generate multiple distinct proteins as a result of alternative splicing of primary transcripts, the presence of sequence polymorphisms, post-translational modifications, and other processing mechanisms. This leads to the fact that the number of proteins in a species' proteome exceeds by far the number of genes in the corresponding genome. As the amino acid sequence of proteins provides a link between proteins and their coding genes via the genetic code, respectively a link between cell physiology and genetics, the identification of proteins can help to understand complex cellular regulatory networks. Thus protein and proteome analysis can provide an opportunity to unravel mechanisms used for cellular regulation [19].

For proteome separation, 1-D and 2-D gel electrophoresis or liquid chromatography (LC) followed by mass spectrometry have become standard techniques. Using gel-based methods, proteins are separated by isoelectric point (pI) and/or molecular weights, detected by staining, and relatively quantified according to staining intensities. Using LC-based methods, proteins or peptides are separated by LC columns, and then detected, identified, and quantified by mass spectrometry [20].

In early proteomic researches the main goal was to identify and characterize proteins. Ongoing developments in chromatography, mass spectrometry and bioinformatics, veered proteomics towards quantitative and comparative studies [20]. One of the most challenging - and rapidly changing – areas of proteomics is the development of methods for accurate protein quantitation. The use of a particular quantitation method depends on factors including the source of the samples, the number of samples, the number of treatments being compared, the type of equipment available, and the expense and time required [21].

Quantitative proteomics strategies can be classified into two types: either absolute or relative. On the one hand absolute quantitation determines changes in protein expression in terms of an exact amount or concentration of each protein present, and on the other hand relative quantitation determines the up- or down-regulation of a protein relative to a control sample [21].

To date, no 'universal usable method' for quantitative proteomics exists. However, specific methods for several biological questions are available. Further improvements of mass spectrometers with respect to sensitivity, dynamic range, mass accuracy and scan rate, as well as development of new multiplexed labeling techniques and improvements in reproducibility of SOPs, will lead to significant improvements in the area of quantitative proteomics [21].

1.2.2 Mass spectrometry

Mass spectrometry (MS) is a method of analysis to determine the mass-to-charge ratio (m/z) of ionized analytes in the high vacuum [18]. As shown on Figure 2 a mass spectrometer consists of three basic components; an ion source, a mass analyzer measuring the mass-to-charge ratio of the analytes and a detector registering the number of ions at each m/z value [22].
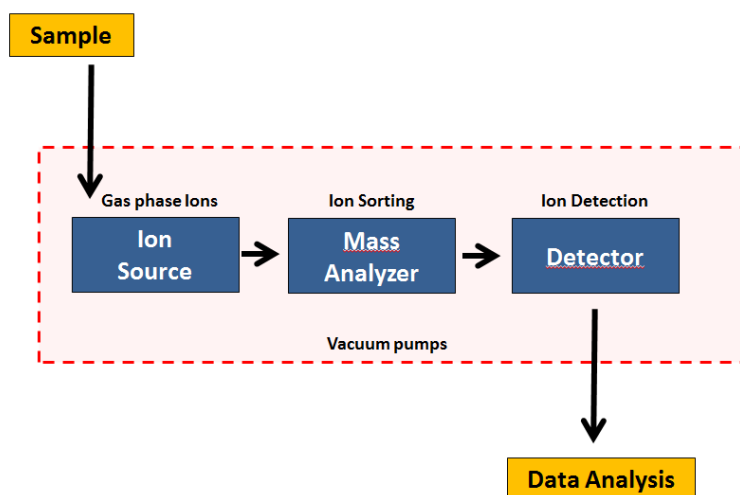
Figure 2: Basic components of a mass spectrometer

Biomolecules and Mass Specrometry – A short historical overview

By the end of the 1970s, the molecular weight of biopolymers was determined using electrophoretic, chromatographic or ultracentrifugation methods. As these results depended also on characteristics other than the molecular weight like the molecule's conformation, the Stokes radius and the hydrophobicity, they were not very precise (10-100 % relative error on average).

At that time applying mass spectrometry to large, non-volatile biological molecules was limited due to an only small selection of available ionization techniques. Ionization techniques like electron impact (EI) and chemical ionization (CI) required the analyte molecules to be present in the gas phase and thus were only suitable for volatile compounds or derivatized samples. Field desorption (FD) ionization method already allowed the ionization of non-volatile molecules but required an experienced operator.

A first breakthrough for mass spectrometry of biomolecules was the development of desorption/ionization methods based on the emission of pre-existing ions from a liquid or solid

phase. Using these methods, such as plasma desorption (PD), fast atom bombardment (FAB) or laser desorption (LD) the problem of ion formation in the field of biomolecules analysis could be solved. But the problem of analyzing high-mass singly charged ions with good sensitivity and good resolution remained. To conclude the challenge was the transfer of large molecules as ions from a liquid or solid phase to the gas phase [23].

Matrix-assisted laser desorption/ionization (MALDI) and electrospray ionization (ESI), until today the two techniques being most commonly used to desorb and ionize proteins or peptides [22], was first mentioned in 1988 [23]. These two techniques continued to revolutionize the role of mass spectrometry in biological research. Today MALDI-MS and ESI-MS allow the high-precision analysis of biomolecules of very high molecular weight [18].

Mass spectrometry with its applications in biological researches of peptides, proteins, nucleic acids, oligosaccharides and lipids, has become one of the most used analytical techniques in the field of life sciences [23].

When MALDI is used for MS analysis, ions are normally created out of a dry, crystalline matrix employing a pulsed laser [22]. As the MALDI process is a pulsed process, it is well suitable for the use with time-of-flight (TOF) mass spectrometers as well as spectrometers that allow the storage of ions like ion traps and fourier transform ion cyclotron resonance mass analyzers (FTICR). Over the last decade, the development of MALDI-TOF spectrometers has rapidly proceeded resulting in an improved performance in terms of mass resolution and accuracy [23].

1.2.2a Principles of MALDI – Mass spectrometry

In general the analysis of samples using MALDI-MS is carried out in two steps. The first step is to embed the analytes of interest in a matrix which absorbs light at the wavelength of the subsequently applied laser. After this mixture is dried, the second step occurs under vacuum conditions inside the mass spectrometer in the so-called ion source. Here bulk portions of the 'solid solution' are ablated by intense laser pulses.

In detail, the laser induces rapid heating of the crystals by the accumulation of a large amount of energy, leading to localized sublimation of the matrix crystals, resulting in the desorption of a portion of the crystal surface and expansion of the matrix into the gas phase entraining intact analytes [24].
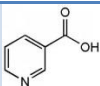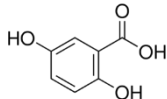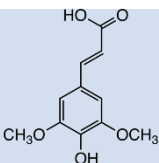
Table 1 shows some common lasers used for MALDI. The most common used lasers are the UV lasers, such as N_2 and Nd:YAG, but also IR lasers like Er:YAG can be used.
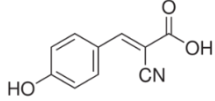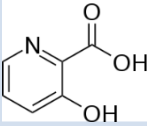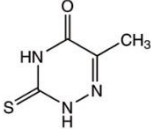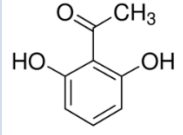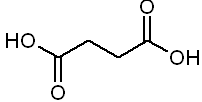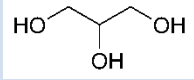
Table 1: Some common lasers used for MALDI

Laser	Wavelength	Energy (eV)	Pulse width
N_2	337 nm	3.68	<1 ns to a few ns
Nd:YAG µ3	355 nm	3.49	5 ns
Nd:YAG µ4	266 nm	4.66	5 ns
Er:YAG	2.94 µm	0.42	85 ns
CO_2	10.6 µm	0.12	100 ns + 1 µs tail

The matrix selection for MALDI analysis is based on the laser used and its wavelength, but also the class of analytes. A number of requirements have to be fulfilled, such as strong absorbance at the laser wavelength, low mass to be effectively sublimated, vacuum stability, ability to promote analyte ionization, solubility in solvents compatible with the analytes and lack of chemical reactivity [23]. Table 2 shows a selection of commonly used MALDI matrices. α-Cyano-4-hydroxycinnamic acid (CHCA) is widely used in proteomics applications for analyzing peptide-mass-fingerprints generated by enzymatic protein digests, because peptides and small proteins below molecular weight 2000 Da are often amenable to analysis using this matrix. Larger proteins may produce better results with either Sinapinic acid (SA) or 2,5-Dihydroxybenzoic acid (DHB) matrix. Using a mixture of matrices often improves the performance of MALDI-MS analysis. In general it is often necessary to test a series of solvents and matrices to optimize the outcome of MALDI-MS experiments [25].

Table 2: A selection of commonly used MALDI matrices

Matrix	Structure	Wavelength	Major applications
Nicotinic acid		UV 266 nm	Proteins, peptides, adduct formation
2,5-Dihydroxybenzoic acid (plus 10 % 2-hydroxy-5-methoxybenzoic acid)		UV 337 nm, 353 nm	Proteins, peptides, carbohydrates, synthetic polymers
Sinapinic acid		UV 337 nm, 353 nm	Proteins, peptides

α-Cyano-4-hydroxycinnamic acid		UV 337 nm, 353 nm	Peptides, fragmentation
3-Hydroxy-picolinic acid		UV 337 nm, 353 nm	Best for nucleic acids
6-Aza-2-thiothymine		UV 337 nm, 353 nm	Proteins, peptides, non-covalent complexes; near-neutral pH
k,m,n-Di(tri)hydroxy-acetophenone (e.g. 2',6'-Dihydroxyacetophenone)		UV 337 nm, 353 nm	Proteins, peptides, non-covalent complexes; near-neutral pH
Succinic acid		IR 2.94 μm, 2.79 μm	Proteins, peptides
Glycerol		IR 2.94 μm, 2.79 μm	Proteins, peptides, liquid matrix

Sample preparation techniques

The sample preparation is one of the most crucial steps in the analysis, as the quality of the results is tremendously dependent upon the quality of sample processing [23]. An overview of the various preparation techniques can be found, for example, on the Internet at: http://chemistry.wustl.edu/~msf/damon/sample_prep_toc.html [25]. The 'dried droplet' standard MALDI sample preparation, which is the most widely used method [23], is very simple. Using this method equal amounts of sample and matrix solution are mixed. First the sample is applied on the target and then the matrix solution is added by direct mixing on the target by means of pipette tip. The small matrix-analyte spot (of typically 1 μL volume) on the target is then slowly dried in air [26]. Figure 3 shows an example of a matrix-analyte spot on the target.
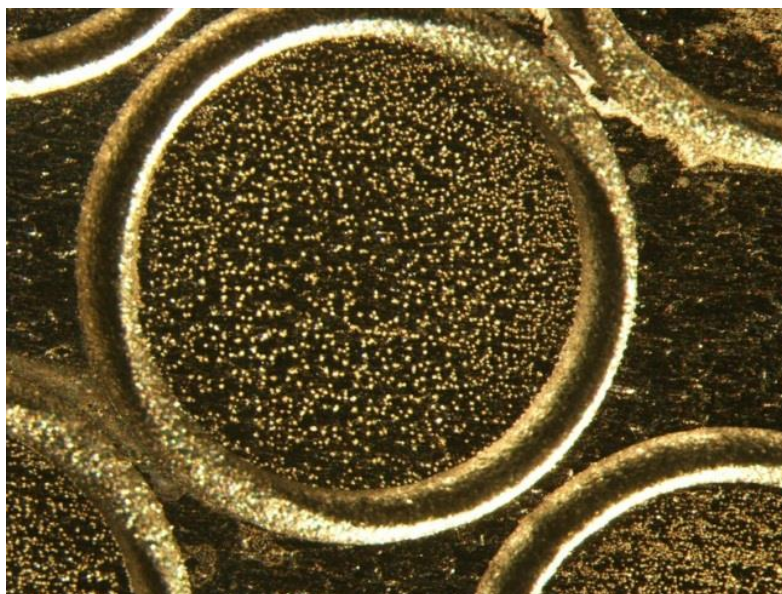
Figure 3: 2µL of a mixture of a peptide mix (500fmol) and CHCA (2.5 mg/mL) in 0.1 % TFA:ACN ratio 1:1 deposited on a stainless steel target

In general the MALDI technique is relatively less sensitive to contamination (salts, buffers, detergents, etc.) compared to other ionization techniques [27]. But prior purification to remove the contaminants leads to improved analysis results. Contaminants may disturb the incorporation of the analyte into the matrix crystals and therefore have to be removed in advance [23].

1.2.2b Ion Source - Desorption/Ionization Process

As shown on Figure 4 using MALDI, ions are generated by irradiating a matrix-analyte mixture with short laser pulses.. Subsequently, ionized molecules are extracted from the thereby generated plume, which expands from the sample plate, into the ion source [28]. Amongst different theories [29] [30] on ionization in MALDI, like gas-phase photoionization, excited state proton transfer, ion-molecule reactions, desorption of preformed ions, etc., the most accepted ion formation mechanism involves gas-phase proton transfer in the expanding plume with photoionized matrix molecules.
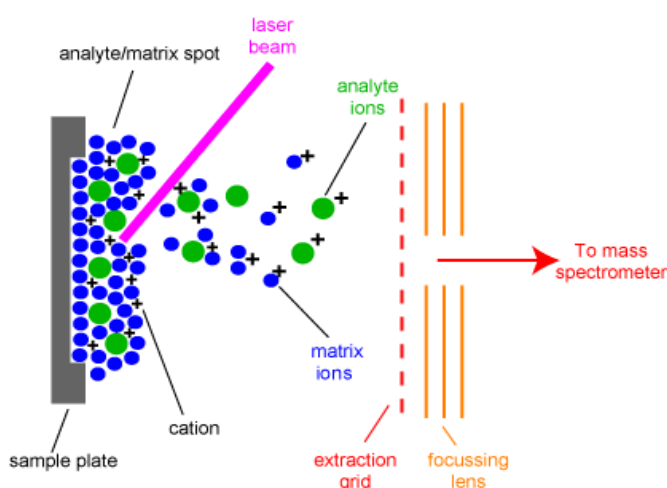
Figure 4: Principle of Desorption/Ionization in MALDI-MS

Using MALDI, known as a 'soft' ionization method, the molecules are ionized as intact molecules and transferred from the condensed phase into the gas phase without excessive fragmentation [19]. Most of the energy from the laser pulse is absorbed by the matrix, minimizing sample damage [23].

1.2.2c TOF, TOF/TOF (LIFT) mass analyzer

Time-of-flight (TOF) mass analyzers were first described by Stephens in 1946. Since the end of the 1980s there has been renewed interest in TOF analyzers. Progress in electronics simplifies the handling of the high data flow [23] and TOF mass analyzers are directly compatible with pulsed ionization techniques such as laser desorption, because they provide short, precisely defined ionization times and a small ionization region [31]. The development of MALDI-TOF has paved the way for new applications, not only for biomolecules but also for synthetic polymers and polymer/biomolecule conjugates [23]. TOF mass analyzers were reviewed by Cotter [32], Mann [24], Weickhardt [33] and Wollnik [34].

Principles of TOF mass analyzers

Using a TOF mass analyzer, the mass-to-charge ratio of an analyte ion is deduced from its flight time through a tube of specific length until the arrival at the detector [19]. In detail, after formation of

ions by the laser pulse, ions are accelerated by an electric field between the sample support and a nearby grid or open electrode. They gain therefore a specific kinetic energy. Accelerated ions travel along a field free drift region of known length to the detector. In the field free path, ions are separated according to their m/z ratio, because same kinetic energy and different masses result in different velocities. In other words the velocity of the ion depends on the mass-to-charge ratio (see v = $(\frac{2zeV_s}{m})^{1/2}$ (2)). The time needed by the particle to reach the detector at a known distance is measured. In this way the mass-to-charge ratio of an ion can be obtained. To conclude, using a defined acceleration voltage as well as a defined length of the flight tube, the m/z value of an ion can be determined by measuring the time of the flight. [25].

Calculating the m/z value of an ion

The kinetic energy of an accelerated ion is calculated according to the following formula.

$$E_k = \frac{mv^2}{2} = qV_s = zeV_s = E_{el} \qquad (1)$$

E_k = kinetic energy

m = mass of the ion

v = velocity of the ion after acceleration

q = total charge

V_s = potential

z = charge number

e = elementary charge

E_{el} = electric potential energy

After rearranging the previous formula the velocity of the ion is given.

$$v = (\frac{2zeV_s}{m})^{1/2} \qquad (2)$$

The time required for the particle to reach the detector is calculated according to the following formula.

$$t = \frac{L}{v} \qquad (3)$$

t = time

L = length of the flight tube

Replacing the velocity of the ion by its deduced from equation (1) gives:

$$t^2 = \frac{m}{z}\left(\frac{L^2}{2eV_s}\right) \qquad (4)$$

From this the mass-to-charge ratio of an ion can be obtained by transforming equation (XX).

$$\frac{m}{z} = \frac{2eV_s}{L^2}t^2 \qquad (5)$$

In this way the unknown mass of an ion can be calculated according to its flight time [23].

Mass analyzer characterization

Mass analyzers are typically characterized by a number of parameters. The most important ones are mass accuracy, sensitivity and mass resolution.

Mass accuracy

Mass accuracy is usually presented in parts per million (ppm) which describes the error of the measured mass-to-charge ratio. To give an example, 20 ppm means that the real mass of an ion measured to 1000 Da has a predicted error margin of ±20 mDa. Limitations are the quality of the calibration and the accuracy of the center determination of the peak [25].

Sensitivity/Limits of detection

Sensitivity means the slope of the intensity/moles of sample plot. Limit of detection is defined as the smallest amount of sample that can be used to achieve a detectable signal. The limit of detection is often defined as a peak with S/N ratio > 3. It is important to know that sample purity has an influence on the limit of detection. In general it is easier to achieve low-femtomole or better limits of detection for clean, synthetic samples or peptides. Samples from biological sources are normally difficult to clean and consequently all other biological molecules and contaminants are well below the concentration of the analyte. To give an example, if a sample contains 1 fmol of peptide but 0.1 pmol of surfactant or salt, the mass spectrometer will detect surfactant or salts [25].

S/N ratio

The S/N ratio defines the signal intensity divided by the nearby noise value. Many methods to calculate the average noise value are available. The most important calculation is the root-mean-square of the noise. Noise spikes are neglected and consequently do not interfere with real sample peaks. [25]. Figure 5 shows a mass spectrum to illustrate the calculation of the S/N ratio.
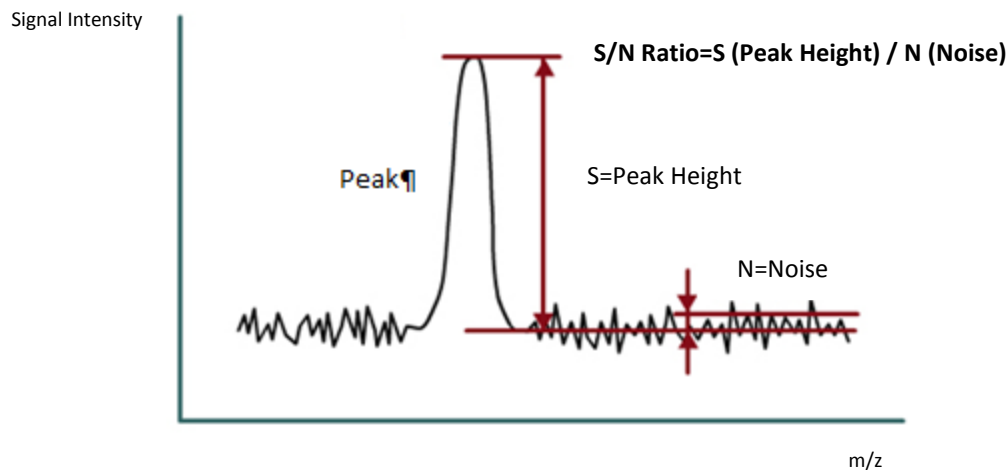
Figure 5: Mass spectrum for calculation of the S/N ratio

Mass resolution R

Resolution power is an important feature of mass analyzers, defined as the ability of the instrument to separate two close masses into two separate signals. The following formula shows, that the mass resolution depends on the ratio of m, which is the smallest mass difference necessary to differentiate m_1 from m_2, to the difference of these two masses.

$$R = \frac{m}{\Delta m} = \frac{m}{(m_2 - m_1)} \tag{6}$$

R = mass resolution

m_1, m_2 = mass$_1$, mass$_2$

Δm = mass difference of mass$_1$ and mass$_2$

To describe the mass resolution of a mass spectrometer different definitions pictured on Figure 6 are used: 10 % valley, 50 % valley and full width at half maximum (FWHM).

The 10 % valley method is widely used for sector field mass spectrometers which use a static electric or magnetic sector or a combination of the two as a mass analyzer. Most modern sector devices are double focusing instruments (focusing of ion beams in direction and velocity). Using the 10 % valley method two peaks are regarded as separated if the valley between them has a relative intensity of 10 % of the smaller peak. **The 50 % valley method** is mainly used for quadrupole mass spectrometers. When using this method, the height of the lowest point between two adjacent peaks must be at 50 % height of the lower peak. The commonly used method for TOF instruments is the use of the **FWHM**, using a single peak to calculate the resolution by calculating the peak width at 50% peak height [18].
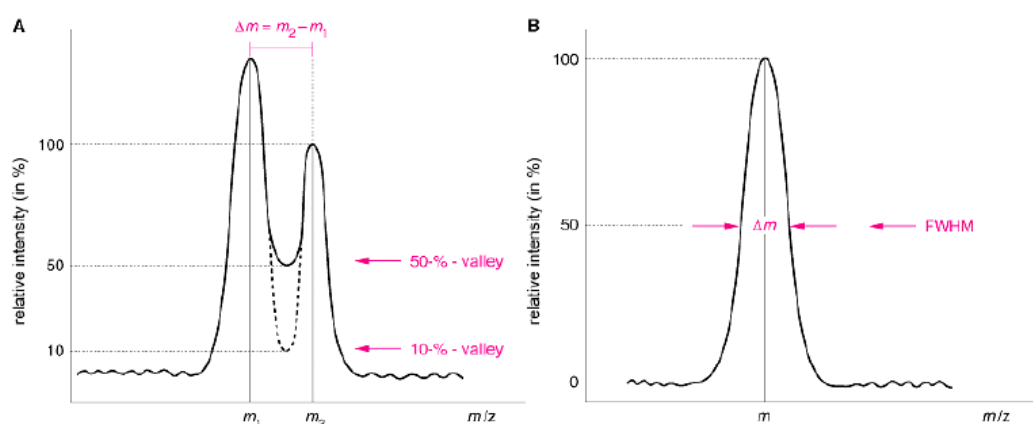
Figure 6: Mass resolution definitions for mass spectrometers. A) Valley 10 % and Valley 50 %, B) Full width at half maximum – FWHM [18]

For TOF mass spectrometry devices two primary sources of error in the arrival times of ions at the detector are present, which have influence on mass resolution. The first one is that MALDI ions are extracted from their desorption plume with an initial velocity distribution which causes ions of a particular mass to arrive at slightly different times at the detector. The second error is that if the surface is irregular, the initial position of the ions in the potential gradient will also affect their final velocity distribution. Modern TOF mass spectrometers can compensate initial energy distribution by pulsed-ion extraction (also called delayed extraction (DE) or time-lag focusing) [25].

Pulsed-ion extraction

Using pulsed-ion extraction to minimize the initial energy spread during the desorption/ionization process, at first the electric energy between sample and the first electrode is kept at zero or very low. After a certain delay (typically tens of nanoseconds) a voltage pulse is applied to extract the ions

into the flight tube. During the initial phase fast ions can move farther towards the first electrode than slower ones. After switching on the electric field, the faster ions experience less of a potential difference than the slower ones, resulting in a compensation of their higher initial energy. By adjusting the pulse potential and timing the point where slow ions will catch up with the fast ones can be chosen. Subsequently, if the ion detector is placed at this 'space focus' the time and mass resolution is greatly increased. Unfortunately, time focusing by delayed extraction is mass-dependent. Improved mass resolution can therefore only be achieved for a limited mass range [25].

Linear and reflectron mode

TOF mass spectrometers can be operated in two different ways: **Linear mode** and **Reflectron mode.** As shown on Figure 7 in the **linear mode** ions are accelerated after ionization and separated according to their m/z ratio during (linear) flight through the flight tube. They are detected at the end of the tube. Heavier ions reach the detector later than the lighter ones. Advantages of mass spectrometers operated in linear mode are the easy setup, no need of additional lenses and high transmission efficiency, which leads to very high sensitivity. As all ions are produced in a short time span and temporal separation of these ions allows all of them to be directed towards the detector, all of these ions, in principle, are analyzed.

The most important drawback of the linear mode is the poor mass resolution. As already described in the previous chapter mass resolution is among other factors dependent on processes that create a difference in flight times among ions having the same m/z ratio. Poor mass resolution is affected by factors like the length of the ion formation pulse **(time distribution),** the size of the volume where the ions are formed **(space distribution)** and the variation of the initial kinetic energy of the ions **(kinetic energy distribution).** Electronics especially digitizers can also have an influence on resolution and precision of the time measurement. One way to handle the problem of poor mass resolution is to lengthen the flight tube, as mass resolution is proportional to the flight time. Another way to increase flight time can be achieved by lowering the acceleration voltage. However, lowering the acceleration voltage reduces the sensitivity. Therefore only the combination of a long flight tube 1-2 m for a higher resolution and an acceleration voltage of at least 20 kV for keeping the sensitivity high can lead to high resolution as well as high sensitivity [23].
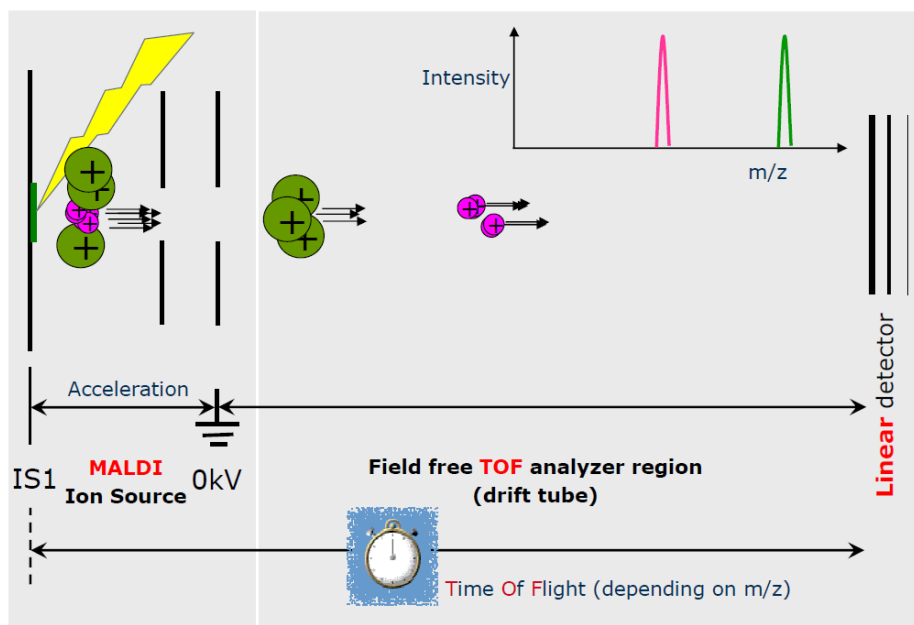
Figure 7: Principles of a linear TOF instrument to analyze ions produced by focusing a laser beam on the sample

As already described one way to improve the initial energy distribution of MALDI ions is the pulsed-ion extraction. Another way to partly compensate the initial velocity/energy distribution of MALDI ions is to use of a **reflector** [25]. The ion reflector was invented by Mamyrin and coworkers in St. Petersburg [35]. Figure 8 shows the scheme of a TOF analyzer operated in reflectron mode. The reflector – also ion mirror – was designed to re-focus the ion packets onto the detector. In principle, the reflection is a series of ring electrodes which, near their center, ideally create a constant electric field through a linear voltage gradient that slows down the ions and turns them around to send them back to a second detector. These mechanism leads to the fact that the higher-energy ions, which arrive the reflectron ahead of the slower ones, will roll up the voltage barrier farther than the low-energy ones, resulting in an increased flight time in the reflectron. By adjusting the reflectron voltage, high- and low-energy ions can be focused to hit the detector at the same time. In this way the resolution power of the instrument can be improved. Using a simple reflectron the flight time dispersion can be corrected to first order, and mass resolutions of over 10 000 can be achieved [25]. Reflectrons with two different electric fields – so-called two-stage reflectrons – can compensate the dispersion to second order [36]. A further reflectron which uses ion mirrors with nonlinear electric field distributions is the so-called 'curved field reflectron'. This reflectron has been designed primarily for post scource decay (PSD) analysis (described in the following chapter) [37].
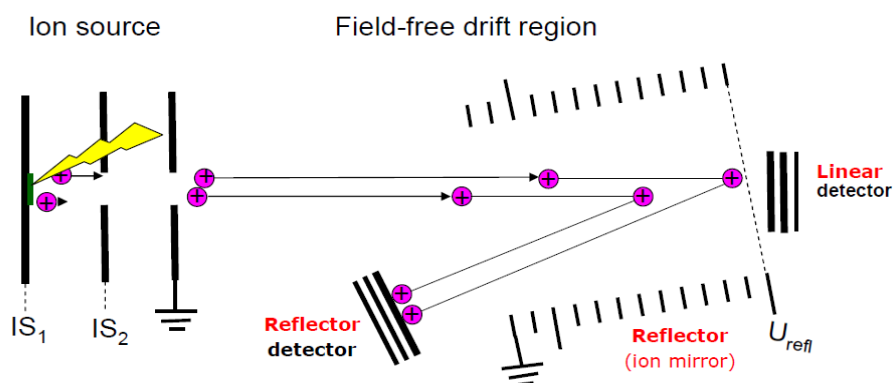
Figure 8: TOF analyzer operated in reflectron mode

Modern TOF mass spectrometers use both reflectrons and pulsed-ion extraction to improve mass resolution as well as mass accuracy. The combination of these two methods can render mass resolutions > 20 000 and a mass accuracy of 5-10 ppm. In selected and very highly tuned experiments even a mass accuracy of 2-5 ppm can be reached [25].

Tandem mass (MS/MS) spectrometry for TOF analyzers

Tandem mass spectrometry is used for the structural analysis of all types of molecules. In general a precursor ion is selected, which is subsequently fragmented to finally get a mass spectrum of the fragments. To gain structural information about the ions, either metastable decay (in which ion selection is avoided) or external induced fragmentation can be used. Obtained fragments will reveal the sequence of the used peptide of interest and often allow determination of modifications like for example phosphorylation [25].

Metastable decay - 'Pseudo-MS/MS' technique

For metastable decay fragments there is a distinction between 'in-source decay' [38] and 'post-source decay' (PSD) [39] ions. 'In-source decay' ions are generated by the desorption/ionization event on a time scale which is short compared to the transit time through the acceleration region (and on the pulsed-ion extraction mode, on the time scale which is short compared to the delay time of the ion extraction) resulting in fragment ions that receive the full acceleration energy. These

fragment ions are detected in the mass spectrum at their correct mass [40]. In contrast, precursor ions that decay in the field-free region of the flight tube are called 'post-source decay' (PSD) fragment ions. It is important that PSD fragment ions will have the same velocity as the precursor. The total kinetic energy of the precursor ion will (in good approximation) be split between the fragments in the ratio of their masses. Using a reflectron – which is as already described an energy-dispersive element – fragment ions can be dispersed and poorly focused on the second detector [39]. By stepping down the reflector voltages, a small range of fragment masses can be shown which are well resolved [41]. The problem of the dispersion of fragment flight times in the simple constant electric field reflectron can be partially compensated over a large mass range by using a nonlinear ('curved') electric reflectron field. [37]. Another possibility to solve this problem is to use the 'LIFT' TOF mass spectrometer (see Chapter 'Principles of the 'LIFT' technique) [42].

External induced fragmentation

To get all the structural information of interest, the previously described metastable fragmentation is not sufficient. Therefore the internal vibrational energy of the molecules has to be increased to generate more fragments. The most common method is the collisionally activated dissociation (CAD) also called collision-induced dissociation (CID). Commonly the increase of the internal vibrational energy is accomplished by collisions with neutral gas molecules, typically in a specially designed collision cell [37]. In a typical tandem TOF instrument at first ions are separated into packets of different m/z values within the first linear tube. The ion gate, placed in front of the collision cell, is then switched open for a properly chosen delay time for a short period. In this way only precursor ions of interest pass this gate. In the collision cell the collision energy can be varied. Useful values are in the range of 25 to a few hundred eV/charge [43]. Using high-energy CID (collision energy >100 eV) additionally ions resulting from a simple dissociation of the peptide-bond backbone types of fragments which can carry specific information such as side-chain structure in peptides can be generated [25]. The nomenclature for peptide fragment ions is outlined in Chapter 1.2.3 Mass spectrometry for protein identification.

To overcome the disadvantages of PSD and to utilize LID, metastable laser induced decay, to its fullest potential triggered the development of the so called 'LIFT' technique. While the basic idea of TOF-TOF, i.e. acceleration of a selected precursor together with its fragments is very simple, major refinement of the ion optics was required to successfully gain high mass resolution and sensitivity in MS/MS mode [42].

Principles of the 'LIFT' technique

Figure 9 shows the principle scheme of the 'LIFT' technique consisting of a TOF1 region which ranges from the MALDI ion source to the 'LIFT' cell, and a TOF2 region which ranges from the second accelerator stage in the 'LIFT' cell to the reflector. In detail, the system consists of a gridless MALDI source with delayed extraction (DE) electronics, a high-resolution timed ion selector (TIS), a 'LIFT' device for raising the potential energy of the ions, a further velocity focusing stage with subsequent post-acceleration, a post lift metastable suppressor (PLMS), a gridless space-angle and energy focusing reflector, and fast ion detectors for the linear and reflectron mode [42].
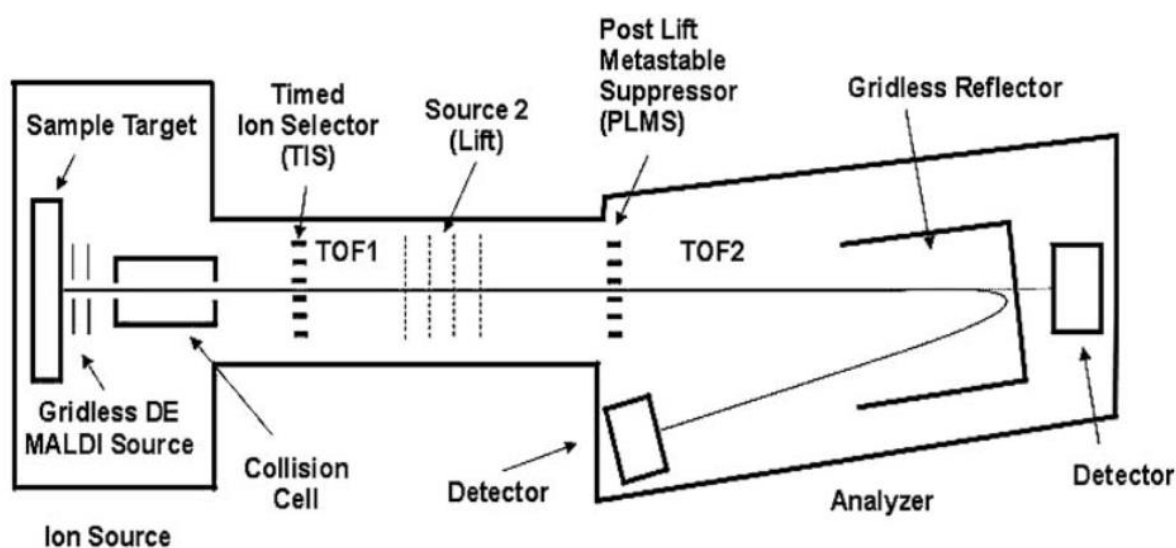
Figure 9: A scheme of the LIFT-TOF/TOF mass spectrometer. TOF1 ranges from the MALDI ion source to the LIFT cell and TOF2 from the second accelerator stage in the LIFT cell to the reflector. [42]

In the **MS mode,** the instrument operates up to 25 kV with all modes of operation: linear, reflector, positive and negative acceleration potential. The instrument is prepared for a full mass-range high-resolution mode (broadband focusing) by modualtion of the delayed extractioln pulse shape. Highest mass resolution is achieved over the mass range of 500 Da to 4000 Da.

In the **LID-MS/MS mode** for protein identification, acquisition conditions must be modified to generate high fragment ion yields. For this laser fluence is increased to provide a larger number of precursor ions per shot. The initial accelerating voltage of 8 kV provides long flight time (10-20 µs) during which fragmentation occurs. All precursor ions have a velocity corresponding to $E = 1/2 \, mv^2$

after acceleration to 8 kV. Fragments that are formed after acceleration have the same velocity as their corresponding precursor. Such an 'ion family' consisting of a precursor ion and its fragments will reach the timed ion selector (TIS) together. Only selected ions pass through the timed ion selector (TIS) by deflecting all ion 'families' except the one under investigation which is done by switching the gate voltage off while the selected ions pass through. The selected 'ion family' leaves the TIS and enters the 'LIFT' device. As ions, that have an identical mass but a small velocity distribution, start to drift away from each other, a velocity-focusing is required. The potential lift is the heart of the LIFT technology. It consists of the following three stages between four grids (Figure 10):

Stage 1: After ions have entirely entered the 'LIFT' cell, which is located between two adjacent grids, the potential between these two grids is rapidly increased from ground potential to 19 kV.

Stage 2: Ions travel at the same speed towards the focusing cell and enter it. In this cell the potential is held at 19 kV. On the third grid the potential is reduced by 2-3 kV and ions are accelerated towards the third cell.

Stage 3: Ions are accelerated to full speed. In this way ions are time-focused onto the detector.

A calculation example of a precursor ion $[M+H]^+$ = 1000 DA:

Initial acceleration in source 1 = 8 kV as shown in Figure 10:

Precursor ion $[M+H]^+$	= 1000 Da	$E_{kin\ precursor}$	= 8 keV (100 %)
Fragment ion f1 $[M+H]^+$	= 500 Da	$E_{kin\ f1}$	= 4 keV (50 %)
Fragment ion f2 $[M+H]^+$	= 100 Da	$E_{kin\ f2}$	= 0.8 keV (10 %)

Reacceleration by 19 kV narrows down the energy spread as shown in Figure 10:

$E_{kin\ precursor}$	= (8 + 19) keV	= 27 keV (100 %)
$E_{kin\ f1}$	= (4 + 19) keV	= 23 keV (85 %)
$E_{kin\ f2}$	= (0.8 + 19) keV	= 19.8 keV (73 %)

In the 'LIFT' cell re-acceleration of fragments and remaining precursor ions as well as re-focusing of the ions occurs. This is necessary because depending on their masses, precursor ions and fragments have different kinetic energies after acceleration in source 1. After reacceleration, even the smallest fragment ions have more than 70% of the energy of the precursor. In this way on the detector the complete fragment ion spectrum at one fixed reflector voltage can be captured [42].
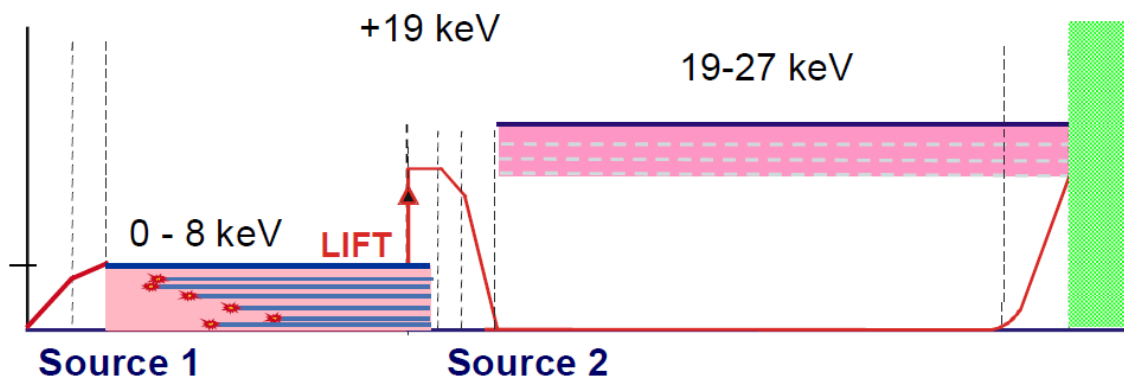
Figure 10: A schematic diagram of the re-acceleration of ions in ion source 2

The instrument is equipped with an additional device to suppress precursor ions, the 'post LIFT metastable suppressor' (PLMS). It is situated between the 'LIFT' cell and the reflector. The PLMS deflects remaining intact precursor ions and thus prevents undesired fragment ion formation after post-acceleration. Due to the elimination of the precursor ion, further fragmentation in the second TOF and the reflector is impossible, this results in low chemical background disrupting the LIFT spectra.

For the **CID-MS/MS mode** for Leu/Ile differentiation, the ion source housing contains a collision region for high-energy collisions. Here a collision gas (typically argon) is introduced under computer control, to increase the source pressure to 6 x 10^{-6} mbar.

1.2.2d Detector

Detectors in MALDI TOF instruments are usually microchannel plates (MCP), and less frequently discrete dynode secondary electron multipliers (SEM). Using these detectors incoming ions are converted into electrons which are then amplified in a cascade by many orders of magnitude.

Microchannel plates (MCP)

MCPs are essentially glass plates with a very large number of channels. These channels have a 2-10 μm diameter and angled at 10-20° to the surface normal. The plates as well as the channels have a specially coated surface to achieve a high ion/electron conversion and electron multiplication yield. The typically applied voltage between two sides of the plates is 1kV. After ions hit the front face of the plate they elicit some electrons which will then cascade down the channels. The typical amplification for every ion is about 10^6 electrons. If two such plates are arranged in series it is called 'chevron' configuration. Finally electrons exiting the last plate are collected by an anode. The electron current is converted to a voltage and amplified to the detector output. The schematic of a single channel (pore) of an MCP showing the mechanism of secondary electron production is pictured on Figure 11.

Secondary electron multipliers (SEM)

In general SEMs have the same principle as MCPs, except that the amplifying electron cascade takes place between properly shaped discrete electrodes, called dynodes. The amplification factor is comparable to that of the MCPs.
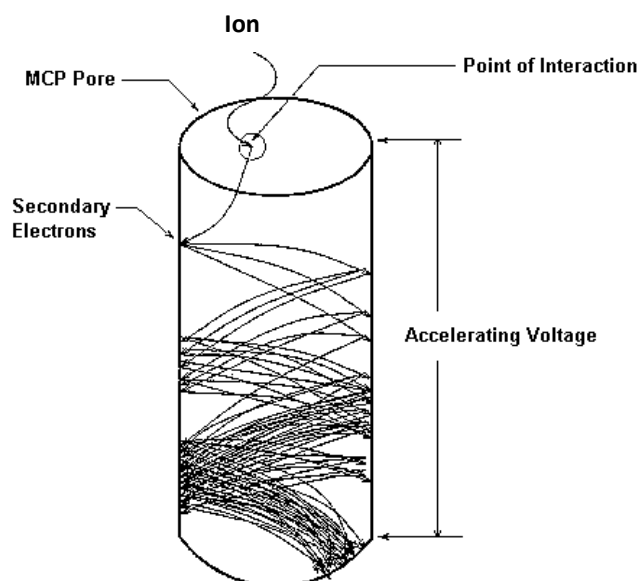
Figure 11: Schematic of an MCP showing the mechanism of secondary electron production

1.2.3 Mass spectrometry for protein identification

The concept of peptide mass mapping (also peptide mass fingerprinting) for protein identification by combination of MS and protein sequence database searching was first proposed in 1993 (Henzel et al., 1993; James et al., 1993; Mann et al., 1993; Pappin et al., 1993; Yates et al., 1993) [25].

In principle this method is based on the insight that the accurate mass of a group of peptides coming from a protein by sequence-specific proteolysis (i.e., a mass map or fingerprint) is a highly effective means of protein identification. After proteolysis of proteins with a specific protease groups of peptides are produced. The masses of these obtained peptides constitute mass fingerprints unique for a specific protein. If a sequence database containing the specific protein sequence is searched using this mass fingerprint (or selected peptide masses), the protein is expected to be correctly identified within this database. Various methods that automate this process have been developed [44].

Basically the established methods vary in specific details but share a typical sequence of steps. At first, peptides are generated by digestion of sample protein using sequence-specific cleavage reagents (e.g. Trypsin) that allow residues at the carboxyl- or amino terminus. These termini can be considered fixed for the database search. The enzyme trypsin used in this work leaves arginine (R) or lysine (K) at the carboxyl-terminus and the N-termini of tryptic peptides (except for the N-terminal one) are expected to be the amino acid following a K or R residue in the protein sequence. Next step is to measure peptide masses as accurately as possible in a mass spectrometer. In general an increase in mass accuracy will decrease the number of isobaric peptides for any given mass in a sequence database resulting in an increase of stringency of the search. Proteins in the databases are 'digested' in silico to generate a list of theoretical masses that are compared to the set of measured masses. To compare the set of measured peptide masses against those sets of masses predicted for each protein an algorithm is used. In this way to each match a score is assigned that ranks the quality of the matches. Therefore for a protein to be identified its sequence has to exist in the sequence database being used for identification. For Identification either protein or DNA sequence databases can be used. The use of a DNA sequence database needs the translation into protein sequences prior to digestion. Generally, if a complete genomic sequence database is available, peptide mass mapping is chosen as the method of choice for protein identification. Peptide mass mapping is also very popular for the identification of proteins purified by 2-DE because information on protein molecular weight and isoelectric point information can be used to aid identification [44].

Several reasons, like the direct correlation between the m/z value of the singly charged ions and the mass of the peptide, the high mass accuracy and sensitivity, and the tolerance towards contaminants, make MALDI-MS the preferred method for peptide mass fingerprinting. Simplicity, good sensitivity and high speed make MALDI-MS the method of choice for large-scale analysis of proteins from 2-D gels and of defined protein bands from SDS-PAGE gels [25].

Amino acid sequencing of peptides

In the field of amino acid sequencing of peptides tandem mass spectrometry (MS/MS) has become a very powerful tool. It has been widely used in protein biochemistry and proteomics to identify proteins, to deduce the sequence of unknown peptides, and to detect and locate post-translational modifications [25].

Different types of fragment ions can be observed in an MS/MS spectrum. These types depend on many factors including primary sequence, the amount of internal energy, the mode of ionization, charge state, etc. The nomenclature for fragment ions (outlined in Figure 12) was first introduced by Roepstorff and Fohlman, 1984 and was subsequently modified by Johnson et al., 1987 [45]. When MALDI peptide ions are fragmented in low-energy collision-induced dissociation (CID) tandem mass spectromters, mainly fragments from backbone cleavages are observed. Very little amino acid side chain framentation is observed. High-collision energy spectra, generated in magnetic sector or TOF/TOF instruments, are more complex than low-energy collision energy spectra. Low-energy CID spectra are relatively simple to interpret, and a straightforward nomenclature for annotating the MS spectra has been adapted (see Figure 12). The nomenclature differentiates fragment ions acccoring to the amide bond that fragments and the end of the pepitde that retains a charge after fragmentation [46] [47].

If the charge is retained on the N-terminal fragment, the ion is classified as either a_n, b_n or c_n. When the charge is on the C-terminal part, the ion type is either x_n, y_n or z_n. Subscripts are used to designate the specific amide bond that was fragmented to generate observed fragment ions. Moreover, using high-energy CID (collision energy >100 eV), additional ion types due to side chain cleavages can be generated. These are denoted w-, v- and d-ions (according to Johnson et al., 1988) [45].

Peptide fragmentation for purpose of protein identification can also be carried out by PSD-MALDI-MS [48]. But fragmentation by PSD-MALDI-MS is least well-controlled partly because only a few parameters of the experiment can be readily varied (i.e., laser energy and type of matrix).

Additionally, peptide ionization by MALDI generates mostly [M + H]$^{+}$ ions that do not produce readily interpretable tandem mass spectra. PSD-MALDI-MS therefore has a lower success rate, and the spectra are in many cases of lower quality than those of low-energy CID in a collision cell. These facts makes CID a more frequently used method for protein identification [49].
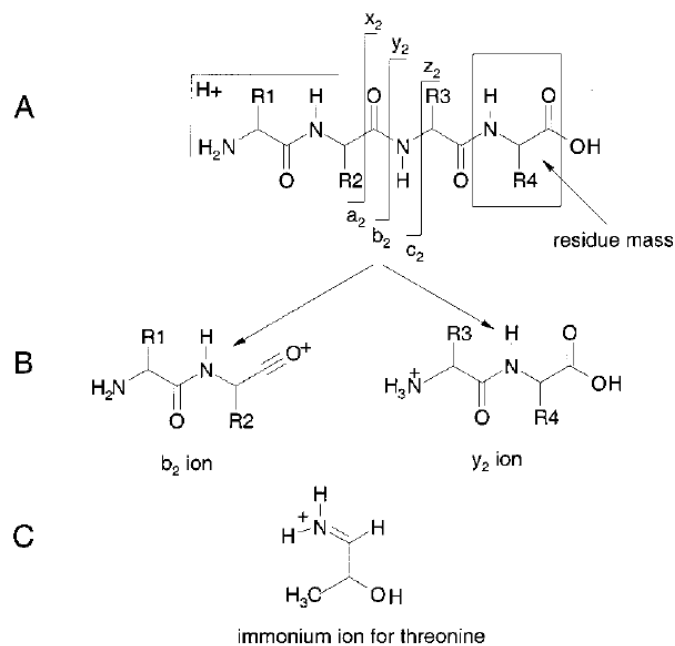
Figure 12: Peptide fragment ion nomenclature (A). Nomenclature for peptide fragment ions that form via cleavage of bonds along the peptide backbone. (B) Example of b- and y-ions. (C) Immonium ion for threonine [50].

Using amino acid sequencing for protein identification, a database search with MS/MS data as query is carried out. Fragment ions are used to score the spectrum against protein sequences in a database. As a result the best match is the peptide that fits the measured mass, the protease cleavage specificity, and the fragment ion pattern in the MS/MS spectrum [25].

1.2.4   Mass spectrometry for protein quantitation

In general the goal of quantitative analysis in mass spectrometry is correlation of the signal intensity with the quantity of the compound present in a sample [23]. Mass spectrometry analyses can be used for absolute and relative quantitation of proteins and peptides [25]. In the field of proteomics, quantitation of differences between two or more physiological states of a biological system ,known as relative quantitation, is one of the most important but also most challenging tasks [20].

For protein quantitation in protein mixtures the first systematic approaches were based on high-resolution two-dimensional electrophoresis (2-DE) [17] and not MS alone. The first and oldest gel-based method was based on statistical analysis via one of the powerful software packages that merge and compare a number of replicate sets of gels for control and treated samples [51]. Using 2-DE proteins are separated according to their isoelectric point by isoelectric focusing in the first dimension, and according to their molecular weight in the second dimension. These two mentioned parameters are unrelated and therefore it is possible to obtain an almost uniform distribution of protein spots across a 2-DE gel [52]. The 2-DE approach still presents advantages, not only due to the overall sensitivity of this technique but also because of its high resolution power as it is able to discriminate protein isoforms and proteins with post-translational modifications [17]. However, this approach requires several replicate runs to overcome variations in running gels, and therefore is very laborious and prone to experimental errors [51]. An alternative - Non-MS-based - approach is the difference gel electrophoresis (DIGE). In this approach, CyDye fluorophors that are spectrally resolvable (e.g., Cy2, Cy3, and Cy5) and matched for mass and charge are used to covalently modify the ε-amino group of lysines in proteins via an amide linkage. In this way the same protein labeled with any of the fluorophors will migrate to nearly the same position on the 2D gel. Control and treated samples are labeled with different dyes (e.g., Cy3 and Cy5, respectively), while a mixture consisting of an equal amount of the control and treated samples is labeled with Cy2. Labeled samples are combined and run in a single 2D gel to allow better spot matching and to minimize gel-to-gel variations. As differently labeled samples are combined and run in a single 2D gel, a better spot matching as well as a minimized gel-to-gel variation can be achieved. The DIGE approach also allows multiplexing for up to three separate protein mixtures [53].

In the past few years gel-based methods have been challenged and complemented by LC-based methods, particularly in the area of high-throughput proteomic research. Some of the reasons for that fact include issues related to reproducibility, poor representation of low abundant proteins, highly acidic/basic proteins, or proteins with extreme size or hydrophobicity, as well as difficulties in

automation [20]. LC-based methods offer flexibility of choosing a wide range of stationary and mobile phases to resolve complex biological samples at the protein or peptide level. LC is recognized as an indispensable tool in proteomics research since it provides high-speed, high-resolution and high-sensitivity separation of macromolecules. Additionally the features of chromatography enable the detection of low-abundance species such as post-translationally modified proteins [54]. In multidimensional LC approaches, proteins are usually digested into peptides prior to separation first by cation exchange, and then with C18 reversed-phase column chromatography. Chemical tagging (usually stable isotope labeling) of proteins/peptides also allows relative quantitation of protein samples by LC-MS analyses [55]. Stable isotope labeling was first introduced into proteomics in 1999 by three independent laboratories [55] [56] [57]. Isotope labels can be introduced into amino acids metabolically, enzymatically or chemically. Recently, label-free methods, that compare two or more experiments by comparing the direct mass spectrometric signal intensity, have emerged [58].

Metabolic labeling

Metabolic labeling means the incorporation of a stable isotope signature into proteins during cell biosynthesis. The first type of metabolic labeling used in MS-based proteomic analysis was ^{15}N labeling. In this approach ^{15}N-enriched medium is used for cell culture leading to a total labeling of the used organism [56]. Metabolic labeling has gained wider popularity by the introduction of a further approach in the form of stable isotope labeling by amino acids in cell culture (SILAC) [59]. SILAC is a simple, robust, yet powerful approach in MS-based quantitative proteomics. Using this method cellular proteoms are labeled through normal metabolic processes, incorporating non-radioactive, stable isotope-containing amino acids in newly synthesized proteins. In the growth medium natural ('light') amino acids are replaced with 'heavy' SILAC amino acids. In this way cells that grow in this medium incorporate the heavy amino acids. An important fact is that SILAC amino acids do not have an effect on cell morphology or growth rates. After mixing 'light' and 'heavy' cell populations, they remain distinguishable by MS and protein abundances can be determined from the relative MS signal intensities. In this way SILAC can provide accurate relative quantitation without any chemical derivatization or manipulation [59]. Compared to the ^{15}N approach, SILAC allows more comparisons within a single experiment due to the availability of several labels. Another advantage is that SILAC has a predictable mass shift. However, the problem of the SILAC approach is that complete incorporation of isotopic amino acids is not the same for all cell lines [60]. The method cannot be used for cell types that are unable to incorporate certain amino acids. In addition, some cells are harder to grow in the dialyzed serum required for SILAC due to the loss of essential growth factors [61].

Enzymatic labeling

Enzymatic labeling can be performed either during proteolytic digestion or after proteolysis in a second incubation step with the protease. To mention an example, trypsin- or Glu-C-catalyzed incorporation of ^{18}O during protein digestion is an elegant and specific way to introduce an isotope label into peptides. Incorporation of ^{18}O into C-termini leads to a mass shift of 2 Da per ^{18}O atom. Enzymes such as trypsin and Glu-C incorporate two oxygen atoms resulting in a 4 Da mass shift which is generally sufficient for differentiation of isotopomers. In general, the presence of an ^{18}O atom label on the carboxyl termini of peptides is advantageous because it eases the assignment of 'y' ions in a spectrum [58] [21]. In MALDI-MS analysis the described trypsin-catalyzed incorporation of ^{18}O into carboxyl groups, facilitates the comparative analysis of protein and peptide samples [25]. One problem of the enzymatic labeling approach is that samples are combined post-digestion, so protein losses that occur during sample preparation are not compensated for and therefore affect experiment reproducibility. A further problem can be that after sample pooling a trypsin-mediated back exchange (the replacement of ^{18}O with ^{16}O) can occur in solvents containing natural water [62]. Another reason why enzymatic labeling is not widely used is that one, two or even three carboxyl oxygens can be incorporated leading to variability in quantitation. The exchange of only one oxygen (mass shift of only 2 Da) can complicate quantitation, especially when low resolution mass spectrometers are used [63]. Another drawback of this method is that different peptides incorporate the label at different rates [64].

Chemical labeling

In addition to enzymatic labeling a further post-biosynthetic labeling method is the chemical derivatization *in vitro*. In general, every reactive amino acid side chain can be used for incorporation of an isotope-coded mass tag by chemical means. Most commonly used side chains are lysine and cysteine [58].

Chemical labeling in the research field of quantitative MS-based proteomics was first shown in 1999 by Gygi *et al.,* who introduced the isotope-coded affinity tag (ICAT) technology. This method comprises cysteine-specific tagging of intact proteins followed by proteolytic digestion. ICAT could not reach widespread application mainly due to limited robustness. Further disadvantages of this method are that ICAT is not applicable to cysteine-free proteins and that the cysteine content of proteins is often low [65].

Another group of chemical labeling targets the peptide N-terminus and the epsilon-amino group of lysine residues [58]. The labeling of the N-terminus of peptides was first introduced by Peter James in 2000, who developed a method for protein quantitation by labeling of the N-terminus of peptides using D_4 or H_4 forms of Nicotinyl-N-Hydroxysuccinimide (Nic-NHS) [21]. The labeling of the N-terminus and the epsilon-amino group is most of the time realized via the very specific *N*-hydroxysuccinimide (NHS) chemistry or other active esters and acid anhydrides as in, e.g., the isotope-coded protein label (ICPL), isobaric tags for relative and absolute quantitation (iTRAQ), tandem mass tags (TMT), and acetic/succinic anhydride [58].

Commercially available alkylating reagents include ICAT (shown on Figure 13), MassTag (shown on Figure 14) and iTRAQ (described in detail in the following chapter), all of which are suitable for MALDI-MS and MS/MS [25].
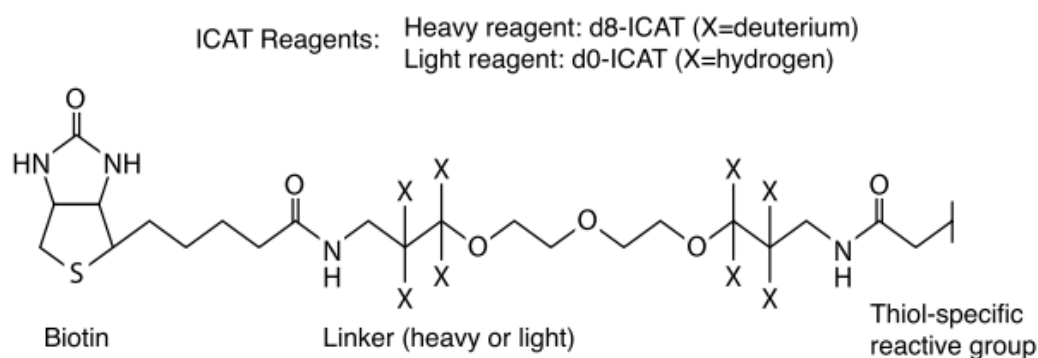
Figure 13: Chemical structure of the ICAT (Isotope Coded Affinity Tag) label [21].
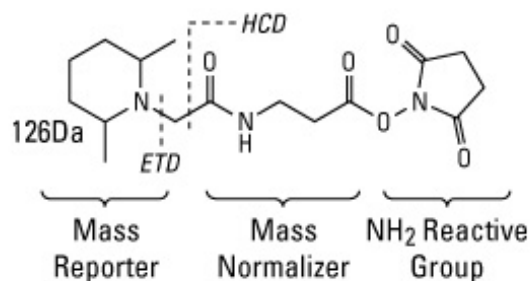
Figure 14: Chemical structure of the TMT (tandem mass tag) label called TMT[0]; further available TMT labels are TMT[2], TMT[6] and TMT[10]

Isobaric tags for relative and absolute protein quantitation (iTRAQ)

The iTRAQ technique was first described by Ross *et al.* in 2004 [21] [66], and was commercialized by Applied Biosystems. In general, iTRAQ reagents employ *N*-hydroxy-succinimide (NHS) chemistry that permits specific and largely complete tagging of α- and ε-amino groups for labeling of peptides after enzymatic digestion [21].

As shown on Figure 15 the iTRAQ label is an isobaric tagging compound consisting of a reporter group (variable mass of 114-117 Da or 113-119 and 121 Da), a balance group and an amino-reactive group that introduces a highly basic group (N-methylpoperazine) at lysine side chains and at peptide N-termini [21]. Especially for immobilized pH gradient isoelectric focusing (IPG-IEF) or off-gel electrophoresis (OGE) it it is important to know that the introduction of this highly basic group can alter the pI or peptides and consequently the isoelectrofocusing [67]. The isobaric iTRAQ labeling reagents can be classified by the type of m/z shift of the chemical modification introduction (during derivatization) and by the number of 'channels'. 'Channels' correspond to the number of samples that can be mixed and analyzed simultaneously. For iTRAQ analysis the 'channels' iTRAQ 4-plex and iTRAQ 8-plex are available [68].
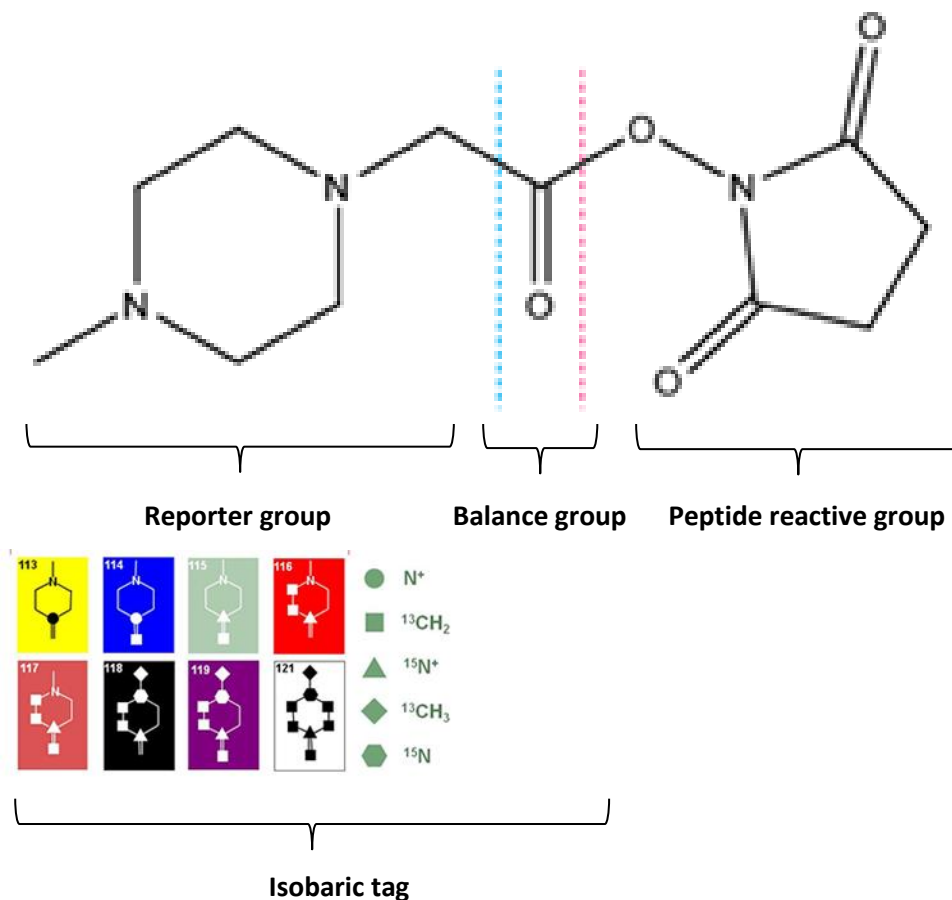
Figure 15: Structure of the iTRAQ reagents. The reporter group with m/z either between 114-117 in iTRAQ 4-plex or m/z of 113-119 and 121 in iTRAQ 8-plex, and the balance group with variable m/z values represent together the isobaric tag of an iTRAQ reagent. The peptide reactive group can covalently link to the N-terminus of the peptide.

In an iTRAQ experiment (as shown on Figure 16) chemical derivatization with different channels with the same isobaric tag leads to molecules with very similar (or identical) mass that appear as a single peak in full MS scans [68]. During the MS/MS mode, the label releases the reporter group as a singly charged ion of masses at m/z 114-117 (4-plex) as shown on Figure 17 or m/z 113-119 and 121 (8-plex). In this way up to four different samples using 4-plex, or up to eight samples using 8-plex can be measured in only one experiment [21].
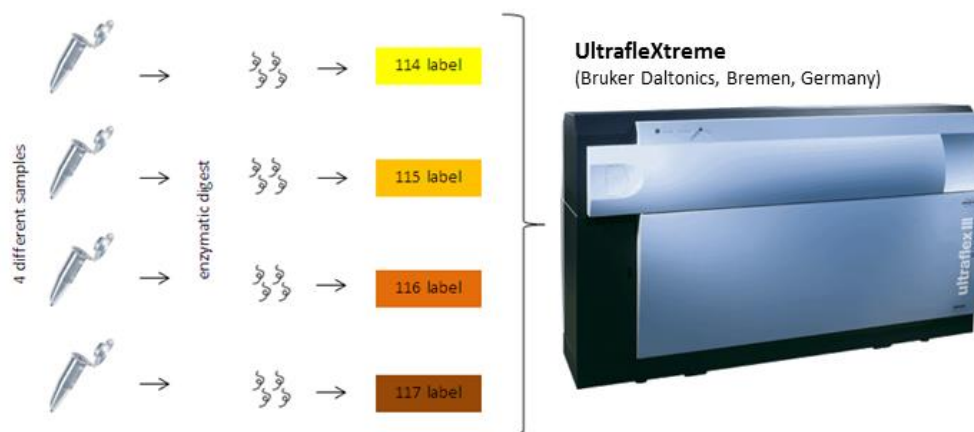
Figure 16: Set-up of an iTRAQ experiment using labels with m/z 114, 115, 116 and 117 (4-plex)
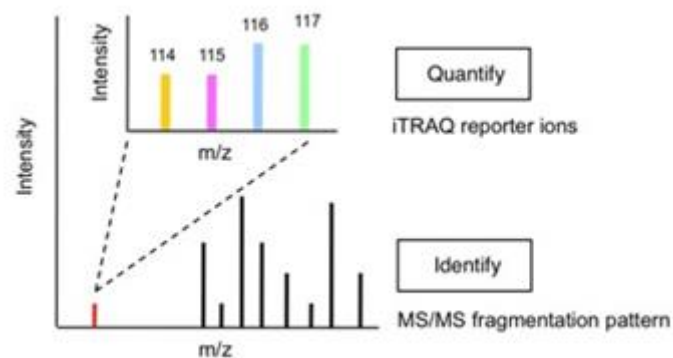
Figure 17: Reporter ions with m/z 114, 115, 116 and 117 which are obtained during MS/MS analysis of an iTRAQ 4-plex experiment

Advantages of iTRAQ

As in iTRAQ, the labeling is done at the peptide level, and because the labeling efficiency of every tryptic peptide should be almost 100%, multiple peptides can be detected for the same protein, resulting in multiple quantitation measurements per protein and therefore increasing the confidence

of protein identification [21]. However, using complex biological samples mass spectrometry analysis proved to be difficult within this study. The huge amount of peptides as well as the presence of disturbing substances resulted in interference and related problems like a decrease of labeling efficiency. Nevertheless, in principle for iTRAQ analysis any sample can be used, e.g. cell lysates or proteins obtained only from other cell compartments, which is different from other approaches, like those that can accommodate incorporation of stable isotopes during cell culture [69]. As already mentioned the iTRAQ reagents consist of different reporter groups, enabling quantification of up to 8 different samples in parallel. As for all iTRAQ experiments suitable software is necessary to analyze generated data, well developed and tested software for iTRAQ labeled samples is also an important advantage [21, 69].

Disadvantages of iTRAQ

In iTRAQ experiments one important aspect which limits the confidence of the output of protein identification and quantitation is the variability. Variability can be introduced in multiple steps of sample preparation, efficiency of chemical tagging, performance of instrumentation, and method of acquisition used, as well as software (algorithms) and thresholds defined for database searches [69]. Current studies [70] [71] also indicate that there is an inherent dynamic range limitation in the results of an iTRAQ experiment. Because of that, observed expression ratios are compressed. According to results of discovery experiments the maximum expression ratios that can be observed seems to be only approximately 3-5. Further disadvantages of this method are the expense of the reagents, the MS/MS quantitation is costly in terms of MS time and that fractionation is required.[21]. To conclude, using iTRAQ, especially for high-throughput quantitative applications, there are a number of key features which must be critically assessed [72].

According to a number of studies in the field of iTRAQ experiments several conclusions can be drawn. The highest fold change value measured differs widely among laboratories, which may be due to analysis limitations rather than a difference in protein change. Secondly, the quantitative protein values appear to be 'flattened', which means that the authors found it difficult to measure relatively high protein ratios [73]. Because of that, relatively high protein ratios are difficult to measure. Reported protein changes rarely seem to exceed the tenfold value. A further problem is the wide range of available quantitation algorithms, resulting in differences in the quantitative results [66]. Nevertheless, iTRAQ-based quantitation has become an attractive method in global proteomic quantitation [69]. It can provide quantitative information from numerous experimental approaches

including affinity pull-downs, time-course analysis, and discovery and elucidation of disease markers, and is therefore a promising tool for various proteomics questions in the future [74].

2   Materials and methods

2.1   Instrumental

During this work the following instruments were used:

The **AXIMA CFRplus** (Shimadzu Biotech Kratos Analytical, Manchester, UK) is a high vacuum MALDI-TOF/TOF device capable of analyzing analytes at even very low concentrations. The curved field reflectron (CFR) enables efficient generation of post source decay (PSD) mass spectra mandatory for identifying analytes based on their fragmentation pattern. Working in continuous or pulsed mode with a 337 nm N_2 laser, the device has furthermore the possibility to easily adapt the acceleration voltage (linear + 30 kV/- 20 kV, Reflectron + 25 kV/- 20 kV) [75].

Figure 18: Axima CFRplus high vacuum MALDI mass spectrometer

Similar to the AXIMA CFRplus **the AXIMA TOF[2]** (Shimadzu Biotech Kratos Analytical, Manchester, UK) is also a MALDI-TOF/TOF device working under high vacuum conditions and equipped with a nitrogen laser (337 nm). However, the TOF[2] is additionally featured with a collision cell enabling high energy collision (20 keV) of the analyte molecules with the collision gas. As a collision gas argon is used. The induced fragment ions provide characteristic information regarding the analyte structure enabling identification of unknown compounds [75].

The **UltrafleXtreme** (Bruker Daltonics, Bremen, Germany) is a MALDI-TOF/RTOF device, equipped with a modified Nd:YAG (neodymium-doped yttrium aluminum garned) laser [76]. The

UltrafleXtreme includes a so called 'LIFT' cell. In general this 'LIFT' cell has two main functions, the re-acceleration of fragments remaining molecular ions and the re-focusing of the ions. Re-acceleration leads to a minimization of the energy spread of the metastable fragments. Thus, the complete fragment ion spectrum at one fixed reflectron voltage can be captured at the detector. Re-focusing leads to an increase of resolution [42].

Figure 19: UltraXtreme MALDI-TOF/TOF mass spectrometer

2.2 Materials

AB Sciex Pte. Ltd. (Foster City, CA, USA):

iTRAQ Reagents Methods Develop Kit (4352160)

iTRAQ Reagents Multi-Plex Kit (4352135)

Acros Organics (New Jersey, USA):

Formic acid (99 %)

AppliChem (Darmstadt, Germany):

Sodium dodecylsulfate (> 99.5 %)

Fluka (Buchs, Switzerland):

Acetonitrile (LC-MS CHROMASOLV ®, 34967)

Ammonium hydrogen carbonate (≥ 99.5 %)

Potassium chloride (> 99,5 %)

Millipore (Bedford, MA, USA):

ZipTip® C18 pipette tips

Roche (Penzberg, Germany):

Trypsin, proteomics grade (03708985001)

Sigma-Aldrich (St. Louis, MO, USA):

Albumin, from bovine serum (≥ 96 %, A8022-10G)

Acetic acid (≥ 99.8 %)

α-Cyano-4-hydroxycinnamic acid (98 %)

β-Mercaptoethanol

Calcium chloride

D,L-Dithiothreitol (99 %)

Iodacetamide (≥ 99 %)

Potassium phosphate (> 99 %)

Triethylammonium bicarbonate buffer pH 8.4–8.6, 25 °C (17902-100mL)

Trifluoroacetic acid (≥ 99 %)

Tris-(2-carboxymethyl)phosphine (≥ 98 %, 75259)

Thermo Scientific (Rockford, IL, USA):

HyperSep C_{18} 96 well plate

2.3 Workflow

Protein quantitation using iTRAQ

Protein identification after 2-d DIGE

| In-solution digestion (see Chapter 2.4.1) |

| HyperSep™ C18 solid phase extraction (see Chapter 2.6) |

| iTRAQ® labeling (see Chapter 2.8) |

| HyperSep™ C18 solid phase extraction (see Chapter 2.6) |

| Cation exchange chromatography (see Chapter 2.5) |

| MALDI-TOF-MS (see Chapter 2.9) |

| In-gel digestion (see Chapter 2.4.2) |

| ZipTip purification (see Chapter 2.7) |

| MALDI-TOF-MS (see Chapter 2.9) |

2.4 Tryptic digestion

2.4.1 In-solution digestion

The procedure for the in-solution digestion was optimized for bovine serum albumin (BSA) and *Exophiala dermatitidis* samples.

Table 3: Buffers and solutions for tryptic in-solution digestion

Solution	Components
Sodium dodecyl sulfate (SDS)	2 % SDS 400 mg SDS in 20 mL UHQ
Tris-(2-carboxyethyl)phosphine (TCEP) (reducing agent)	110 mM TCEP in UHQ 3.15 mg TCEP/mL UHQ
Iodacetamide (IAA) solution (alkylation solution)	84 mM IAA in UHQ 15.54 mg IAA/mL UHQ *store in the dark*
Triethylammonium bicarbonate (TEAB) (digestion buffer)	0.5 M TEAB, pH 8.4-8.6, 25 °C 500 µL TEAB + 500 µL UHQ (1:1)
Calcium chloride (CaCl$_2$)	100 mM CaCl$_2$ in UHQ 111 mg CaCl$_2$ in 10 mL
Trypsin solution	0.1 µg trypsin/µL 50 mM CH$_3$COOH 1.5 µg trypsin in 15 µL 50 mM CH$_3$COOH stored at -20 °C

Procedure

- To each of up to four sample tubes containing 5 to 100 µg of sample (BSA samples; *Exophiala dermatitidis* samples extracted according to [14]), add UHQ to get a final volume of 200 µL.
- Add 10 µL of prepared **SDS** solution and vortex to mix.
- To each sample tube add 10 µL of the **reducing agent** to get a final concentration of 5 mM TCEP.
- Vortex to mix, then spin.
- Incubate the tubes at 60 °C for 1 hour.
- Spin to bring the sample to the bottom of the tube.

- To each tube add 10 μL *freshly prepared alkylation solution* to get a final concentration of 3.7 mM IAA.

- Vortex to mix, then spin.

- Incubate the tubes at room temperature for 30 minutes.

- Dry the sample in a vacuum centrifuge.

- To get rid of interfering substances for the tryptic digestion, the samples have to be diluted at least 20 fold with 0.5 M TEAB (volume depends on the initial buffer amount).

- To each sample add the needed amount of the prepared $CaCl_2$ solution to get a final volume of 1 mM $CaCl_2$.

- Vortex to mix, then spin.

- Thaw *trypsin* aliquots and add needed trypsin to each sample tube (trypsin:protein ratio should be 1:50).

- Vortex to mix, then spin.

- Incubate the tubes at 37 °C overnight.

- Spin to bring the sample digest to the bottom of the tube.

2.4.2 In-gel digestion

Destaining of silver stained gels [77].

Table 4: Buffers and solutions for destaining and tryptic in-gel digestion

Solution	Components
Destain **(until gel is completely destained, gels become yellow, but brown silver spots disappear)**	50 % 100 mM $Na_2S_2O_3$ 50 % 30mM $K_3Fe(CN)_6$ (III)
NH₄HCO₃	100 mM NH_4HCO_3 pH 8.5 790.6 mg NH_4HCO_3 + 90 mL UHQ, use NH_3 to adjust pH bring final volume to 100 mL
Dithiotreitol (DTT) solution **(reducing solution)**	10 mM DTT in 100 mM NH_4HCO_3 1.54 mg DTT/mL 100 mM NH_4HCO_3

Iodacetamide (IAA) solution (alkylation solution)	54 mM IAA in 100 mM NH$_4$HCO$_3$ 10 mg IAA/mL 100 mM NH$_4$HCO$_3$ *store in the dark*
Digestion buffer	95 % 50 mM NH$_4$HCO$_3$/5 % ACN 5 mL 100 mM NH$_4$HCO$_3$ + 500 µL ACN bring to final volume of 10 mL
Trypsin solution	12.5 ng trypsin/µL 1 µg trypsin in 10 µL UHQ (stored at -20 °C) add 90 µL digestion buffer before use

Procedure

- Wash the gel slab with UHQ (2 changes, each).
- Use a clean scalpel to excise the spot of interest from the gel. Cut as close to the protein band as possible to reduce the amount of background gel. Excise a gel piece of roughly the same size from a gel region which does not carry any protein to use it as a control.
- Cut the excised piece into roughly 1 mm^3 cubes, and transfer them to a clean 0.5 mL microfuge tube.

Silver stained gels:

- Wash the gel particles with N$_2$S$_2$O$_3$/ K$_3$Fe(CN)$_6$ (III)– one or two changes each, 5 min/change. Solvent volumes used in the washing steps should roughly equal to the gel volume.
- Wash the gel pieces with UHQ until they are clear (the yellow color has to be removed entirely).
- Remove all liquid and add enough ACN to cover the gel pieces.
- After the gel pieces have shrunk (they become milky and stick together) remove the ACN and rehydrate the gel pieces in 100 mM NH$_4$HCO$_3$ for 5 min.
- Add an equal volume of ACN (to get 100 mM NH$_4$HCO$_3$ /ACN, 1:1) and incubate for 15 min.

For all destained gels:

- Remove all liquid and dry gel particles in a vacuum centrifuge.
- Swell the gel particles in **reducing solution** and incubate for 45 min at 50-56 °C to reduce the protein.
- Chill tubes to room temperature, spin down condensate. Remove excess liquid, and replace it quickly with roughly the same volume of **freshly prepared alkylation solution.** Incubate at room temperature for 30 min in the dark.
- Remove alkylation solution and wash the gel particles with 100 mM NH_4HCO_3 for 5 min.
- Add an equal volume of ACN (to get 100 mM NH_4HCO_3/ACN, 1:1) and incubate for 15 min.
- Remove all liquid and dry gel particles in a vacuum centrifuge.
- Rehydrate gel particles by adding trypsin solution. Add more if all the initially added volume is soaked up. Incubate for 45 min.
- Remove remaining enzyme supernatant and replace it with 5-20 μL of the **digestion buffer** (without enzyme).

For all digestions:

- Digest overnight at 37 °C and/or for 10 min at approximately 170 W in the domestic microwave oven.
- The first peptide analysis can be performed already after 3-4 h (or after overnight digestion). If some liquid has evaporated and condensed on the side or on the lid of the microcentrifuge tube, centrifuge briefly to gather the liquid at the bottom of the tube.
- After overnight digestion add a sufficient volume of 50 mM NH_4HCO_3 to cover the gel pieces and incubate for 15 min.
- Add the same volume of ACN. Incubate for 15 min and recover the supernatant.
- Repeat the extraction two times with 1 % HCOOH and ACN (1:1, v/v).
- Pool all the extracts.
- Dry the sample in a vacuum centrifuge.
- Redissolve peptides in 10 μL 0.1 % TFA, sonicate briefly.

2.5   Cation exchange chromatography

The following substances in an iTRAQ® Reagent-labeled sample mixture may interfere with LC/MS/MS analysis:

- Dissolution Buffer
- 75 % organic solvent (ethanol and acetonitrile)
- 1 mM Reducing Reagent (tris(2-carboxyethyl) phosphine [TCEP])
- 0.02 % SDS
- 5 mM calcium chloride
- Excess iTRAQ® Reagents

Therefore before performing LC/MS/MS analysis, the sample mixture has to be cleaned up using cation exchange chromatography.

Table 5: Buffers and solutions for cation exchange chromatography

Solution	Components
Buffer-Load	10 mM Potassium phosphate in 25 % ACN at pH 3.0, use HCl to adjust pH
Buffer-Elute	10 mM Potassium phosphate in 25 % ACN at pH 3.0, 350 mM Potassium chloride
Buffer-Clean	10 mM Potassium phosphate in 25 % ACN at pH 3.0, 1 M Potassium chloride
Buffer-Storage	10 mM Potassium phosphate in 25 % ACN at pH 3.0, 0,1 % Sodium azide

Procedure

- After HyperSep™ C18 solid phase extraction (see Chapter 2.6), reduce the concentrations of buffer salts and organics by diluting the sample mixture at least 10 fold with cation exchange *Buffer-Load.*
- Vortex to mix.
- Check the pH using pH paper. If the pH is not between 2.5 and 3.3, adjust by adding more cation exchange *Buffer-Load.*
- To condition the cartridge, inject 1 mL of the cation exchange *Buffer-Clean.* Divert to waste.
- Inject 2 mL of the cation exchange *Buffer-Load.* Divert to waste.

- Slowly inject (≈ 1 drop/second) the diluted sample mixture onto the cation exchange cartridge and collect the flow-through in a sample tube.

- Inject 1 mL of the cation exchange ***Buffer-Load*** to wash the TCEP, SDS, calcium chloride, and excess iTRAQ® Reagents from the cartridge. Collect the flow-through in the same sample tube used in the previous step. (Keep the flow-through until verification by MS/MS analysis that loading on the cation exchange cartridge was successful. If loading fails, loading can be repeated using the flow-through after troubleshooting the cause of the loading failure.)

- To elute the peptides, slowly inject (≈ 1 drop/second) 500 µL of the cation exchange ***Buffer-Elute.*** Capture the eluate in a fresh 1.5 mL tube. Collect the eluted peptides as a single fraction.

- Wash the undigested proteins such as trypsin from the cation exchange cartridge by injecting 1 mL of the cation exchange ***Buffer-Clean.*** Divert to waste.

- For further samples repeat the point 5 through 8. After finishing, store the cartridge as follows.

- After cleaning the cartridge (point 9 above), inject 2 mL of the cation exchange ***Buffer-Storage.***

- Remove the cartridge, then seal the ends of the cartridge with the two end caps.

- Record the number of times the cartridge has been used.

- Store the cartridge at 2 to 8 °C.

- Clean the needle-port adapter, outlet connector, and syringe with water.

2.6   HyperSep™ C18 solid phase extraction

To purify peptides after in-solution digestion and before MS/MS analysis HyperSep™ C18 SPE Columns were used.

Procedure

- **Wet** each column three times with 1 mL ACN.
- **Equilibrate** each column by wetting it five times with 1 mL 0.25 % TFA.
- **Bind** the peptides (≈ 1 mL/min flow rate).
- **Wash** each column five times with 1 mL 0.25 % TFA.
- **Elute** the peptides with 100 µL 80 % ACN + 0.1 % Formic acid.

2.7   ZipTip purification

To purify peptides after in-gel digestion Millipore ZipTips$_{C18}$ tips were used.

<u>**Procedure**</u>

- **Wet** the ZipTip three times with ACN.
- **Equilibrate** the ZipTip by wetting the ZipTip three times with 0.1 % TFA.
- **Bind** the peptides by sucking in the redissolved peptides eight times.
- **Wash** the ZipTip three times with 0.1 % TFA.
- **Elute** the peptides with 5 µL 0.1 % TFA/ACN (1:1).

2.8   iTRAQ labeling

- After HyperSep™ C18 solid phase extraction (see Chapter 2.6), add to each sample 10 µL 0.5 M TEAB.
- Vortex each tube to mix, then spin.
- Allow each vial of iTRAQ® Reagent required to reach room temperature.
- Spin to bring the solution to the bottom of the tube.
- Add 70 µL of ethanol to each iTRAQ® Reagent vial.
- Vortex each vial to mix, then spin.
- To each sample tube transfer 23,3 µL of the needed iTRAQ® Reagent. For example, for a duplex experiment, transfer the contents of the iTRAQ® Reagent 114 vial to sample 1, sample 2 and sample 3 and transfer the contents of the iTRAQ® Reagent 117 vial to sample 4, sample 5 and sample 6.
- Vortex each tube to mix, then spin.
- Incubate the tubes at room temperature for 1 hour.
- To each sample tube add 16,7 µL UHQ to quench the iTRAQ® reaction and incubate at room temperature for 30 minutes.
- Combine the contents of each iTRAQ® Reagent-labeled sample tube into one tube. For example, combine sample 1 and 4, sample 2 and 5 and sample 3 and 6.
- Vortex to mix, then spin.

2.9   MALDI-TOF-MS

2.9.1   Peptide analysis

Peptide mass fingerprint (PMF) analysis was performed in the positive ion, reflectron mode on the AXIMA-CFRplus (Shimadzu Biotech Kratos Analytical, Manchester, UK), the AXIMA-TOF[2] (Shimadzu Biotech Kratos Analytical, Manchester, UK) or the UltraXtreme (Bruker Daltonics, Bremen, Germany).

Instrumentation settings for the AXIMA CFRplus and the AXIMA TOF[2]:

Laser power:	50 – 90
Mass range:	1.0 – 5000.0 Da
Peak extraction (PE) optimized for:	2000.0 Da
Blank:	500.0 Da
Accumulation of shots per profile:	2
Profiles summed up for one spectrum:	100

Instrumentation settings for the UltraXtreme:

Laser power:	30-35 %
Mass range:	600.0-3500.0 Da
Accumulation of laser shots per profile:	500
Profiles summed up for one spectrum:	5-10

Post-source decay (PSD) fragment analysis was measured in the reflectron mode on the AXIMA-CFRplus (Shimadzu Biotech Kratos Analytical, Manchester, UK), the AXIMA-TOF[2] (Shimadzu Biotech Kratos Analytical, Manchester, UK) or the UltraXtreme (Bruker Daltonics, Bremen, Germany). For PSD analysis the mass range and the laser power were adapted to the respective peptide.

2.9.2 Database search

Peptide mass fingerprint spectra (PMF) as well as Post-source decay fragment spectra were searched in Mascot (http://matrixscience.com) and manually interpreted using the free software program mMass (www.mmass.org) and the Bruker Daltonics software package Compass™.

The database searching was performed in the MASCOT database.

For database search of PMF spectra the parameters were set as follows:

Database:	NCBI
Taxonomy:	Fungi
Enzyme:	Trypsin
Missed cleavages up to:	2
Fixed modifications:	Carbamidomethyl (C)
Variable modifications:	Oxidation (M)
Mass values:	Monoisotopic
Peptide mass tolerance:	± 0.8 Da
Peptide charge state:	1+

For database search of PSD spectra the following parameters were set:

Database:	NCBI
Taxonomy:	Fungi
Enzyme:	Trypsin
Missed cleavages up to:	2
Fixed modifications:	Carbamidomethyl (C)
Variable modifications:	Oxidation (M)
Mass values:	Monoisotopic
Peptide mass tolerance:	± 0.8 Da
Fragment mass tolerance:	± 0.5 Da
Instrument type:	MALDI-TOF-TOF

In addition to database search, spectra were manually processed using various software tools available as open source products, e.g. Protein Prospector (MS digest) or PeptideMass.

3 Results and discussion

3.1 Overview of Method Development

As already described, the extreme stress tolerance of black micro-colonial fungi is a relatively new field of research. The intended goal of the study was to develop a proteomics-based approach for relative protein quantitation, because knowledge on differential protein regulation allows deeper insight into biological functions. The applied methodology is mainly based on the standard iTRAQ protocol (according to the iTRAQ reagent provider AB Sciex), the work of Ping Lan et al., 2011 [78], as well as the protocol obtained from the working group of Univ.Prof.Mag.Dr. Christian Huber at the University of Salzburg. iTRAQ has never been used for fungal species containing high concentrations of melanin and therefore a robust sample preparation protocol had to be established. For this, first a standard protein sample of moderate complexity, bovine serum albumin (BSA), was used to test different clean-up steps necessary to remove interfering substances from sample preparation which are critical for trypsin digestion, the labeling process of the samples or for the subsequent MS analysis. For the actual fungal samples the strain *Exophiala dermatitidis* was used as model organism. The main sources of interfering substances for the fungal samples are mainly buffer constituents necessary to lyse the thick melanized cell walls and important for effective protein extraction from (Protein extraction was carried out at the University of Natural Resources and Life Sciences, Vienna).

At first the influence of a cation exchange chromatography clean-up step and a HyperSep™ C18 solid phase extraction clean-up step were evaluated. The cation exchange chromatography step was recommended by the standard iTRAQ protocol (according to the iTRAQ reagent provider AB Sciex) and the HyperSep™ C18 solid phase extraction step was chosen as an alternative routine suggested by literature to be suitable with respect to sample nature and sample amount. Different to literature an additional dilution step prior to tryptic digestion had to be introduced to decrease buffer component concentration to an amount suitable for mass spectrometry. After comparing the efficiency of all clean-up steps, the finally established method was statistically evaluated using results obtained from experiment facilitating a trytic BSA digests.

To evaluate the established relative protein quantitation method on biological samples also experiments with *Exophiala dermatitidis* samples were processed. For this, five different biological conditions in four replicates were studied.

As not only the quantitation of different peptides is of interest to get deeper insight to biological functions of black fungi, also protein identification for *Exophiala dermatitidis* samples were carried out. 25 spots of an extract of *Exophiala dermatitidis separated by* 2D gel electrophoresis were cut out, digested and measured by MALDI mass spectrometry. An online available reference gel of *Saccharomyces cerevisiae* was used have a first indication for protein identity as protein databases are not yet available for this species.

3.2 Method development using bovine serum albumin

3.2.1 Evaluation of a cation exchange chromatography step

As already mentioned, the first step during the development of a relative protein quantitation method was the study of the influence of a cation exchange chromatography step performed according to Chapter 2.4. Figure 20 shows a scheme of the experimental setup.

Total protein was first denatured with 2 % (w/v) SDS and then reduced by adding tris(2-carboxyethyl)phosphine (TCEP) to a final concentration of 5 mM. After incubation at 60 °C for one hour, iodoacetamide (final concentration 3.7 mM) was used for alkylation. To test also the influence of different sample concentrations, 5 µg BSA and 10 µg BSA were used without changing the amount of reducing and alkylation agent.

Trypsin (ratio 1: 50, trypsin: protein) was used to digest the samples at 37 °C over night. Subsequently the digested samples were purified using either a micro reversed-phase clean-up step (see Chapter 2.6) or cation exchange chromatography (see Chapter 2.4) in combination with the same reversed-phase clean-up (see Chapter 2.6).

Finally MALDI-TOF-MS analysis (see Chapter 2.8) was carried out. Peptide mass fingerprint (PMF) analysis as well as post-source decay (PSD) fragment analysis was performed in the positive ion mode using the AXIMA-TOF[2] (Shimadzu Biotech Kratos Analytical, Manchester, UK). Measured m/z values were compared to m/z values which can be expected from an *in-silico* BSA digest (theoretical digest). Information on theoretical BSA peptides were obtained from the UniProtKB/Swiss-Prot database using the accession number P02769 on the ExPASy bioinformatics resource portal (www.expasy.com). For the theoretical BSA digestion the following parameters for peptide masses were chosen: Treated with Iodoacetamide and oxidized with Methionines. The enzyme Trypsin was used and no missed cleavages were allowed. In this way 54 expected peptides for a BSA digestion could be obtained.
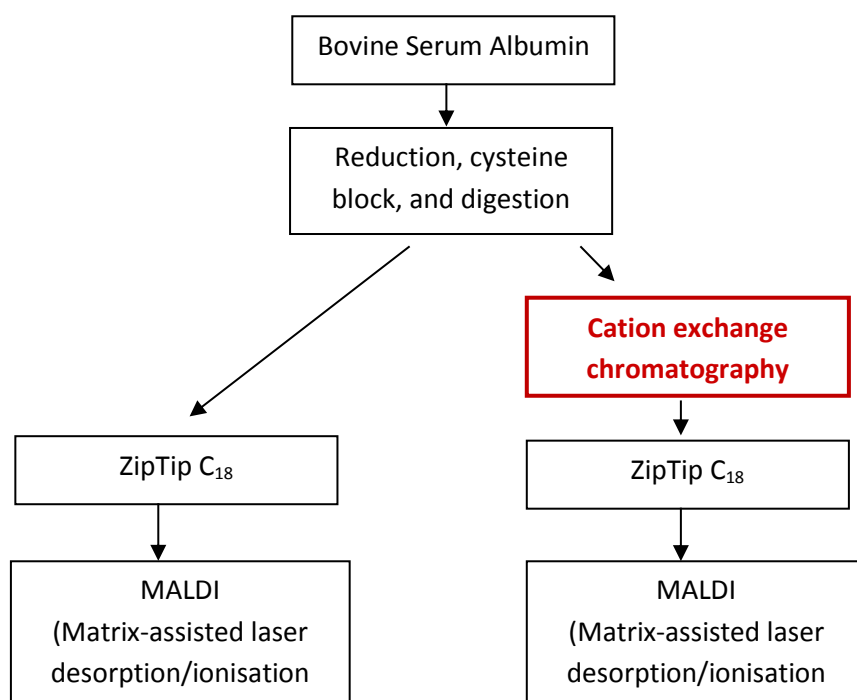
Figure 20: Sample preparation with/without cation exchange chromatrography

3.2.1a Results obtained without cation exchange chromatography

As shown on Table 6 and **Fehler! Verweisquelle konnte nicht gefunden werden.**, a large number of BSA peptides could be detected and assigned to be relevant for BSA. The total number of peptides which could be assigned to BSA based on m/z comparison of detected and expected peptides varied in samples with 5 µg BSA and 10 µg BSA.

Table 6: List of peptides resulting from BSA digestion using
5 µg BSA and 10 µg BSA without a cation exchange chromatography step.

Nb of Experiment	BSA amount (µg)	Number of peptides which can be assigned to BSA based on m/z comparison	Number of detected peptides resulting from BSA digestion
1	5	25	49
2	10	26	43
3	5	30	54
4	10	24	32

Figure 21 illustrates the reproducibility of the experiments. Peptide mass fingerprints of two independent experiments for 5 µg BSA are shown. In experiment 1 marked in blue 25 peptides can be assigned to be relevant for BSA and in experiment 3 marked in green 30 peptides.

Figure 21: Peptide mass fingerprint (PMF) of a BSA spot (5 µg)
without a cation exchange chromatography step. Experiment 1 is marked in blue and Experiment 3 is marked in green.

3.2.1b Results obtained with cation exchange chromatography

Implementing an additional cation exchange chromatography step before the reversed-phase enrichment of peptides did not improve peptide recovery, in fact a loss of peptides was observed.

Table 7 shows a list of peptides detected using a cation exchange chromatography step. The number of peptides decreased significantly compared to experiments without cation exchange chromatrophray. Cation exchange chromatography usually uses buffer substances not suitable for mass spectrometry. This can be the reason for the reduced number of detected peptides as these buffer substances very likely cause ion suppression effects reducing the number of detected peptides significantly. Additionally it has to be stated, that mass spectra of samples treated with an additional cation exchange chromatography step exhibited many background signals like polyethylene glycol and polypropylene glycol.

Table 7: List of detected peptides resulting from BSA digestion using 5 µg BSA and 10 µg BSA with a cation exchange chromatography step.

Nb of Experiment	BSA amount (µg)	Number of peptides which can be assigned to BSA based on m/z comparison	Number of detected peptides resulting from BSA digestion
1	5	20	38
2	10	25	41
3	5	20	33
4	10	22	35

As visible on Figure 22, the peptide mass fingerprint of experiment 1 marked in blue with 5 µg BSA using a cation exchange chromatography step shows only 20 peptides which can be assigned to be relevant for BSA. In experiment 3 marked in green also 20 peptides can be assigned to be relevant for BSA.
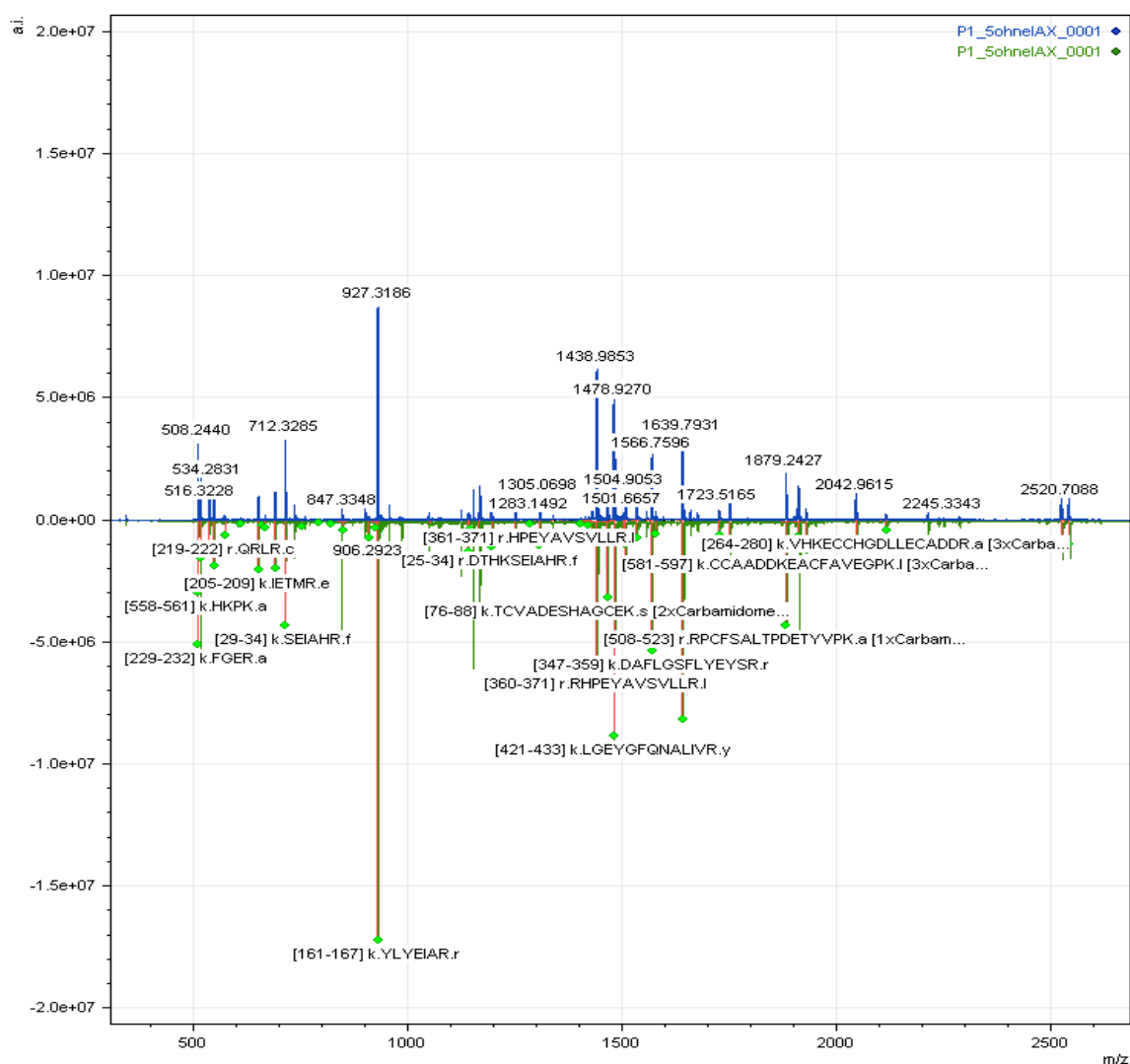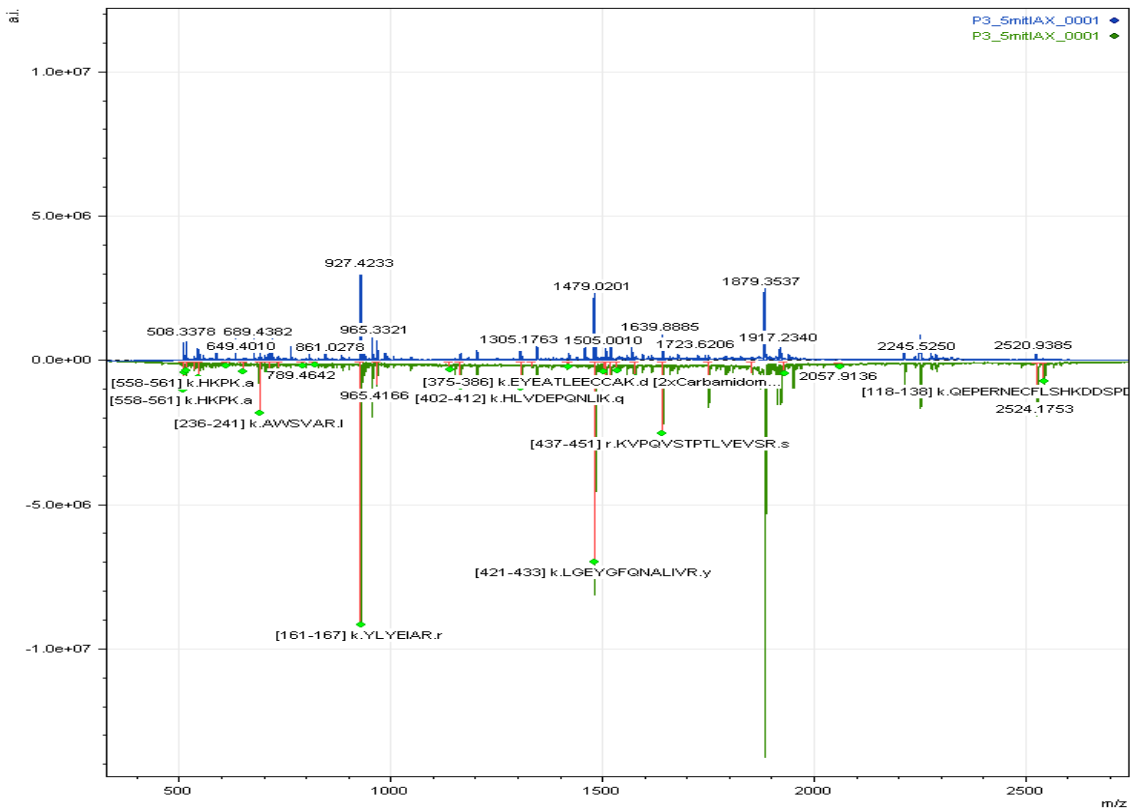
**Figure 22: Peptide mass fingerprint (PMF) of a BSA spot (5 µg)
with a cation exchange chromatography step. Experiment 1 is marked in blue and Experiment 3 is
marked in green.**

Table 8 shows an overview of all gathered results. To confirm results, experiments were performed more than once. In general it can be said, that with and without cation exchange chromatography if peptides could be assigned to BSA in the respective mass spectra the detected peptides were identical. In mass spectra obtained from experiments not implementing cation exchange chromatography, signal intensities were more intensive and even more peptides could be assigned to BSA. Interestingly it was observed that for 10 µg BSA some peptides were not detected when compared to 5 µg BSA samples. The reason for this effect is not clear at the moment but it can be assumed that this loss occurred because these signals could not be distinguished from noise signals because of their low peak intensities. Nevertheless, based on these results the use of an additional cation exchange chromatography step was omitted and a more thorough clean-up using reversed-phase enrichment was aimed for.

Table 8: Comparison of detected peptides resulting from BSA digestion without and with a cation exchange chromatography step

Nb of Experiment	Without IEC — Number of peptides which can be assigned to BSA based on m/z comparison	With IEC — Number of peptides which can be assigned to BSA based on m/z comparison	% loss trough IEC
1 (5 µg BSA)	25	20	20 %
2 (10 µg BSA)	26	25	4 %
3 (5 µg BSA)	30	20	34 %
4 (10 µg BSA)	24	22	8 %

3.2.2 Evaluation of peptide enrichment prior to a cation exchange chromatography step

However, before an eventual replacement of the cation exchange chromatography step, the influence of iTRAQ labeling prior to a cation exchange chromatography step was tested. The reason for this was to evaluate the influence of the labeling step relating to an eventual enrichment of labeled peptides prior to a cation exchange chromatography step because of the charge of the iTRAQ label.

For this, 5 µg BSA were reduced, alkylated and digested as described before (see Chapter 2.3.1), subsequently labeled with iTRAQ m/z 114 and 117 (see Chapter 2.7) and analyzed (see Chapter 2.8) using the AXIMA-TOF2. For relative quantification, to assess the reproducibility and the efficiency of the iTRAQ labeling step itself as well as the clean-up with a cation exchange chromatography the ratios of m/z 114 and m/z 117 of labeled peptides were determined in post-source decay fragment analysis.

To asses peptides actually labeled with the 114 and 117 iTRAQ label, peptide mass analysis was conducted. All observed BSA peptides were listed and compared to the theoretical masses of all expected peptides derived from a tryptic digest. Peptides not successfully labeled exhibited the m/z value which could be expected for the instrument's mass accuracy. Subtracting the theoretical molecular mass of the iTRAQ label from those peptides not yet assigned to BSA revealed all peptides successfully labeled with the respective iTRAQ label. Table 9 shows a list of iTRAQ obtained labeled BSA peptides.

Table 9: List of iTRAQ labeled BSA peptides

m/z labeled peak	m/z unlabeled peak	iTRAQ label
1072 Da	927 Da	145 Da
1624 Da	1479 Da	145 Da
2170 Da	2025 Da	145 Da

Figure 23 shows the comparison of two independent experiments for an iTRAQ labeled BSA digest. The first experiment is marked in blue and the second experiment carried out to check for reproducible results is marked in green.

It has to be mentioned, that iTRAQ labeled peptides exhibited higher intensities when compared to the corresponding unlabeled BSA peptides. This effect is possibly due to an enrichment of labeled peptides during a cation exchange chromatography. However in spectra without an iTRAQ labeling step prior to the cation exchange chromatography step more peaks could be detected especially peaks with low m/z values. The reason for this is not known but it can be assumed that the additional steps necessary for an iTRAQ labeling are responsible for the loss of peptides.
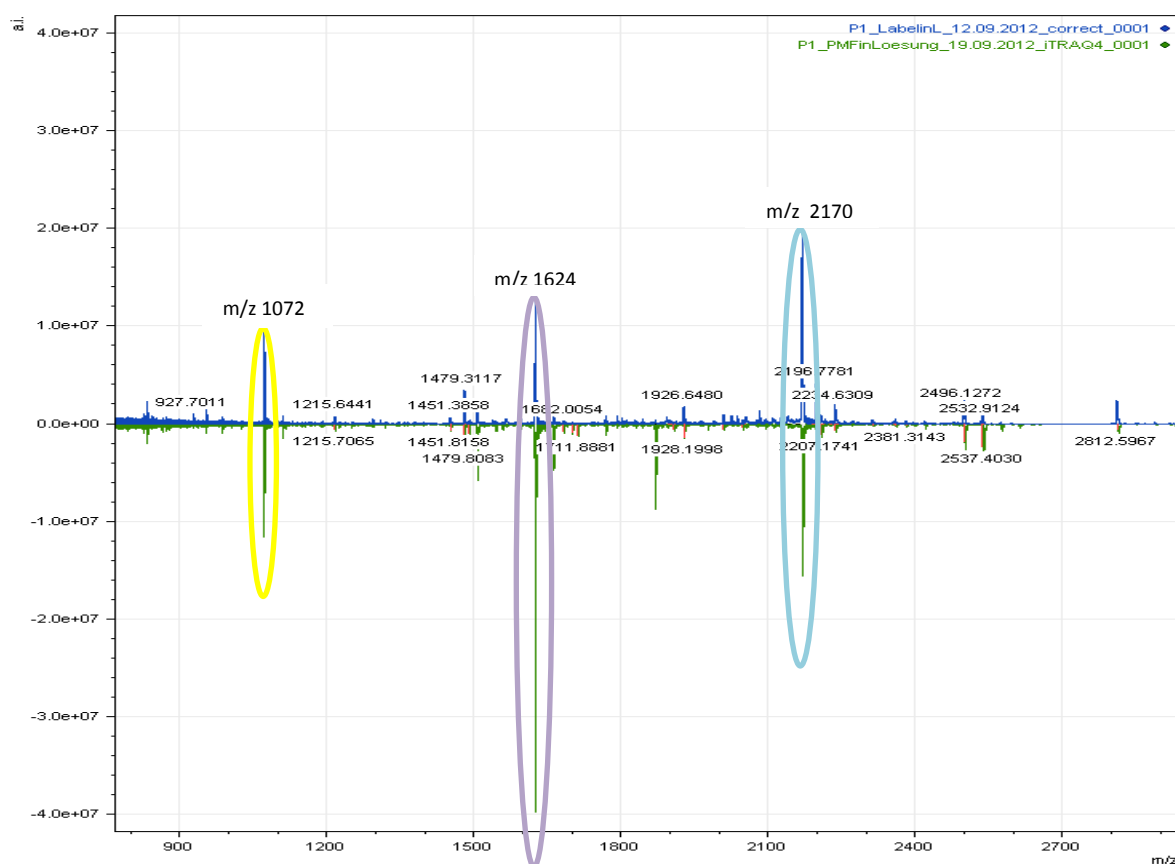
Figure 23: Peptide Mass Fingerprint of a BSA spot (5 µg) labeled with iTRAQ 114 and 117. The first experiment is marked in blue and the second experiment using equal conditions is marked in green.

For quantitative analysis the fragment ions characteristic for the respective labels have to be studied in detail. For this, a precursor ion is selected and fragmented (e.g. by post-source decay fragmentation). The isolated precursor represents in fact the mixture of isobaric peptides originating from different samples, labeled with the iTRAQ label 114 and 117 respectively. As an example of a post-source decay fragmentation of a labeled BSA peak Figure 24 shows detected reporter ions of the labeled BSA peptide with m/z 1624. The measured reporter group ratio 1.126 of label 114 and 117 shows good correlation with the expected ratio of 1. This result indicates strong evidence of a well working iTRAQ labeling step.
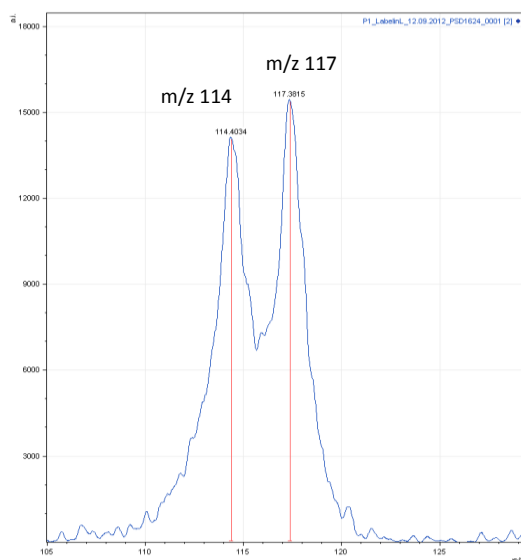
Figure 24: iTRAQ reporter group with m/z 114 and 117 of a post-source decay experiment of peptide with m/z 1624

Findings of all experiments testing the influence of a cation exchange chromatography step indicate that on the one hand an additional cation exchange chromatography step may lead to more impurities like polyethylene glycol and polypropylene glycol in the generated spectra and on the other hand a combination of an iTRAQ labeling step and a subsequent cation exchange chromatography step may lead to an enrichment of labeled peptides.

3.2.3 Development of a method fit for use with an extraction buffer used for *Exophiala dermatitidis*

The initial workflow includes a tryptic digestion after reduction and alkylation, an iTRAQ labeling step, a cation exchange chromatography step and a ZipTip C18 purification prior to MALDI-TOF-MS and PSD experiments analysis. However this workflow was regarded as not suitable for the prepared *Exophiala dermatitidis* samples, because especially the buffer constituents were not effective enough for cell lysis itself or protein pellet reconstitution after cell lysis (experiments conducted at the University of Natural Resources and Life Sciences, Vienna). To find a buffer suitable for the established iTRAQ workflow different buffer systems were tested. Changes in the workflow were tested using *Exophiala dermatitidis* samples as well as BSA samples. BSA samples were used as control because all theoretical peptides are known. *Exophiala dermatitidis* samples were chosen to evaluated if additional steps are necessary to remove disturbing substances.

The main sources of interfering substances of *Exophiala dermatitidis* samples are buffer constituents necessary to lyse the thick melanized cell walls and essential for effective protein extraction and pellet re-suspension. At the University of Natural Resources and Life Sciences, Vienna the protein extraction and pellet re-suspension was done according to Marzban Gorji et. al, 2013 [15]. The main problem was the buffer system necessary for the pellet re-suspension containing 7 M Urea, 2 M Thiourea, 4 % 3-[(3-cholamidopropyl)dimethylammonio]-1-propanesulfonate (CHAPS) and 300 mM Tris. On the one hand the most severely intereferring substance, CHAPS, is a strong detergent necessary for membrane disruption and pellet re-suspension but also interferes with MALDI MS analysis and furthermore it is difficult to remove it from a sample prior to analysis. So for DIGE analyses, the second approach for relative quantitation (not presented in this thesis), CHAPS is not a problem and the mentioned buffer system can be used. But for the iTRAQ approach an alternative buffer system had to be implemented. Therefore among the following three buffer systems, only iTRAQ experiments with buffer 1 were carried out.

Buffer 1

7 M Urea

2 M Thiourea

200 mM Triethylammonium bicarbonate (TEAB)

1 mM Ethylenediaminetetraacetic acid (EDTA)

Buffer 2:

7 M Urea

2 M Thiourea

1 % 3-[(3-cholamidopropyl)dimethylammonio]-1-propanesulfonate (CHAPS)

1 mM Ethylenediaminetetraacetic acid (EDTA)

Buffer 3:

7 M Urea

2 M Thiourea

1 % 3-[(3-cholamidopropyl)dimethylammonio]-1-propanesulfonate (CHAPS)

200 mM Triethylammonium bicarbonate (TEAB)

1 mM Ethylenediaminetetraacetic acid (EDTA)

To reach buffer concentrations tolerable for tryptic in solution digestion for a relative quantitation using iTRAQ labeling, samples had to be diluted with 0.5 M triethylammonium bicarbonate and 1 mM $CaCl_2$ to reduce the urea concentration to less than 0.6 M according to Ping Lan et al, 2011 [78]. Figure 25 shows the workflow for *Exophiala dermatitidis* samples. 25 µg total protein extract (measured at at the University of Natural Resources and Life Sciences using Bradford protein assay) was reduced, alkylated, diluted with 0.5 M triethylammonium bicarbonate and 1 mM $CaCl_2$, digested, desalted using HyperSep™ C18 solid phase columns and labeled with iTRAQ reagents.

Trypsin digestion

Trypsin digestion

HyperSep C18 Reversed Phase Chromatography

HyperSep C18 Reversed Phase Chromatography

Label with an iTRAQ reagent

Label with an iTRAQ reagent

Combination of labeled samples into one sample mixture
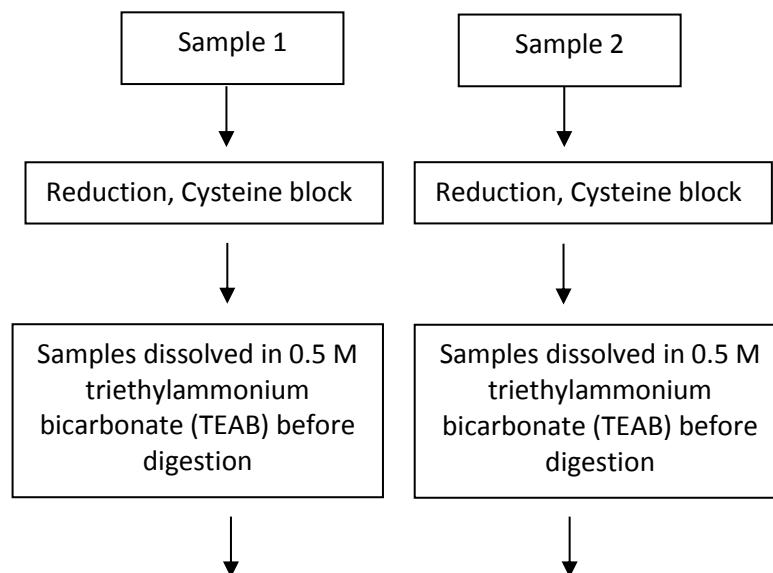
Figure 25: Initial workflow for *Exophiala dermatitidis* samples

Interestingly we observed that by implementing this workflow the samples became a brownish, sticky residue/solution after drying the supposedly derived iTRAQ labeled peptides. Mass spectrometric analysis was therefore not possible for these samples.

3.2.4 Evaluation of various clean-up steps for a method fit for use with *Exophiala dermatitidis* samples

Skipping the drying process and combining the labeled samples without drying, followed by the cation exchange and reversed-phase cleaned-up showed after MS analysis that an extensive amount of sample was lost. To detect sample loss, samples were measured by MS analysis before and after the cation exchange chromatography step. For this 25 µg respectively 50 µg BSA were reduced, alkylated, diluted by 0.5 M triethylammonium bicarbonate and 1 mM $CaCl_2$, digested, desalted using HyperSep™ C18 solid phase columns and labeled with iTRAQ reagents. Samples were measured by MS analysis before and after the following cation exchange chromatography step. In the sample with 25 µg BSA eight BSA peptides could be found prior to the cation exchange and in the samples with 50 µg BSA 12 BSA peptides could be detected. After the cation exchange chromatography step no BSA peptides and two eventually labeled BSA peptides could be detected. The reason for this effect is

not known but it can be assumed that either peptides remained in the columns or were lost in the flow through of the cation exchange chromatography. To evaluate also the influence of iTRAQ labeling on cation exchange chromatography a second experiment was carried out using unlabeled BSA samples. Using the same condition as in the previous experiment, after the cation exchange chromatography step 15 BSA peptides respectively 19 BSA peptides could be detected. These findings indicate a possible interference of an iTRAQ labeling step and a cation exchange chromatography step and therefore this introduced clean-up step had to be replaced by an alternative cleaning step.

To find an alternative method, experiments were carried out using a HyperSep™ C18 reversed-phase chromatography. To assess sample preparation with respect to peptide loss the HyperSep™ C18 reversed-phase chromatography step was evaluated. For standardization this experiment was not only carried out for the fungal samples but also for the BSA digest. Replacing the cation exchange chromatography step with a second HyperSep™ C18 reversed-phase chromatography step showed the following results: using the same conditions as in the previous experiments labeled BSA samples were analyzed. MS analysis of samples after the second HyperSep™ C18 reversed-phase chromatography step showed 15 BSA peptides as well as five eventually labeled BSA peptides. Further PSD analysis could show that the BSA peptides with m/z 1624 and 1928 were iTRAQ labeled.

After the evaluation experiments of various clean-up steps the following protocol for *Exophiala dermatitidis* samples could be established.

3.2.5   Established iTRAQ protocol for *Exophiala dermatitidis* samples

The initial workflow shown on Figure 25 was modified as follows: Total protein (25 µg) was reduced, alkylated, diluted by 0.5 M triethylammonium bicarbonate and 1 mM $CaCl_2$, digested, desalted using HyperSep™ C18 solid phase co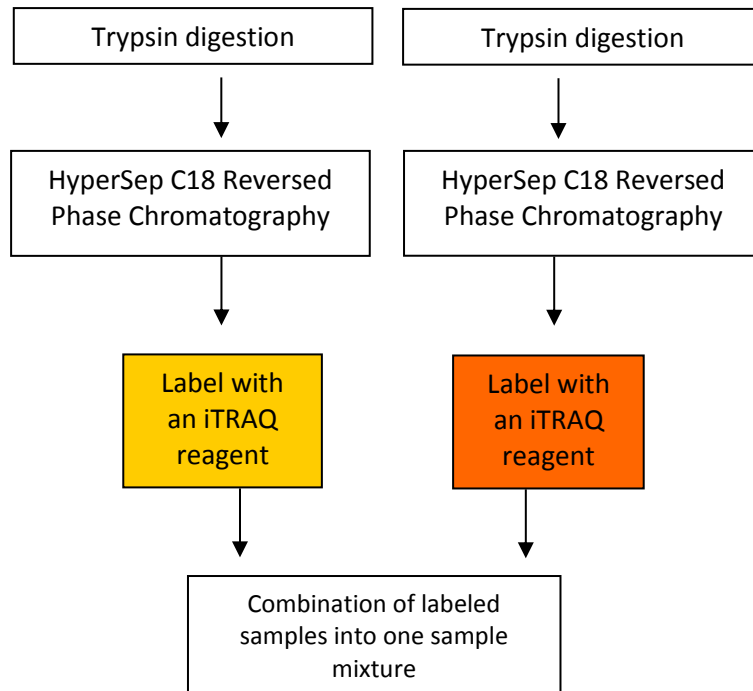lumns and labeled with iTRAQ reagents. After the combining the labeled samples the mixture was cleaned up using HyperSep™ C18 solid phase columns. Purified samples were mixed with the MALDI matrix α-cyano-4-hydroxycinnamic acid (2-3 mg/mL 0.1% trifluoroacetic acid: acetonitrile ratio 1: 1), ratio of 1: 1, and immediately spotted on an anchor chip target. Finally MALDI analysis was carried out. Peptide mass fingerprint (PMF) analysis as well as post-source decay (PSD) fragment analysis was performed in the reflectron mode on the MALDI mass spectrometer UltrafleXtreme.

3.2.6 Statistical evaluation of the established iTRAQ workflow for *Exophiala dermatitidis* samples

For statistical evaluation of particular steps as well as the overall established workflow BSA was used. As shown on Figure 26, the labeling step, the clean-up step and the digest procedure including the labeling step were separately evaluated. Additionally the dynamic range for relative quantitation was studied by using samples with a high concentration variation. For statistical evaluation iTRAQ label 114 and 117 were used to produce mass spectrometric data for BSA concentration ratios of 1:1, 1:2 and 2:1. Measured m/z 114 to 117 ratios were plotted over the concentration ratios. To generate reliable values for data evaluation the analysis was carried out in triplicates.
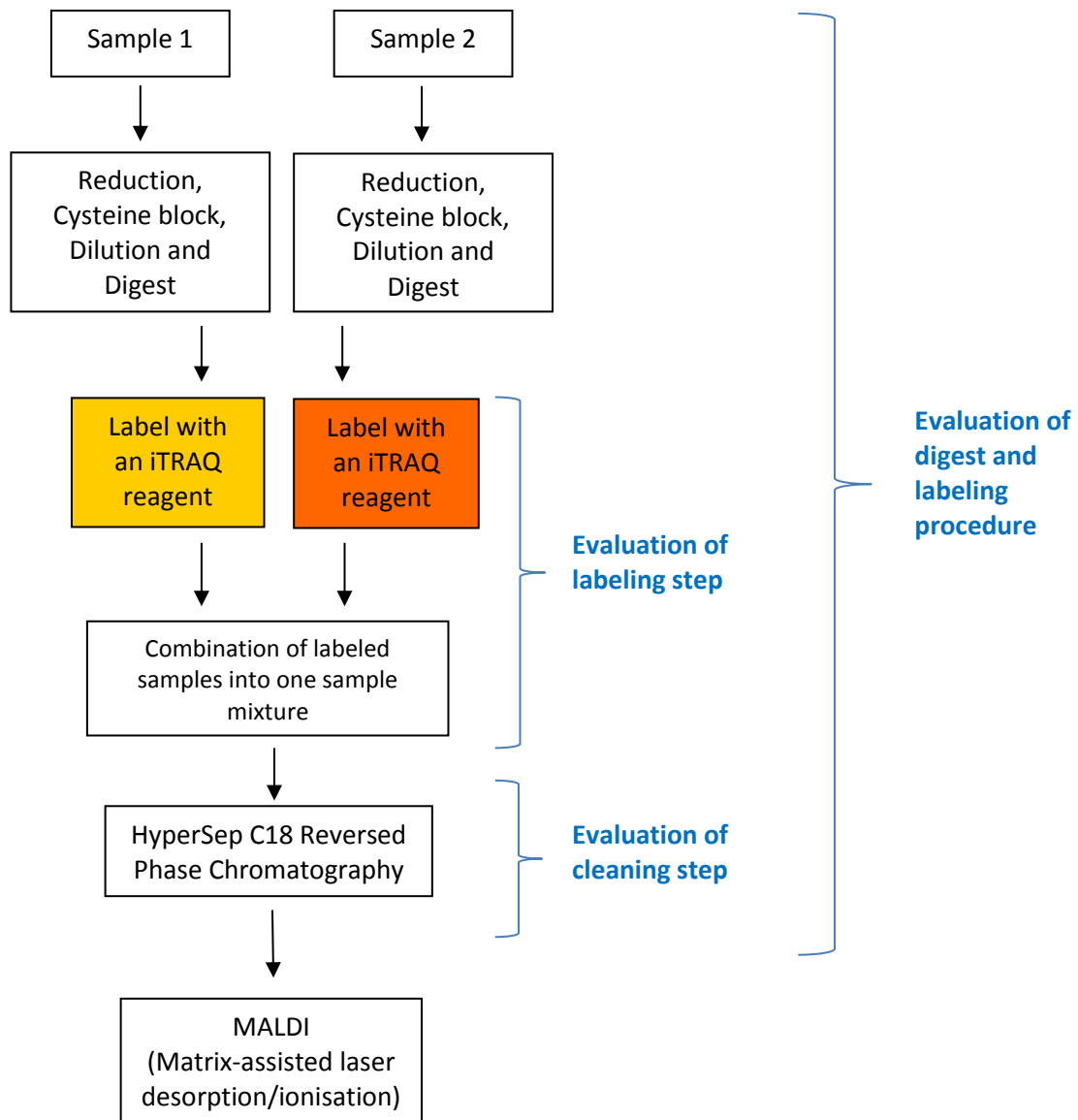
Figure 26: Established workflow for *Exophiala dermatitidis* samples

3.2.6a Evaluation of suitable peptides for statistical evaluation of the established iTRAQ workflow

Prior to statistical evaluation of the established iTRAQ protocol it was necessary to find out which of the experimentally obtained peptides of nine independent tryptic BSA digests are suitable for data analysis. For this at first all obtained peptides were listed as shown in column 1 in Table 10. To get an idea of peptide masses of labeled BSA peptides, a theoretical BSA digestion was carried out followed by an addition of the iTRAQ label with m/z 145. In this way 54 expected peptides for a BSA digestion could be obtained. Received theoretical BSA peptides carrying an iTRAQ label with m/z 145 are shown in column 2 on Table 10. Peptides with m/z 1072, 1624 Da and 1713 encircled in red could be detected in all independent experiments. Therefore for evaluation of the various method steps these three mentioned peptides were used. It has to be stated that peptides with m/z values smaller than 1000 Dalton were excluded because for peptides with low m/z values it is more likely that they belong to different proteins and therefore it is better to use peptides with higher masses to assure higher significance of results.

Table 10: Recovery rate of theoretical labeled BSA peptides;
m/z values smaller than 1000 Dalton excluded

Peptide mass	Inkl. label (m/z 145)	Digest 1_l1	Digest 1_l2	Digest 1_l3	Digest 2_l1	Digest 2_l2	Digest 2_l3	Digest 3_l1	Digest 3_l2	Digest 3_l3
2435,2427	2580,2427	-	-	+	-	-	-	-	-	-
1955,9596	2100,9596	-	-	-	-	-	-	-	-	-
1888,9268	2033,9268	-	-	-	-	-	-	+	+	-
1850,8993	1995,8993	-	-	-	-	-	-	-	-	-
1823,8996	1968,8996	+	-	-	-	-	+	-	-	-
1667,8131	1812,8131	-	-	-	-	-	-	-	-	-
1633,6621	1778,6621	+	-	-	-	-	-	+	-	-
1578,5981	1723,5981	-	-	+	-	-	-	-	-	-
1567,7427	1712,7427	+	+	+	+	+	+	+	+	+
1519,7461	1664,7461	+	-	-	-	-	-	-	-	-
1511,8427	1656,8427	-	-	-	+	-	-	-	-	-
1497,6314	1642,6314	-	-	+	-	-	-	-	-	-
1479,7954	1624,7954	+	+	+	+	+	+	+	+	+
1399,6926	1544,6926	-	-	-	-	-	-	+	-	-
1388,5708	1533,5708	-	-	-	-	-	-	-	-	-
1386,6206	1531,6206	-	-	-	-	-	-	+	-	-
1364,4803	1509,4803	-	-	-	+	-	-	-	-	-
1362,6722	1507,6722	-	-	+	-	-	-	+	-	-
1349,546	1494,546	-	-	-	-	-	-	-	-	+
1305,7161	1450,7161	-	-	+	+	+	+	+	+	+
1283,7106	1428,7106	-	-	-	-	-	-	-	-	-

72

1177,5591	1322,5591	-	+	-	+	+	+	-	+	-
1163,6306	1308,6306	-	-	+	+	+	+	-	-	+
1052,4499	1197,4499	-	-	-	-	-	+	+	+	-
1050,4924	1195,4924	-	+	+	+	+	+	-	+	+
1024,455	1169,455	-	-	-	-	-	+	-	-	-
1015,4877	1160,4877	-	-	-	+	+	+	-	+	+
1014,6193	1159,6193	-	-	+	+	-	-	-	-	+
1011,42	1156,42	-	-	-	-	-	-	-	-	-
1002,583	1147,583	-	-	-	-	-	-	-	-	-
977,4509	1122,4509	-	-	-	-	-	-	-	-	-
974,4577	1119,4577	-	-	-	-	-	-	-	-	-
927,4934	1072,4934	+	+	+	+	+	+	+	+	+
922,488	1067,488	-	-	-	-	-	-	-	-	-
886,4152	1031,4152	-	-	-	-	-	-	-	-	-
841,46	986,46	-	-	-	-	-	-	-	-	-
818,4254	963,4254	-	-	-	+	-	+	-	-	-
789,4716	934,4716	-	-	-	-	-	-	-	-	-
752,3573	897,3573	+	+	+	+	+	+	-	+	+
725,2593	870,2593	-	-	-	-	-	-	-	-	-
712,3736	857,3736	+	-	-	-	+	+	-	-	+
703,4097	848,4097	+	-	-	-	-	-	-	-	-
701,4014	846,4014	-	-	-	-	-	-	-	-	-
689,3729	834,3729	+	+	+	+	+	-	+	+	+
660,3563	805,3563	-	-	-	-	-	-	-	-	-
658,3155	803,3155	-	-	+	-	-	-	-	-	-
649,3338	794,3338	+	+	-	+	+	+	-	+	+
609,2878	754,2878	-	-	-	-	-	-	-	-	-
545,3405	690,3405	+	+	-	+	+	+	-	-	-
537,282	682,282	-	-	-	-	-	-	-	-	-
517,298	662,298	-	-	-	-	-	-	-	-	-
509,3194	654,3194	-	-	-	-	-	-	-	-	-
508,2514	653,2514	+	+	+	+	+	+	+	+	+
500,2463	645,2463	-	-	-	-	-	-	-	-	-

3.2.6b Evaluation of the labeling step of relative quantitation using iTRAQ

The aim of this evaluation analysis was to detect possible variation of the labeling step within the established workflow. For this 100 µg protein were reduced, alkylated, digested and desalted using HyperSep™ C18 solid phase columns. Eluted peptides were subsequently split in six equal 10 µg protein parts and separately labeled with iTRAQ m/z 114 and iTRAQ m/z 117. Labeled peptides were mixed in the ratios 1:1, 1:2 and 2:1. In this way for each ratio three independent experimental data can be achieved guaranteeing a detection of a possible labeling step variation. After a second reversed-phase clean-up the peptides were measured by MALDI-TOF-MS and PSD experiments.

Figure 27: Various concentrations of BSA labeled with iTRAQ label 114 and 117. The reported ratios are in all cases relative to the reporter ion 114.

As shown on Figure 27 the expected ratios of 1:1 and 1:2 are within the calculated standard deviation. Ratio 2:1 is a little bit lower than the expected value but still in a relatively good range. Reproducible data achieved with this experiment show no significant variation of the labeling step within the established method.

3.2.6c Evaluation of the clean-up step of relative quantitation using iTRAQ

As not only the labeling of the samples is a crucial step within the established workflow, also the clean-up step had to be evaluated relating to any possible variation. To determine the influence of different amounts of protein cleaned-up using reversed-phase chromatography, experiments with 4 µg and 60 µg protein were carried out. Following the established workflow total protein was reduced, alkylated, digested, desalted using HyperSep™ C18 solid phase columns and separately labeled with iTRAQ m/z 115 respectively m/z 116. Before the second reversed-phase clean-up step labeled peptides were mixed and then split in equal parts. Each labeled part was separately cleaned-up using HyperSep™ C18 solid phase columns. In this way a possible variation within the clean-up step could be detected. As already described to test also the influence of varied protein amounts, the

HyperSep™ C18 step was carried out using 4 µg as well as 60 µg total protein. Subsequently cleaned-up peptides were measured by MALDI-TOF-MS and PSD experiments.
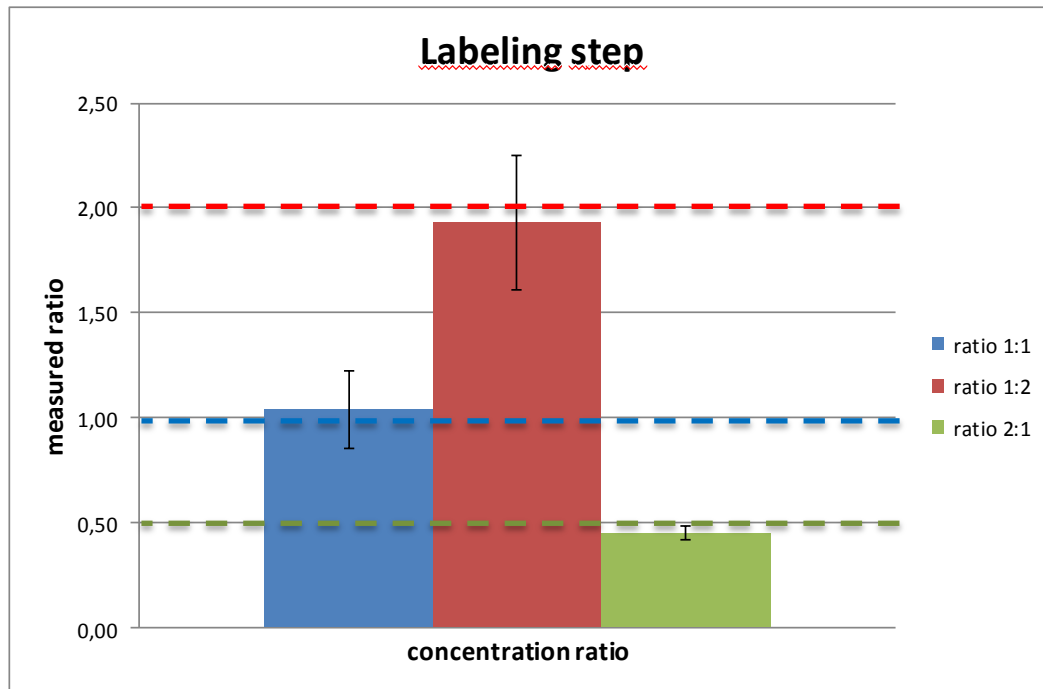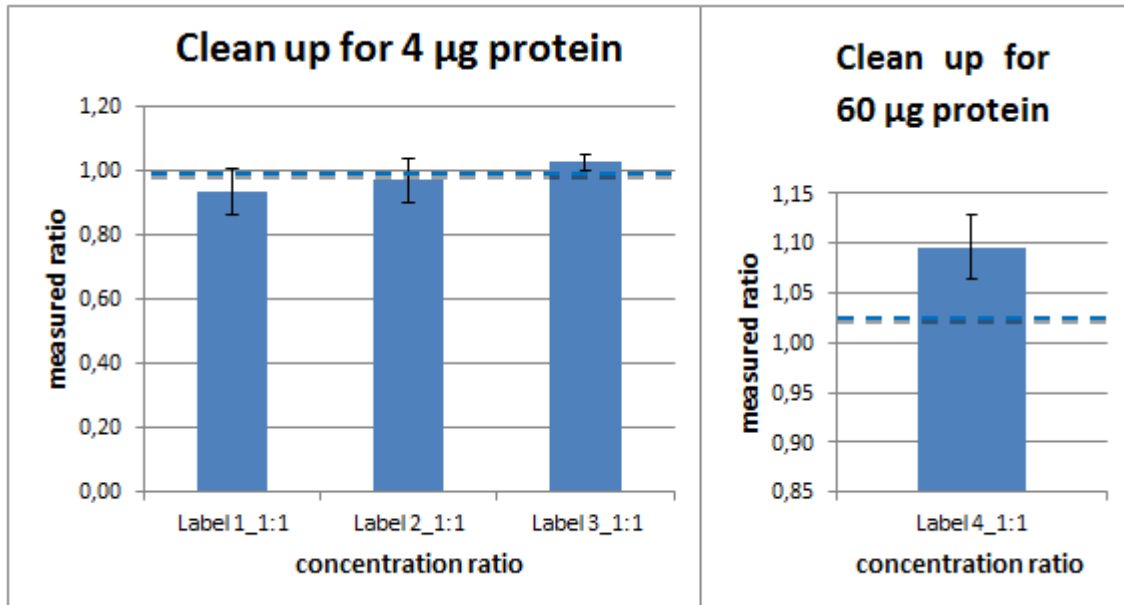

Figure 28: Various concentrations of BSA labeled with iTRAQ label 115 and 116 in a 1:1 ratio. The reported ratios are in all cases relative to the reporter ion 115.

Figure 28 shows that in experiments with lower protein amounts better results could be achieved. Therefore the use of low protein amounts may prevent from high errors originating from the clean-up step.

3.2.6d Evaluation of the digest and the labeling step of relative quantitation using iTRAQ

To get information about possible variation of the overall workflow, three independent digestions had to be analyzed. In this way it can be approved that the established workflow is not influenced by any variation at all. For evaluation of the overall digestion including the labeling step and the clean-up step total protein was first split in three 100 µg protein parts. Each part was reduced, alkylated, digested, desalted using HyperSep™ C18 solid phase columns and separately labeled with iTRAQ m/z 114 respectively m/z 117. Subsequently labeled peptides were mixed in the ratios 1:1, 1:2 and 2:1. After a second reversed-phase clean-up the peptides were measured by MALDI-TOF-MS and PSD experiments.

Figure 29: Overall ratios calculated from all executed evaluation steps. The reported ratios are in all cases relative to the reporter ion with the lower m/z value.

Figure 29 shows that on the one hand the measured 1:2 ratio is in all cases higher than the expected ratio and on the other hand the 2:1 ratios are lower than the expected ratio, but nevertheless all ratios are in a good range. As the measured 1:2 and 2:1 ratios shows in all three independent experiments similar values, the workflow seems to be almost unaffected by any variation. The higher respectively lower measured values compared to the calculated values is eventually occurred due to inaccurate sample preparation.

3.2.6e Influence of a high BSA concentration ratio variation on relative quantitation using iTRAQ

As also the influence of various BSA concentrations is important for a good working protocol, experiments using different amounts of BSA were carried out to show if any variations can be detected. For this 200 µg protein were reduced, alkylated, digested, desalted using HyperSep™ C18 solid phase columns and separately labeled with iTRAQ m/z 114 respectively iTRAQ m/z 117. Subsequently labeled peptides were mixed in the ratio 1:50. After a second reversed-phase clean-up the peptides were measured by MALDI-TOF-MS and PSD experiments.
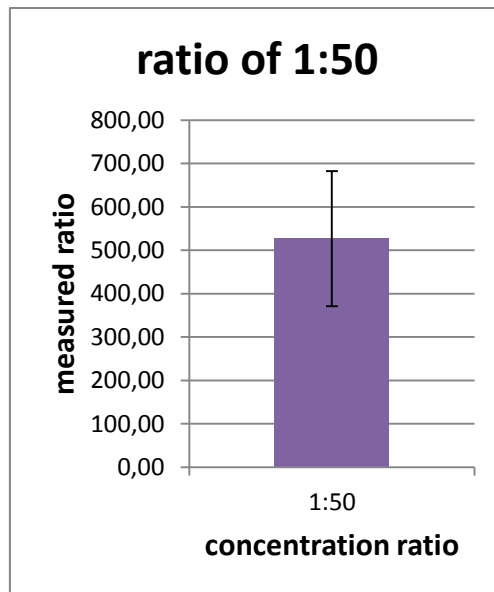
Figure 30: BSA labeled with iTRAQ label 114 and 117 in a 1:50 ratio.
The reported ratio is relative to the reporter ion 114.

As shown on Figure 30 the expected ratio of 1:50 could not be reached at all. Possible explanations could be the dynamic range for detection and fragmentation of peptides (4 pmol on target) or a high clean-up step bias.

3.2.6f Evaluation of the overall established workflow of relative quantitation using iTRAQ

Figure 31 shows the evaluation of calculated ratios of all executed evaluation steps. As visible on this chart the measured 1:2 ratio is higher than the expected value and the 2:1 lower than the expected value, but all ratios are anyway in a good range. In general, the findings of all statistically evaluated steps showed strong evidence of a well working iTRAQ labeling protocol.
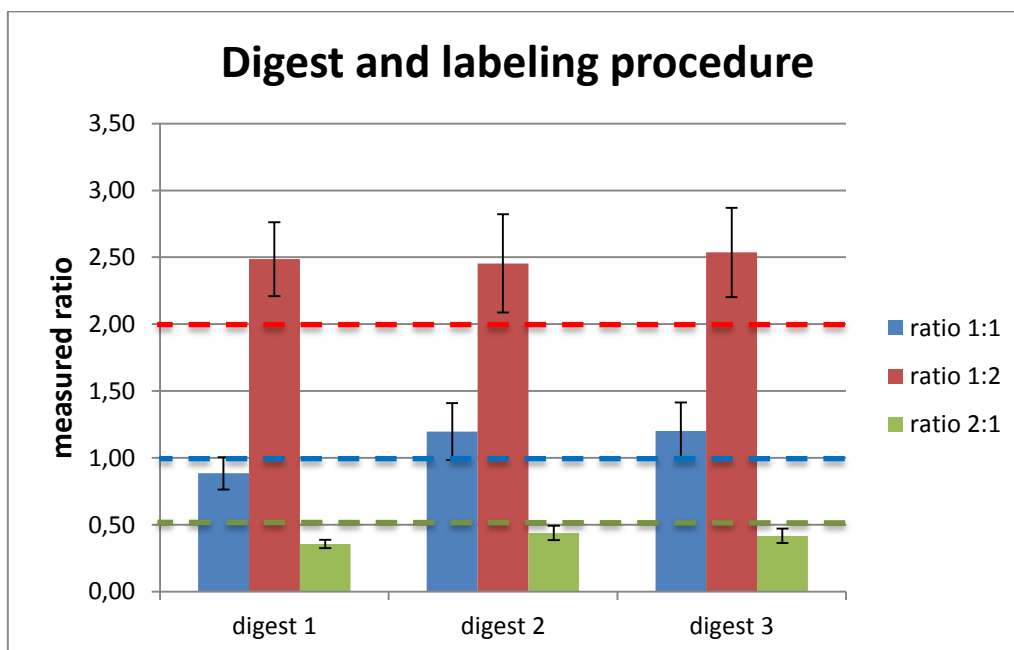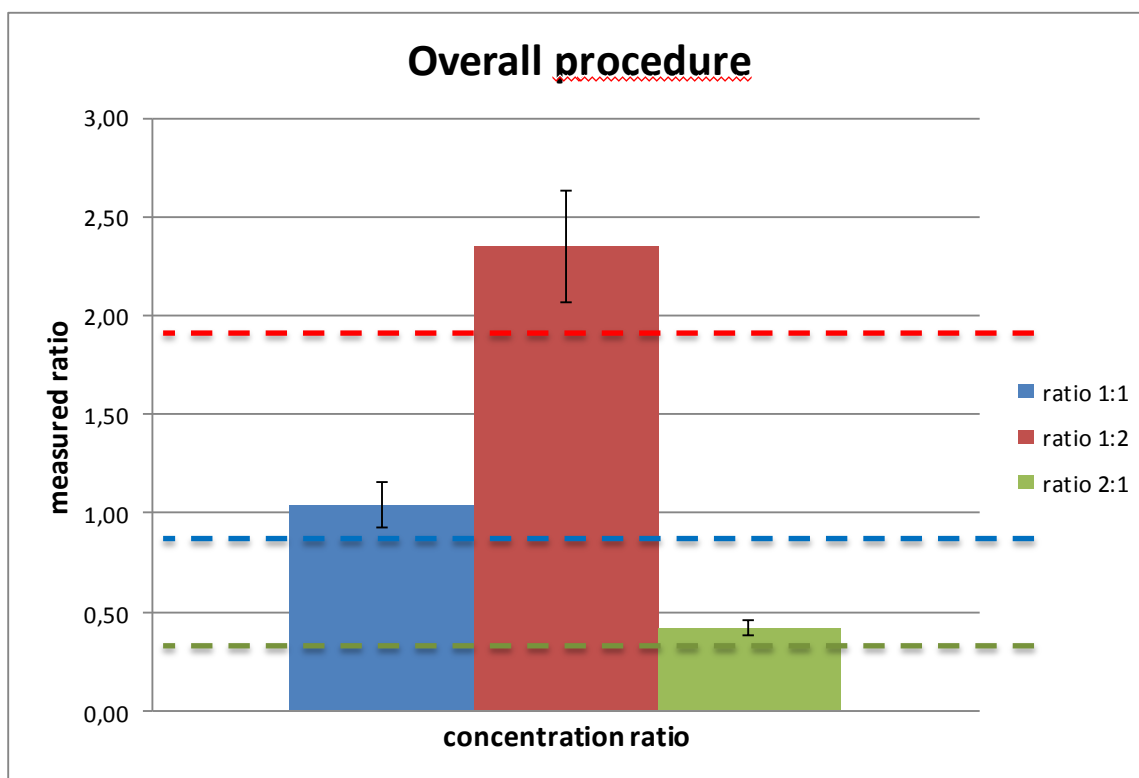

Figure 31: Overall ratios calculated from all executed evaluation steps. The reported ratios are in all cases relative to the reporter ion with the lower m/z value.

3.3   Quantitative protein analysis of *Exophiala dermatitidis* samples

3.3.1   Exophiala dermatitidis samples

To evaluate the established relative protein quantitation method on complex biological samples iTRAQ experiments with *Exophiala dermatitidis* samples were processed. As shown on Table 11 five different conditions in four replicates of *Exophiala dermatitidis* samples were tested. Protein extraction was carried out according to Donatella Tesei et al., 2012 [14] at the University of Natural Resources and Life Sciences, Vienna.

Table 11: *Exophiala dermatitidis* samples, five different conditions in four replicates

ID	Sample name	Protein amount [µg]	Volume [µL]	Concentration [µg/µL]
Condition 1a	E.d. 37°C 8weeks tube 1 TU	430.0	268.8	1.60
Condition 1b	E.d. 37°C 8weeks tube 2 TU	265.0	265.0	1.00
Condition 1c	E.d. 37°C 8weeks tube 3 TU	512.5	269.7	1.90
Condition 1d	E.d. 37°C 8weeks tube 4 TU	366.7	267.7	1.37
Condition 2a	E.d. 1°C 1week tube 1 TU	309.0	266.4	1.16
Condition 2b	E.d. 1°C 1week tube 2 TU	281.5	265.6	1.06
Condition 2c	E.d. 1°C 1week tube 3 TU	265.0	265.0	1.00
Condition 2d	E.d. 1°C 1week tube 4 TU	402.5	268.3	1.50
Condition 3a	E.d. 1°C 1hour tube 1 TU	325.5	266.8	1.22
Condition 3b	E.d. 1°C 1hour tube 2 TU	449.2	269.0	1.67
Condition 3c	E.d. 1°C 1hour tube 3 TU	325.5	266.8	1.22
Condition 3d	E.d. 1°C 1hour tube 4 TU	273.2	265.3	1.03
Condition 4a	E.d. 45°C 1week tube 1 TU	336.5	267.1	1.26
Condition 4b	E.d. 45°C 1week tube 2 TU	375.0	267.9	1.40
Condition 4c	E.d. 45°C 1week tube 3 TU	430.0	268.8	1.60
Condition 4d	E.d. 45°C 1week tube 4 TU	402.5	268.3	1.50
Condition 5a	E.d. 45°C 1hour tube 1 TU	457.5	269.1	1.70

Condition 5b	E.d. 45°C 1hour tube 2 TU	430.0	268.8	1.60
Condition 5c	E.d. 45°C 1hour tube 3 TU	300.7	266.2	1.13
Condition 5d	E.d. 45°C 1hour tube 4 TU	265.0	265.0	1.00

3.3.2 Experimental Design

At first a suitable design of experiments was necessary to get reproducible data. To get labeling ratios of biological as well as technical replicates the design of experiments was set up according to Table 12. To avoid an eventual influence of the four different used iTRAQ labels, samples treated under equal conditions were labeled with either iTRAQ 114, 115, 116 or 117. This label-swap is necessary to get results that are independent from the possible influence of a particular iTRAQ label. This label-swap as well as the use of four biological replicates of each condition is the basis to obtain reproducible data. Experiments shown on Table 12 should give information of possible up- or down-regulation patterns of peptides under different conditions.

The four independent experiments were processed as described in Chapter 3.2.5 Established iTRAQ protocol for *Exophiala dermatitidis* samples. The iTRAQ labeling step was done with iTRAQ label m/z 114, iTRAQ m/z 115, iTRAQ m/z 116 and iTRAQ m/z 117.

Table 12: Design of experiments

Experiment 1: Comparison of Condition 1, Condition 2, Condition 3, Condition 4 — Experiment 1

ID	iTRAQ label	ID	iTRAQ label	ID	iTRAQ label	ID	iTRAQ label	
Condition 1a	114	Condition 2a	115	Condition 3a	116	Condition 4a	117	A
Condition 1b	117	Condition 2b	116	Condition 3b	115	Condition 4b	114	B
Condition 1c	116	Condition 2c	117	Condition 3c	114	Condition 4c	115	C

Experiment 2: Comparison of Condition 1, Condition 2, Condition 3, Condition 5 — Experiment 2

ID	iTRAQ label	ID	iTRAQ label	ID	iTRAQ label	ID	iTRAQ label	
Condition 1a	114	Condition 2a	115	Condition 3a	116	Condition 5a	117	A
Condition 1b	117	Condition 2b	116	Condition 3b	115	Condition 5b	114	B
Condition 1c	116	Condition 2c	117	Condition 3c	114	Condition 5c	115	C

Experiment 3: Comparison of Condition 1, Condition 2, Condition 3, Condition 4 — Experiment 3

ID	iTRAQ label	ID	iTRAQ label	ID	iTRAQ label	ID	iTRAQ label	
Condition 1d	114	Condition 2d	115	Condition 3d	116	Condition 4d	117	A
Condition 1a	117	Condition 2a	116	Condition 3a	115	Condition 4a	114	B
Condition 1b	116	Condition 2b	117	Condition 3b	114	Condition 4b	115	C

Experiment 4: Comparison of Condition 1, Condition 2, Condition 3, Condition 5 — Experiment 4

ID	iTRAQ label	ID	iTRAQ label	ID	iTRAQ label	ID	iTRAQ label	
Condition 1d	114	Condition 2d	115	Condition 3d	116	Condition 5d	117	A
Condition 1a	117	Condition 2a	116	Condition 3a	115	Condition 5a	114	B
Condition 1b	116	Condition 2b	117	Condition 3b	114	Condition 5b	115	C

3.3.3 Biological replicates

To detect biological reproducibility by means of the received labeling ratios Table 13 shows an overview of executed experiments. Ratios of conditions encircled in red, green or blue were calculated relative to condition 1 (*Exophiala dermatitidis* CBS 525.76; 37 °C; 8 weeks).

Table 13: Experimental design for biological replicates

At first, peptides of each experiment (e.g. experiment 1A, 1B, 1C) were listed. Post-source decay fragment analysis spectra of peptides with identical m/z values within one independent experiment were compared. Peptides with comparable fragment patterns were used for statistical evaluation of labeling ratios. To highlight some results of executed experiments, Figure 32 shows four calculated ratios of experiment 3. Due to bad peak intensities of obtained spectra, analysis proved to be difficult for *Exophiala dermatitidis.* Insufficient peak intensities led to unfavourable database search results and consequently no identification could be achieved. Therefore obtained peptides could not be assigned to a particular protein. This fact made it impossible to draw conclusions from these four mentioned peptides to a possible up-or down regulation pattern of certain proteins. The ratios of each peptide had to be calculated separately. Peptides with m/z 1657 and m/z 1705 show similar up- and down regulation patterns. Peptides with m/z 1711 and m/z 1763 also show similar patterns. As

detected peptides of all executed experiments could not be significantly identified, the findings should only be regarded as a hypothesis of a possible up- or down regulation of proteins. Detailed information of all received ratios are provided in a separate excel sheet on a DVD-ROM as additional material.
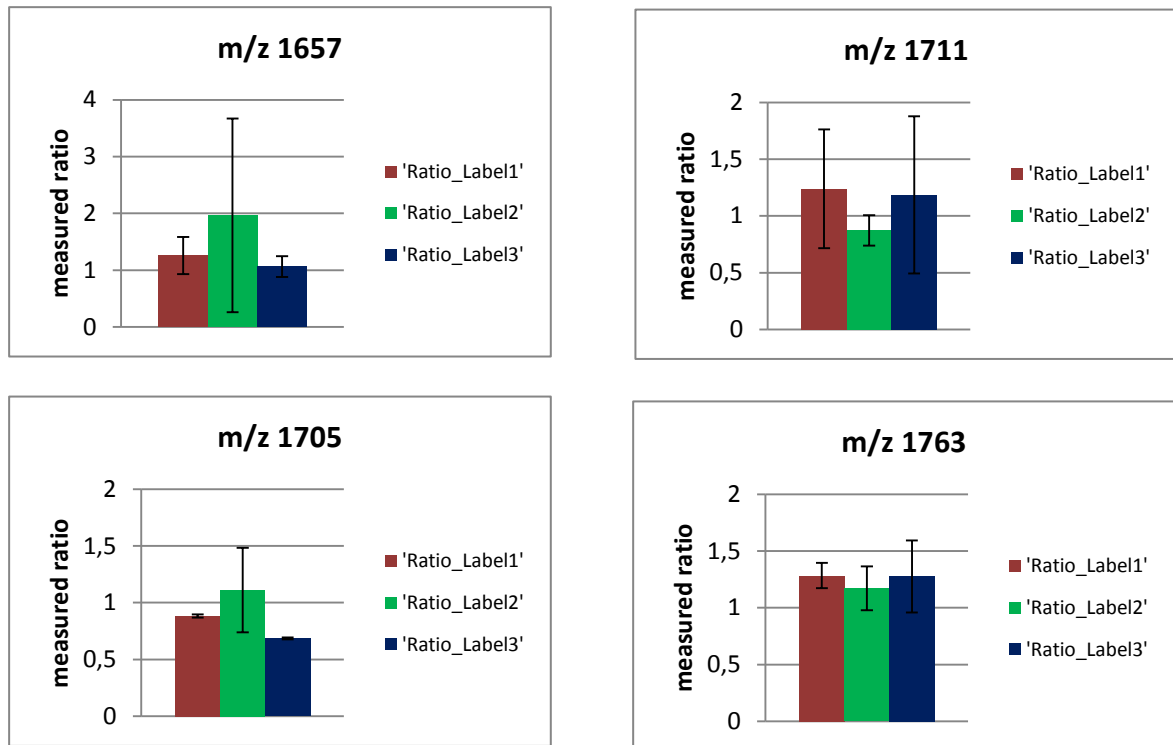
Figure 32: Labeling ratios of peptides with m/z 1657, 1705, 1711 and 1763 of experiment 3. The reported ratios are in all cases relative to condition 1 (*Exophiala dermatitidis* CBS 525.76; 37 °C; 8 weeks).

3.3.4 Technical replicates

In comparison to the studies performed for BSA the technical reproducibility was also assessed for fungal samples. The calculated labeling ratios are shown in Table 14 giving an overview of executed experiments. To get data that are independent from a possible label influence like improved labeling efficiency using a particular label or improved detection of a particular label, biological replicates were labeled with either iTRAQ 114, 115, 116 or 117.

Ratios of condition 2 and 3 were calculated relative to condition 1 (*Exophiala dermatitidis* CBS 525.76; 37 °C; 8 weeks). At first, ratios of experiment 1 and 2 as well as ratios of experiment 3 and 4 were calculated, and then ratios of all executed experiments were determined.

Table 14: Experimental design for technical replicates

At first, peptides of each experiment (e.g. experiment 1A, 1B, 1C) were listed. Post-source decay fragment analysis spectra of peptides with identical m/z values within one independent experiment were compared. Peptides with comparable fragment patterns were used for statistical evaluation of labeling ratios. Unfortunately within all experiments only the ratio of one peptide with m/z 1274 as shown on Figure 33 could be used for statistical evaluation. As no significant identification of this peptide could be obtained, the up- or down regulation pattern should only be regarded as a hypothesis. Detailed information of all received ratios are provided in an excel sheet.
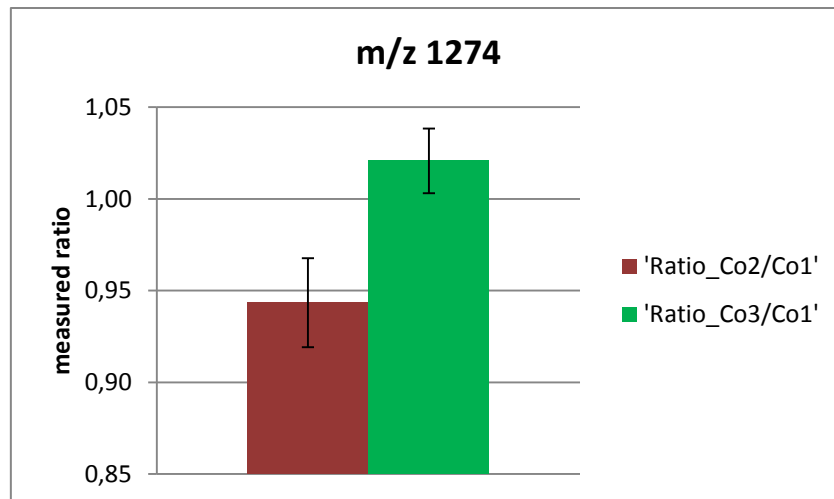
Figure 33: Labeling ratio of peptide with m/z 1274.
The reported ratio is relative to condition 1 (*Exophiala dermatitidis* CBS 525.76; 37 °C; 8 weeks).

3.3.5   Exophiala dermatitidis sample results compared to BSA results

Basically measured ratios of experiments using BSA showed relative good correlation with the calculated labeling ratio. The average measured value of the 1:1 ratio of all executed experiments was 1.04 with a standard deviation of 0.12, the average measured value of the 1:2 ratio 2.35 with a standard deviation of 0.28 and the average measured value of the 2:1 ratio 0.42 with a standard deviation of 0.04. Compared to these results obtained using BSA samples, results of *Exophiala dermatitidis* samples showed in general a higher variation. Bad peak intensities of *Exophiala dermatitidis* samples resulted in a lack of data suitable for statistical evaluation. As no significant identification of peptides could be obtained, a possible up- or down regulation of analyzed peptides can only be regarded as a hypothesis.

In summary, it can be stated that findings of quantitative protein analysis of *Exophiala dermatitidis* samples proved to be difficult to interpret as obtained peptides could not be significantly identified. Possible up- or down regulation patterns of proteins can only be regarded as a hypothesis without any significance. In general low intensity signals of reporter groups made statistical evaluations difficult. Further experiments using for example liquid chromatography (LC) prior to MALDI MS analysis may lead to an improvement of signal intensities.

3.4   Protein identification after 2D gel electrophoresis
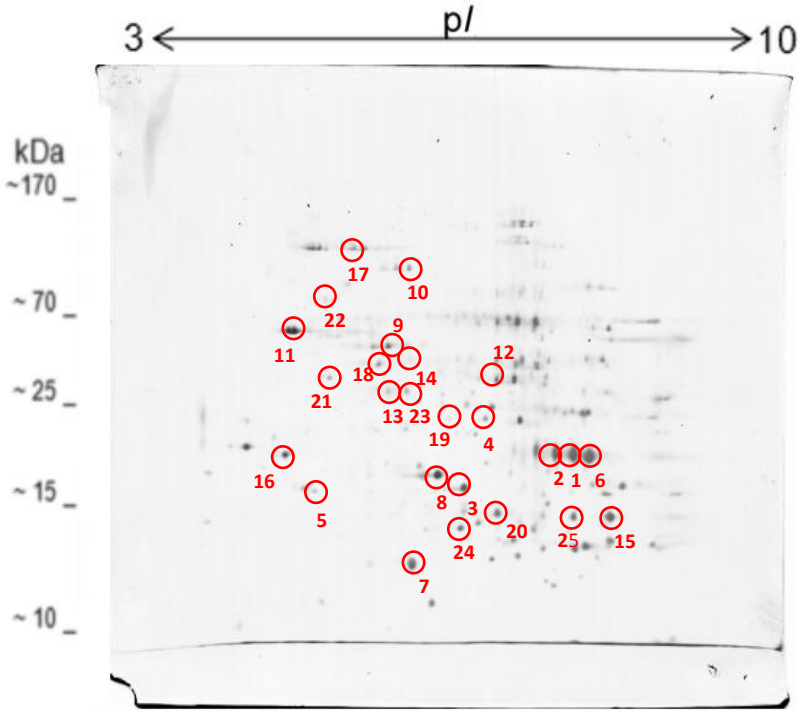
Figure 34: 2D gel electrophoresis of an extract of *Exophiala dermatitidis* at 37 °C. MS - compatible silver staining. Numbers refer to gel spots selected for protein identification.
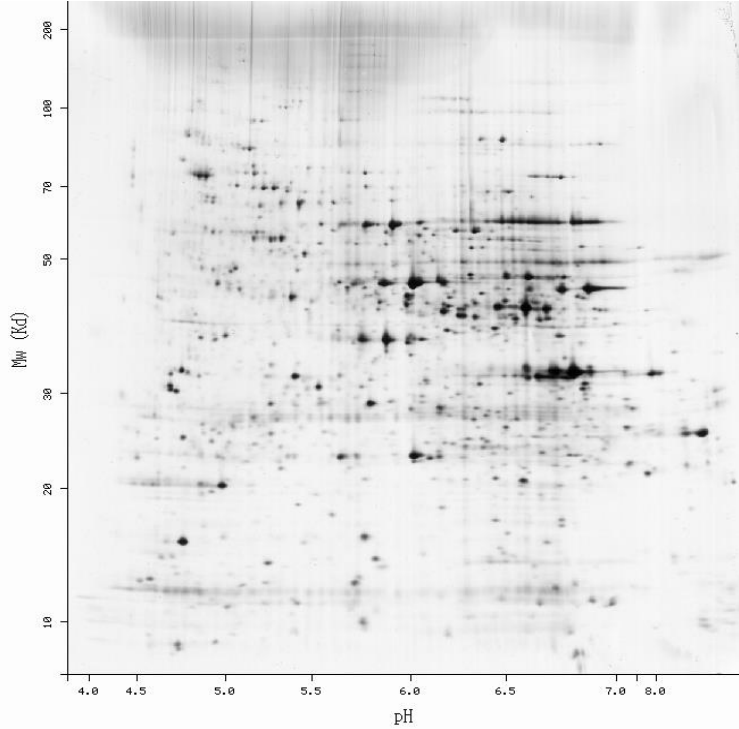
Figure 35: 2D gel electrophoresis of *Saccharomyces cerevisiae* (according to http://world-2dpage.expasy.org/swiss-2dpage/data/gifs/swiss_2dpage/YEAST.gif)

The 2D gel of an extract of *Exophiala dermatitidis* at 37 °C shown on Figure 34 was prepared at the University of Natural Resources and Life Sciences Vienna. The selected protein spots were *in-gel* digested and analyzed using the MALDI mass spectrometer UltrafleXtreme (Bruker Daltonics, Bremen, Germany). Figure 35 shows an online available reference 2D gel of *Saccharomyces cerevisiae* used to get an idea which protein could eventually be to protein of interest.

3.4.1 Peptide mass fingerprint (PMF) analysis

As described in Chapter 2.8.1 peptide analysis spectra were recorded in the positive ion reflectron mode as singly charged ions employing a mass range between 600.0-3500.0 Da. Interpretation of mass spectra within this region is very difficult and database search rarely leads to satisfactory results. Nevertheless obtained mass spectra were used for selecting particular peptides for further MS/MS analysis. In addition recorded gel blank spectra were used for excluding background signals from the peaklist.

To highlight one PMF analysis result Figure 36 shows the PMF spectrum of spot 11. Trypsin peaks, blank peaks and peaks identified as interferences or contaminants encountered in mass spectrometry [79] were excluded.

The following peptide masses were detected in the blank spectrum as blank peaks:

625.566, 639.566, 796.517, 798.525, 842.532, 864.512, 868.543, 880.486, 899.552, 906.531, 1006.524, 1045.594, 1063.544, 1071.609, 1083.549, 1102.616, 1106.103, 1517.822, 1526.803, 1707.821, 1766.835, 1882.897, 1939.923, 2167.109, 2193.147, 2196.096, 2197.964, 2211.170, 2221.119, 2232.122, 2234.215, 2236.229, 2246.156, 2249.123, 2268.188, 2282.236, 2284.236, 2293.241, 2295.213, 2299.230, 2300.214, 2326.230, 2340.246, 2410.262, 2435.217, 3113.544, 3184.445, 3216.427

The following peptide masses were detected in the trypsin spectrum as either trypsin or blank peaks:

606.145, 672.184, 842.547, 864.524, 868.564, 880.489, 906.552, 928.526, 932.554, 934.486, 944.501, 955.537, 1001.599, 1006.524, 1030.578, 1045.611, 1050.893, 1054.551, 1067.594, 1071.631, 1083.564, 1103.575, 1106.096, 1119.598, 1126.614, 1127.597, 1150.634, 1220.640, 1387.671, 1435.801, 1494.788, 1722.824, 1734.853, 1751.846, 1764.830, 1766.848, 1769.868, 1774.930 1780.837, 1782.856, 1788.827, 1791.840, 1794.617, 1798.846, 1804.806, 1809.356, 1809.855, 1884.941, 1911.957, 1928.959, 1940.996, 1962.968, 2041.060, 2091.074, 2157.115, 2167.152, 2173.118, 2193.153, 2196.098, 2197.963, 2211.181, 2218.918, 2233.162, 2237.200, 2246.222,

2249.135, 2255.146, 2259.178, 2268.241, 2271.109, 2275.143, 2284.270, 2293.093, 2297.300, 2300.278, 2306.245, 2322.241, 2338.221, 2473.307, 2835.334, 2867.329, 3011.390, 3124.367, 3161.626, 3177.622, 3441.564

The following peptide masses were used for database search:

1116.644, 1166.589, 1304.608, 1307.679, 1321.620, 1359.666, 1361.650, 1423.800, 1436.714, 1475.758, 1493.731, 1537.823, 1585.823, 1601.818, 1675.958, 1716.861, 1773.920, 1779.969, 1791.734, 1969.050, 1993.982, 2216.041, 2228.149, 2234.147, 2246.108, 2268.133, 2276.149, 2285.107, 2292.149, 2321.133, 2342.135, 2383.955, 2399.030, 2522.148, 2536.157, 2602.179, 2651.204, 2705.169, 2717.081, 2722.436, 3069.329, 3177.486, 3182.319, 3185.394, 3193.506, 3535.601, 3653.728, 3828.948
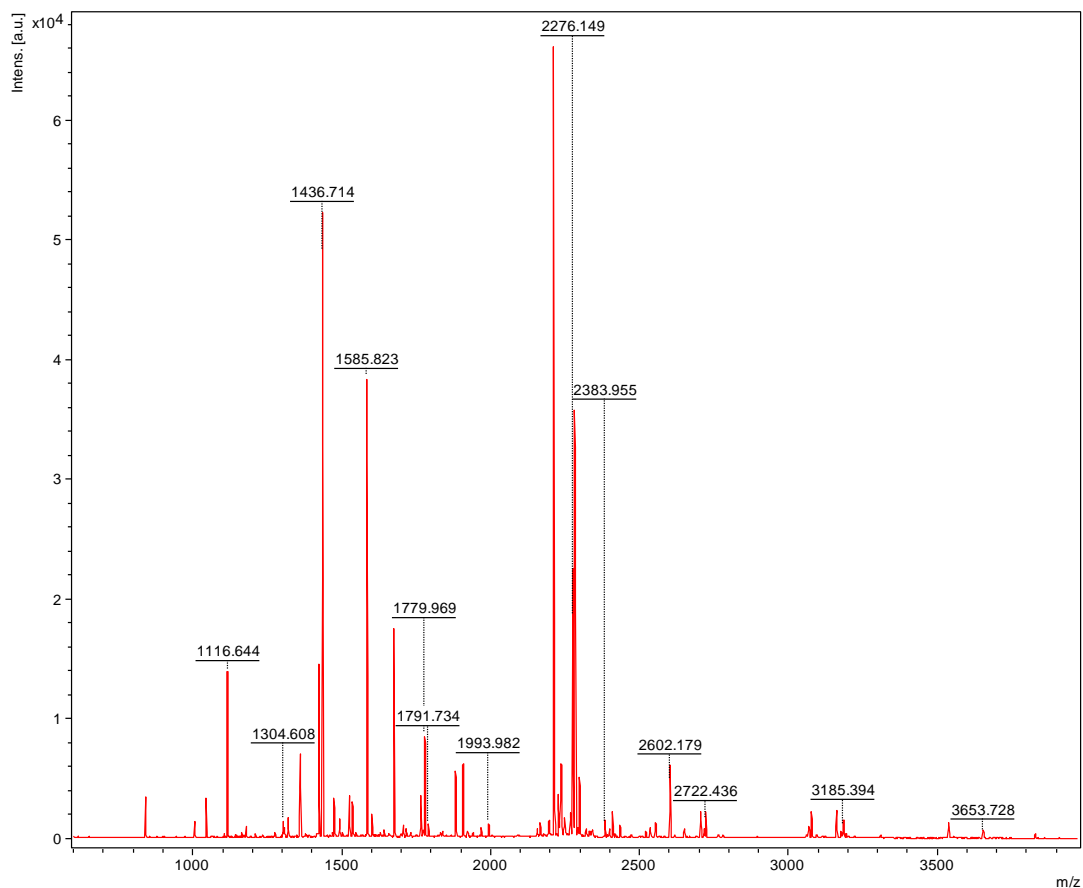
Figure 36: Peptide Mass Fingerprint of gel spot 11 recorded in the positive reflectron ion mode. Within the list of relevant peptide masses for database search, a selection of peptides with the highest intensities is marked in the spectrum. Trypsin peaks, blank peaks and peaks identified as interferences or contaminants encountered in mass spectrometry [2] are excluded.

As mentioned earlier PMF database searches proved to be difficult for protein identification, especially for unknown and hardly known species as *Exophiala dermatitidis.* Mass spectrometric based protein identification depends on the availability of the protein in the database. For organism with unsequenced genome cross-species protein identifications can help identifying proteins. Using MS and available protein sequences, cross-species protein identifications are accomplished by partially aligning an analyzed protein from an organism with an unsequenced genome to database sequence from a related organism. PMF allows for cross-species protein identification in some cases because only a part of all peptides from a protein digest need to be recognized. Especially the high mass accuracy of modern TOF instruments increases the confidence of in cross-species peptide mass mapping because of the fact that less peptide masses would be required to produce a confident hit [80].

As protein identification using PMF proved to be difficult within this study, only PMF spectrum of spot 11 (Figure 36) has returned significant protein identification from *Exophiala dermatitidis.* The identified protein is called ATP synthase subunit beta, mitochondrial. The score of this identification is 97 (Protein scores greater than 76 are significant (<0.05)). 22 mass values of the 48 searched mass values matched the sequence. The protein sequence coverage is 64 %. Detailed information about PMF spectra identifications are outlined in the part identified proteins of Chapter 3.2.1.

As already described, although all other PMF spectra did not return significant protein identifications, spectra can be used as indication for further evaluations. Therefore PMF spectra of all 25 analyzed spots are provided on a DVD-ROM as additional material.

3.4.2 Tandem mass spectrometry (MS/MS) analysis

Today a peptide mass fingerprint (PMF) is no longer accurate enough for an unambiguous identification of protein. Therefore, the 'LIFT' technique (see chapter 1.2.2c) operated in the laser induced dissociation (LID) MS/MS mode was used to perform fragment analysis of selected peptides. As described in Chapter 2.8.1 all spectra were recorded in the positive ion reflectron mode.

To highlight one spectra of tandem mass spectrometry analysis Figure 37 shows the MS/MS spectrum of precursor ion with m/z 1675.96 Da of spot 11. Unfortunately only a part of the sequence could be annotated of this spectrum because of low signal intensities in the upper m/z region. A detailed list of all fragment ions of the identified sequence RVVNEGLHQAVELVL is shown on Table 15. Nevertheless the database search of this part of the sequence RVVNEGI/LH of the precursor ion with m/z 1675.96 of spot 11 resulted in the following identification:

1. gi|119182499   **Mass:** 55808   **Score: 108**

    ATP synthase beta chain, mitochondrial [*Coccidioides immitis RS*]

Table 15: List of fragment ions of the identified sequence RVVNEGLHQAVELVL. Matches are marked in red: 58/254 fragment ions using 58 most intense peaks

#	Immon.	a	a*	a⁰	b	b*	b⁰	d	Seq.	v	w	y	y*	y⁰	#
1	86.0964	86.0964			114.0913			44.0495	L						15
2	72.0808	185.1648			213.1598			171.1492	V	1518.8023	1531.8227	1562.8649	1545.8384	1544.8544	14
3	86.0964	298.2489			326.2438			256.2020	L	1405.7183	1404.7230	1463.7965	1446.7700	1445.7859	13
4	102.0550	427.2915		409.2809	455.2864		437.2758	369.2860	E	1276.6757	1275.6804	1350.7124	1333.6859	1332.7019	12
5	72.0808	526.3599		508.3493	554.3548		536.3443	512.3443	V	1177.6072	1190.6276	1221.6698	1204.6433	1203.6593	11
6	44.0495	597.3970		579.3865	625.3919		607.3814		A	1106.5701		1122.6014	1105.5749	1104.5909	10
7	101.0709	725.4556	708.4291	707.4450	753.4505	736.4240	735.4400	668.4341	Q	978.5116	977.5163	1051.5643	1034.5378	1033.5538	9
8	110.0713	862.5145	845.4880	844.5039	890.5094	873.4829	872.4989		H	841.4526		923.5057	906.4792	905.4952	8
9	86.0964	975.5986	958.5720	957.5880	1003.5935	986.5669	985.5829	933.5516	L	728.3686	727.3733	786.4468	769.4203	768.4363	7
10	30.0338	1032.6200	1015.5935	1014.6095	1060.6150	1043.5884	1042.6044		G			673.3628	656.3362	655.3522	6
11	102.0550	1161.6626	1144.6361	1143.6521	1189.6576	1172.6310	1171.6470	1103.6572	E	542.3045	541.3093	616.3413	599.3148	598.3307	5
12	87.0553	1275.7056	1258.6790	1257.6950	1303.7005	1286.6739	1285.6899	1232.6997	N	428.2616	427.2663	487.2987	470.2722		4
13	72.0808	1374.7740	1357.7474	1356.7634	1402.7689	1385.7423	1384.7583	1360.7583	V	329.1932	342.2136	373.2558	356.2292		3
14	72.0808	1473.8424	1456.8158	1455.8318	1501.8373	1484.8108	1483.8267	1459.8267	V	230.1248	243.1452	274.1874	257.1608		2
15	129.1135								R	74.0237	73.0284	175.1190	158.0924		1

Figure 37: MS/MS spectrum of precursor ion with m/z 1675.96 Da of spot 11

As mentioned above in the field of amino acid sequencing of peptides tandem mass spectrometry (MS/MS) has become a very powerful tool. In contrast to only few protein identifications obtained in PMF analysis because of the fact that a PMF spectrum can only represent the series of m/z values of peptides which sequences will have many possibilities for amino acid combination, MS/MS analysis often leads to a higher rate of identifications. To emphasize this statement MS/MS analysis of the 25 gel spots (Figure 34) led to 6 significantly identified proteins, (some proteins were confirmed based on different MS/MS spectra). Detailed information about all these identifications based on MS/MS analyses are outlined in the part identified proteins of Chapter 3.2.1. Additionally all MS/MS spectra are provided on a DVD-ROM.

3.4.3 Identified Proteins

3.4.3a Database search of PMF spectra

Spot 11

The following peptide masses were chosen:
1116.64, 1166.59, 1304.61, 1307.68, 1321.62, 1359.67, 1361.65, 1423.80, 1436.71, 1475.76, 1493.73, 1537.82, 1585.82, 1601.82, 1675.96, 1716.86, 1773.92, 1779.97, 1791.73, 1969.05, 1993.98, 2216.04, 2228.15, 2234.15, 2246.11, 2268.13, 2276.15, 2285.11, 2292.15, 2321.13, 2342.14, 2383.96, 2399.03, 2522.15, 2536.16, 2602.18, 2651.20, 2705.17, 2717.08, 2722.44, 3069.33, 3177.49, 3182.32, 3185.39, 3193.51, 3535.60, 3653.73, 3828.95

For database search settings outlined in Chapter 2.8.2 were used.

Search results:

1. gi|378728418   **Mass:** 55935   **Score: 97**

    ATP synthase subunit beta, mitochondrial [*Exophiala dermatitidis NIH/UT8656*]

2. gi|310798044   **Mass:** 55639   **Score:** 50

    ATP synthase F1 [*Colletotrichum graminicola M1.001*]

    gi|380488786   **Mass:** 60282   **Score:** 34

    ATP synthase subunit beta [*Colletotrichum higginsianum*]

    gi|471567117   **Mass:** 54945   **Score:** 32

    putative atp synthase beta mitochondrial precursor protein [*Eutypa lata UCREL1*]

3. gi|340516338   **Mass:** 54898   **Score:** 45

    predicted protein [*Trichoderma reesei QM6a*]

    gi|358379235   **Mass:** 54868   **Score:** 45

    hypothetical protein TRIVIDRAFT_75569 [*Trichoderma virens Gv29-8*]

    gi|358398002   **Mass:** 54920   **Score:** 39

    ATP synthase beta chain mitochondrial precursor [*Trichoderma atroviride IMI 206040*]

Detailed results:

Taxonomy: *Exophiala dermatitidis*   *NIH/UT8656*

Score: 97

Expect: 0.00039

Nominal Mass: 55935

Calculated pI: 5.29

Mass values searched: 48

Mass values matched: 22

Protein sequence coverage: 64 %

As the score of this identification is 97 and protein scores greater than 76 are significant (<0.05), this identification can be identification can be regarded as significant.

Figure 38 shows the protein sequence of the identified protein, ATP synthase subunit beta, mitochondrial. Detailed information about the matched peptides marked in red are shown on Table 16. Additionally the root-mean-square deviation, which shows the differences between predicted values of the peptides and the observed peptide values.

1	**MLKSGIARSL**	**GR**SAFARPSI	ARRAFEPLRR	QAVPAIAQRW	ASTDSGRVGK
51	IHQVIGAVVD	VKFDSEQLPP	ILNALETENN	GNK**LVLEVAQ**	**HLGENVVRCI**
101	**AMDGTEGLVR**	GRK**ATDTGAP**	**ISIPVGPGTL**	**GRIMNVTGDP**	**IDER**GPIKAT
151	K**LAPIHADAP**	**EFVEQSTSAE**	**VLVTGIKVVD**	**LLAPYAR**GGK	IGLFGGAGVG
201	K**TVFIQELIN**	**NIAKAHGGYS**	**VFTGVGERTR**	**EGNDLYHEMQ**	**ETSVIQLDGE**
251	**SKVALVFGQM**	**NEPPGAR**ARV	**ALTGLTVAEF**	**FR**DEEGQDVL	LFIDNIFRFT
301	QAGSEVSALL	GR**IPSAVGYQ**	**PTLAVDMGLM**	**QER**ITTTRKG	**SITSVQAVYV**
351	**PADDLTDPAP**	**ATTFAHLDAT**	**TVLSRGISEL**	**GIYPAVDPLD**	**SK**SRMLDPRV
401	**VGQEHYDTAS**	**RVQQMLQEYK**	SLQDIIAILG	MDELSEADKL	TVERARKIQR
451	**FLSQPFTVAQ**	**VFTGIEGKLV**	**DLKDTISSFQ**	**KIINGEGDDL**	**PEGAFYMVGD**
501	**FESAR**AKGEK	ILAELEKSS			

Figure 38: Protein sequence of the identified protein, ATP synthase subunit beta, mitochondrial. Matched peptides are marked in red.

Table 16: List of identfied peptides of the identified protein, ATP synthase subunit beta, mitochondrial.

Start – End	Observed	Mr(expt)	Mr(calc)	Delta	M	Peptide
1 – 12	1304.6077	1303.6004	1303.7394	-0.1390	2	-.MLKSGIARSLGR.S + Oxidation (M)
84 – 98	1675.9575	1674.9502	1674.9417	0.0085	0	K.LVLEVAQHLGENVVR.C
99 – 110	1321.6198	1320.6125	1320.6166	-0.0041	0	R.CIAMDGTEGLVR.G
114 – 132	1779.9688	1778.9616	1778.9527	0.0089	0	K.ATDTGAPISIPVGPGTLGR.I
133 – 144	1359.6662	1358.6589	1358.6500	0.0089	0	R.IMNVTGDPIDER.G
152 – 177	2722.4358	2721.4285	2721.4225	0.0060	0	K.LAPIHADAPEFVEQSTSAEVLVTGIK.V
178 – 187	1116.6437	1115.6364	1115.6339	0.0025	0	K.VVDLLAPYAR.G
202 – 230	3177.4860	3176.4787	3176.6731	-0.1944	2	K.TVFIQELINNIAKAHGGYSVFTGVGERTR.E
215 – 228	1436.7135	1435.7063	1435.6844	0.0218	0	K.AHGGYSVFTGVGER.T
231 – 252	2522.1476	2521.1404	2521.1278	0.0125	0	R.EGNDLYHEMQETSVIQLDGESK.V
253 – 267	1585.8230	1584.8157	1584.8082	0.0075	0	K.VALVFGQMNEPPGAR.A
253 – 267	1601.8181	1600.8108	1600.8032	0.0076	0	K.VALVFGQMNEPPGAR.A + Oxidation (M)
270 – 282	1423.7998	1422.7925	1422.7871	0.0054	0	R.VALTGLTVAEFFR.D
313 – 333	2276.1489	2275.1417	2275.1341	0.0076	0	R.IPSAVGYQPTLAVDMGLMQER.I
313 – 333	2292.1490	2291.1417	2291.1290	0.0127	0	R.IPSAVGYQPTLAVDMGLMQER.I + Oxidation (M)
339 – 375	3828.9475	3827.9403	3827.9582	-0.0179	1	R.KGSITSVQAVYVPADDLTDPAPATTFAHLDATTVLSR.G
376 – 392	1773.9197	1772.9124	1772.9196	-0.0072	0	R.GISELGIYPAVDPLDSK.S
400 – 411	1361.6505	1360.6432	1360.6371	0.0061	0	R.VVGQEHYDTASR.V
412 – 420	1166.5888	1165.5815	1165.5801	0.0014	0	R.VQQMLQEYK.S
451 – 468	1969.0497	1968.0424	1968.0357	0.0067	0	R.FLSQPFTVAQVFTGIEGK.L
469 – 481	1493.7311	1492.7238	1492.8137	-0.0899	1	K.LVDLKDTISSFQK.I
482 – 505	2602.1785	2601.1713	2601.1693	0.0019	0	K.IINGEGDDLPEGAFYMVGDFESAR.A
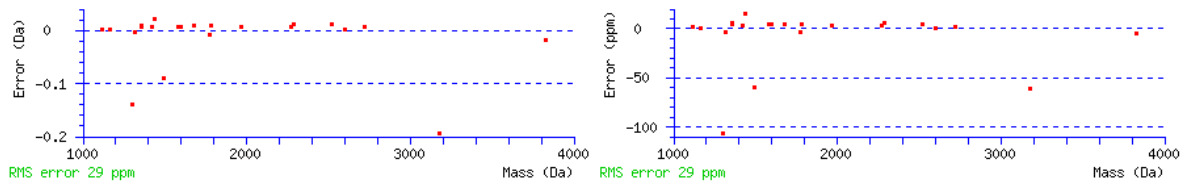
Figure 39: Root-mean-square deviation graph of obtained peptides; The left graph shows the Error in Dalton and the right graph shows the error in ppm.

3.4.3b Database search of PSD spectra

Spot 1: Precursor ion with m/z 1674.72

For database search settings outlined in Chapter 2.8.2 were used.

Search results:

1. gi|169783178   **Mass:** 36228   **Score: 70**

    glyceraldehyde-3-phosphate dehydrogenase [*Aspergillus oryzae RIB40*]
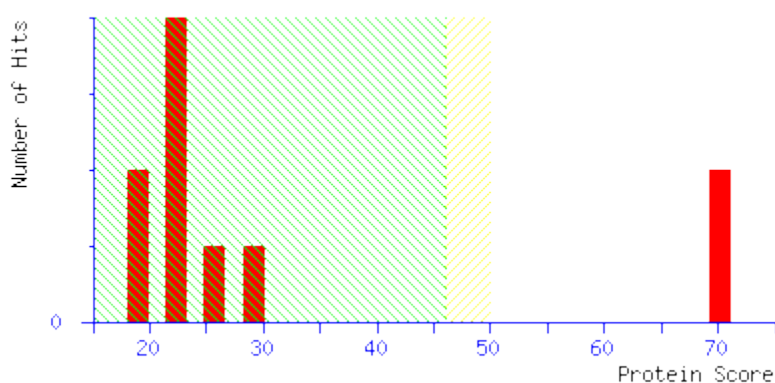
Detailed results:

Taxonomy: *Aspergillus oryzae RIB40*

Score: 70

Expect: 0.00057

Nominal Mass: 36228

Calculated pI: 6.40

Database search of the part of the sequence RSYGWENDYWS of the spectrum shown on Figure 41 resulted in the identification of the protein glyceraldehyde-3-phosphate dehydrogenase of the species *Aspergillus oryzae.* As the species *Aspergillus oryzae* belongs to class Eurotiomycetes and the species *Exophiala dermatitidis* belongs to the class Chaetothyriomycetes a subclass of Eurotiomycetes, these species can be regarded as related organisms and therefore the identification can be regarded as relevant.

A detailed list of all fragment ions of the identified sequence RSYGWENDYWSVI is shown on Table 17.

Table 17: List of fragment ions of the identified sequence RSYGWENDYWSVI. Matches are marked in red: 52/195 fragment ions using 62 most intense peaks.

| #	Immon.	a	a*	a⁰	b	b*	b⁰	d	Seq.	v	w	y	y*	y⁰	#
1	86.0964	86.0964			114.0913			44.0495	I						13
2	72.0808	**185.1648**			**213.1598**			171.1492	V	1517.6080	1530.6284	1561.6706	1544.6441	1543.6601	12
3	60.0444	272.1969		254.1863	**300.1918**		**282.1812**	256.2020	S	1430.5760	1429.5808	1462.6022	1445.5757	1444.5917	11
4	159.0917	**458.2762**		440.2656	486.2711		**468.2605**		W	1244.4967		***1375.5702***	1358.5436	1357.5596	10
5	136.0757	**621.3395**		603.3289	649.3344		631.3239		Y	1081.4334		***1189.4909***	1172.4643	1171.4803	9
6	88.0393	736.3665		718.3559	764.3614		746.3508	692.3766	D	966.4064	965.4112	***1026.4275***	1009.4010	1008.4170	8
7	87.0553	850.4094	833.3828	832.3988	878.4043	861.3777	860.3937	807.4036	N	852.3635	851.3682	***911.4006***	894.3741	893.3900	7
8	102.0550	979.4520	962.4254	961.4414	**1007.4469**	990.4203	989.4363	921.4465	E	723.3209	722.3257	***797.3577***	780.3311	**779.3471**	6
9	159.0917	1165.5313	1148.5047	1147.5207	1193.5262	1176.4997	1175.5156		W	537.2416		***668.3151***	651.2885	650.3045	5
10	30.0338	1222.5527	1205.5262	1204.5422	**1250.5477**	1233.5211	1232.5371		G			***482.2358***	465.2092	464.2252	4
11	136.0757	1385.6161	1368.5895	1367.6055	1413.6110	1396.5844	1395.6004		Y	317.1568		***425.2143***	408.1878	407.2037	3
12	60.0444	1472.6481	1455.6216	1454.6375	1500.6430	1483.6165	1482.6325	1456.6532	S	230.1248	229.1295	***262.1510***	245.1244	**244.1404**	2
13	129.1135								R	74.0237	73.0284	***175.1190***	158.0924		1

Figure 40: Root-mean-square deviation graph of obtained fragment ions; The left graph shows the Error in Dalton and the right graph shows the error in ppm.


Figure 41: MS/MS spectrum of precursor with m/z 1674.72 Da of spot 1

Spot 2: Precursor ion with m/z 1674.76

For database search settings outlined in Chapter 2.8.2 were used.

Search results:

1. gi|120690　　　　　　　**Mass:** 36285　　　　　　　**Score: 47**

   RecName: Full=Glyceraldehyde-3-phosphate dehydrogenase; Short=GAPDH; AltName: Full=GPD-1 [*Cryphonectria parasitica]*
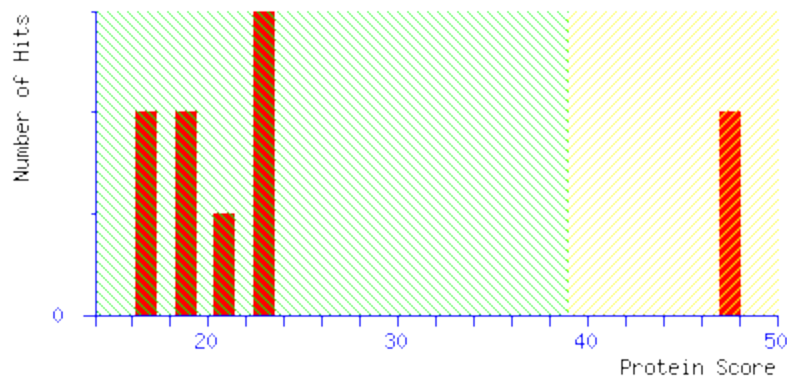
Detailed results:

Taxonomy:　　　*Cryphonectria parasitica*

Score:　　　　　47

Expect:　　　　　0.095

Nominal Mass:　36285

Calculated pI:　6.40

Database search of the part of the sequence RSYGWEND of the spectrum shown on Figure 43 resulted in the identification of the protein glyceraldehyde-3-phosphate dehydrogenase of the species *Cryphonectria parasitica.* As the species *Cryphonectria parasitica* belongs to the subphylum Pezizomycotina as well as the species *Exophiala dermatitidis* belongs to Pezizomycotina, these species can be regarded as related organisms resulting in a relevant identification.

A detailed list of all fragment ions of the identified sequence RSYGWENDYWSVL is shown on Table 18.

Table 18: List of fragment ions of the identified sequence RSYGWENDYWSVL. Matches are marked in red: 39/195 fragment ions using 47 most intense peaks

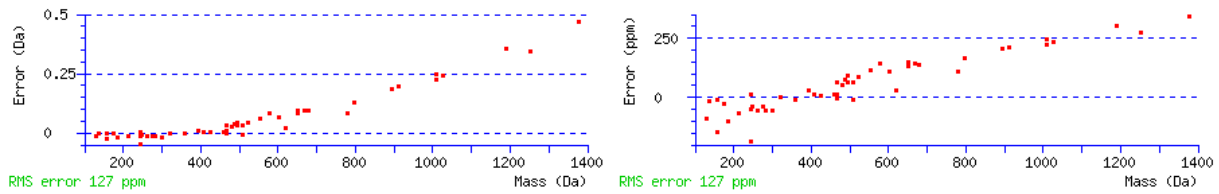| #	Immon.	a	a*	a⁰	b	b*	b⁰	d	Seq.	v	w	y	y*	y⁰	#
1	86.0964	86.0964			114.0913			44.0495	L						13
2	72.0808	185.1648			213.1598			171.1492	V	1517.6080	1530.6284	1561.6706	1544.6441	1543.6601	12
3	60.0444	272.1969		254.1863	300.1918		282.1812	256.2020	S	1430.5760	1429.5808	1462.6022	1445.5757	1444.5917	11
4	159.0917	458.2762		440.2656	486.2711		468.2605		W	1244.4967		1375.5702	1358.5436	1357.5596	10
5	136.0757	621.3395		603.3289	649.3344		631.3239		Y	1081.4334		1189.4909	1172.4643	1171.4803	9
6	88.0393	736.3665		718.3559	764.3614		746.3508	692.3766	D	966.4064	965.4112	1026.4275	1009.4010	1008.4170	8
7	87.0553	850.4094	833.3828	832.3988	878.4043	861.3777	860.3937	807.4036	N	852.3635	851.3682	911.4006	894.3741	893.3900	7
8	102.0550	979.4520	962.4254	961.4414	1007.4469	990.4203	989.4363	921.4465	E	723.3209	722.3257	797.3577	780.3311	779.3471	6
9	159.0917	1165.5313	1148.5047	1147.5207	1193.5262	1176.4997	1175.5156		W	537.2416		668.3151	651.2885	650.3045	5
10	30.0338	1222.5527	1205.5262	1204.5422	1250.5477	1233.5211	1232.5371		G			482.2358	465.2092	464.2252	4
11	136.0757	1385.6161	1368.5895	1367.6055	1413.6110	1396.5844	1395.6004		Y	317.1568		425.2143	408.1878	407.2037	3
12	60.0444	1472.6481	1455.6216	1454.6375	1500.6430	1483.6165	1482.6325	1456.6532	S	230.1248	229.1295	262.1510	245.1244	244.1404	2
13	129.1135								R	74.0237	73.0284	175.1190	158.0924		1

Figure 42: Root-mean-square deviation graph of obtained fragment ions; The left graph shows the Error in Dalton and the right graph shows the error in ppm.
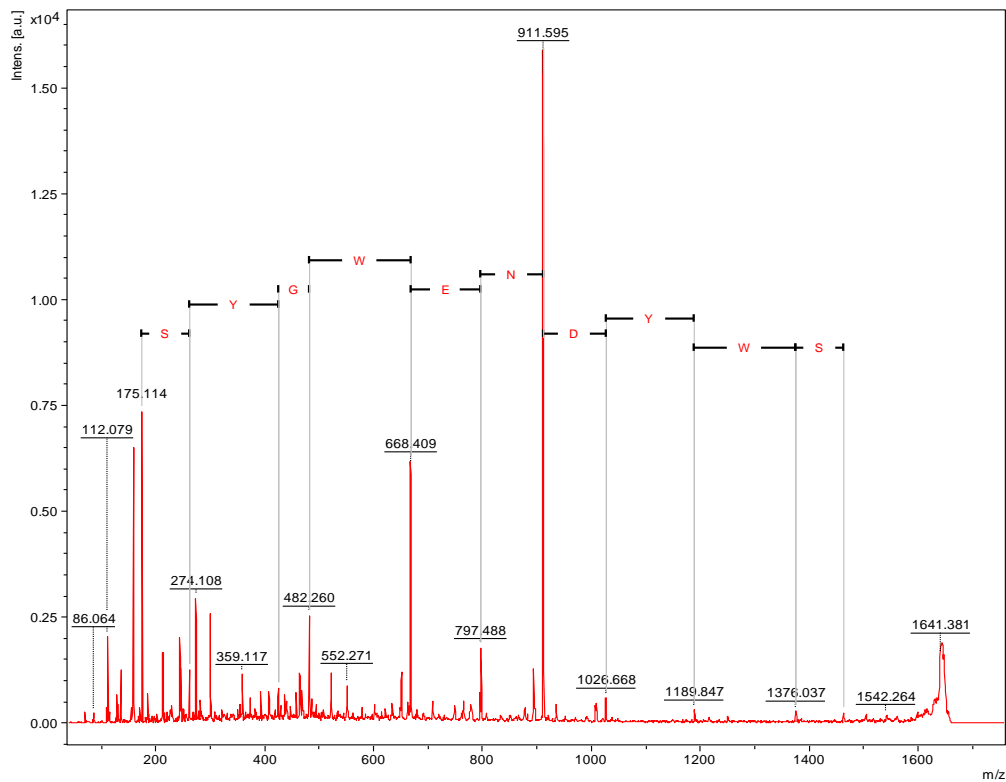

Figure 43: MS/MS spectrum of precursor with m/z 1674.76 Da of spot 2

Spot 11: Precursor ion with m/z 1116.64

For database search settings outlined in Chapter 2.8.2 were used.

Search results:

1. gi|164657588   **Mass:** 47468   **Score: 88**

   hypothetical protein MGL_2906 [*Malassezia globosa CBS 7966*]

2. gi|171110   **Mass:** 54947   **Score: 85**

   F1-ATPase beta-subunit precursor [*Saccharomyces cerevisiae*]

3. gi|82491928   **Mass:** 71564   **Score: 54**

   white collar one A [*Phycomyces blakesleeanus*]
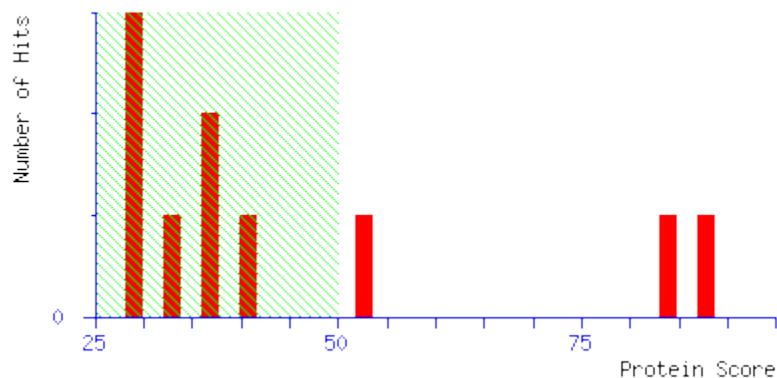
Detailed results (of F1-ATPase beta-subunit precursor):

Taxonomy: *Saccharomyces cerevisiae*

Score: 85

Expect: 1.8e-05

Nominal Mass: 54947

Calculated pI: 5.71

Database search of the part of the sequence RAYPALLDV of the spectrum shown on Figure 45 resulted in the identification of the protein F1-ATPase beta-subunit precursor of the species *Saccharomyces cerevisiae.* As the species *Saccharomyces cerevisiae* belongs to the subphylum Saccharomycotina a so called sister group of Pezizomycotina, and the species *Exophiala dermatitidis* belongs to Pezizomycotina these organisms can be regarded as related.

A detailed list of all fragment ions of the identified sequence RSYGWENDYWSVL is shown on Table 19.

Table 19: List of fragment ions of the identified sequence RAYPALLDVV. Matches are marked in red: 53/133 fragment ions using 50 most intense peaks

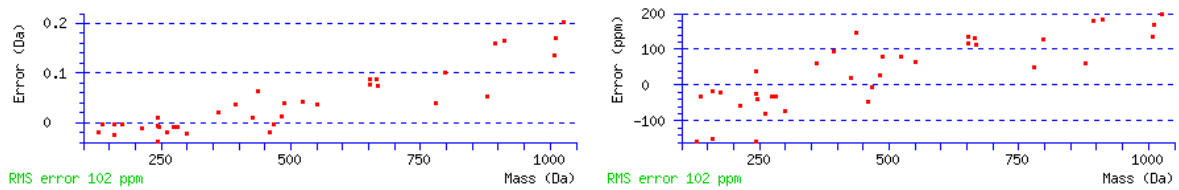| #	Immon.	a	a⁰	b	b⁰	d	Seq.	v	w	y	y*	y⁰	#
1	72.0808	**72.0808**		100.0757		44.0495	**V**						10
2	72.0808	171.1492		**199.1441**		157.1335	**V**	973.5102	986.5306	*1017.5728*	1000.5462	999.5622	9
3	88.0393	286.1761	268.1656	**314.1710**	296.1605	242.1863	**D**	858.4832	857.4880	*918.5043*	901.4778	900.4938	8
4	86.0964	**399.2602**	381.2496	**427.2551**	409.2445	357.2132	**L**	745.3992	744.4039	*803.4774*	786.4509		7
5	86.0964	**512.3443**	494.3337	**540.3392**	522.3286	470.2973	**L**	632.3151	631.3198	*690.3933*	673.3668		6
6	44.0495	583.3814	565.3708	**611.3763**	593.3657		**A**	561.2780		*577.3093*	560.2827		5
7	70.0651	**680.4341**	662.4236	708.4291	690.4185	654.4185	**P**	464.2252	463.2300	*506.2722*	489.2456		4
8	136.0757	843.4975	825.4869	871.4924	853.4818		**Y**	301.1619		*409.2194*	392.1928		3
9	44.0495	914.5346	896.5240	942.5295	924.5189		**A**	230.1248		*246.1561*	229.1295		2
10	129.1135						**R**	74.0237	73.0284	*175.1190*	158.0924		1
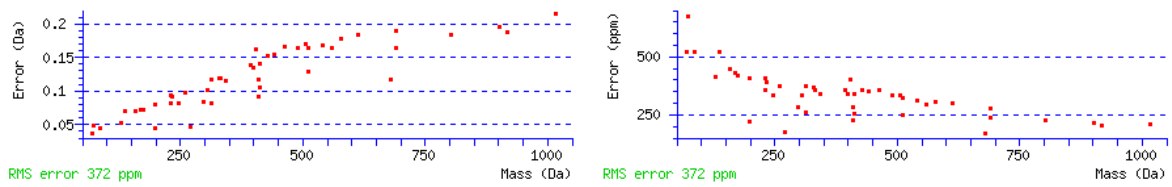
Figure 44: Root-mean-square deviation graph of obtained fragment ions; The left graph shows the Error in Dalton and the right graph shows the error in ppm.
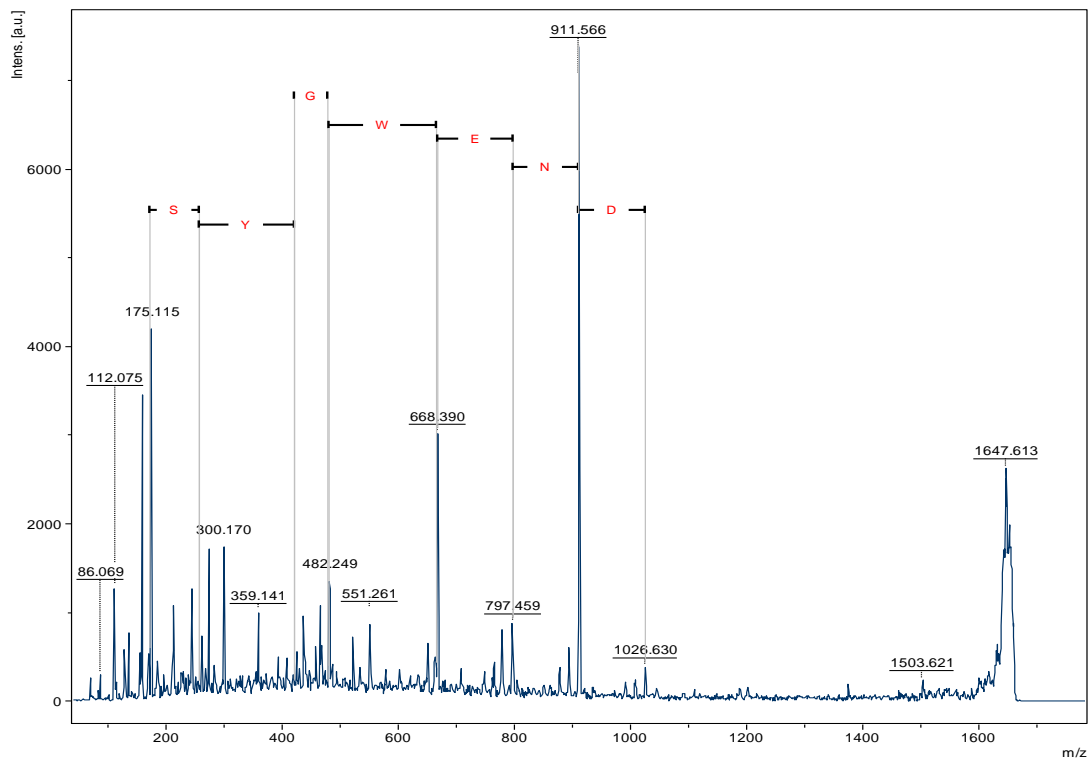

Figure 45: MS/MS spectrum of precursor with m/z 1116.64 Da of spot 11

99

Spot 11: Precursor ion with m/z 1423.80

For database search settings outlined in Chapter 2.8.2 were used.

Search results:

1. gi|378728418 **Mass:** 55935 **Score: 68**

   ATP synthase subunit beta, mitochondrial [*Exophiala dermatitidis NIH/UT8656*]
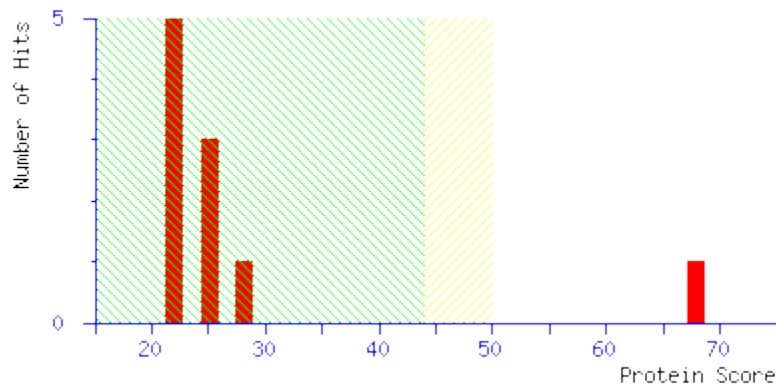
Detailed results:

Taxonomy: *Exophiala dermatitidis NIH/UT8656*

Score: 68

Expect: 0.00082

Nominal Mass: 55935

Calculated pI: 5.29

Database search of the part of the sequence RFFEAVTLG of the spectrum shown on Figure 47 resulted in the identification of the protein ATP synthase subunit beta, mitochondrial of the species *Exophiala dermatitidis.*

A detailed list of all fragment ions of the identified sequence RFFEAVTLGTLAV is shown on Table 20.

Table 20: List of fragment ions of the identified sequence RFFEAVTLGTLAV. Matches are marked in red: 57/205 fragment ions using 58 most intense peaks

| #	Immon.	a	a⁰	b	b⁰	d	d'	Seq.	v	w	w'	y	y*	y⁰	#
1	72.0808	72.0808		100.0757		44.0495		V							13
2	44.0495	143.1179		**171.1128**				A	1308.6947			1324.7260	1307.6994	1306.7154	12
3	86.0964	256.2020		**284.1969**		214.1550		L	1195.6106	1194.6154		**1253.6889**	1236.6623	1235.6783	11
4	74.0600	357.2496	339.2391	**385.2445**	367.2340	341.2547	343.2340	T	1094.5629	1107.5833	1109.5626	1140.6048	1123.5782	1122.5942	10
5	30.0338	414.2711	396.2605	**442.2660**	424.2554			G				**1039.5571**	1022.5306	1021.5465	9
6	86.0964	527.3552	509.3446	**555.3501**	537.3395	485.3082		L	924.4574	923.4621		**982.5356**	965.5091	964.5251	8
7	74.0600	628.4028	610.3923	**656.3978**	638.3872	612.4079	614.3872	T	823.4097	836.4301	838.4094	**869.4516**	852.4250	851.4410	7
8	72.0808	727.4713	709.4607	755.4662	737.4556	713.4556		V	724.3413	737.3617		**768.4039**	751.3774	750.3933	6
9	44.0495	798.5084	780.4978	**826.5033**	808.4927			A	653.3042			**669.3355**	652.3089	651.3249	5
10	102.0550	927.5510	909.5404	955.5459	937.5353	869.5455		E	524.2616	523.2663		**598.2984**	581.2718	580.2878	4
11	120.0808	1074.6194	1056.6088	1102.6143	1084.6037			F	377.1932			**469.2558**	452.2292		3
12	120.0808	1221.6878	1203.6772	1249.6827	1231.6721			F	230.1248			**322.1874**	305.1608		2
13	129.1135							R	74.0237	73.0284		**175.1190**	158.0924		1
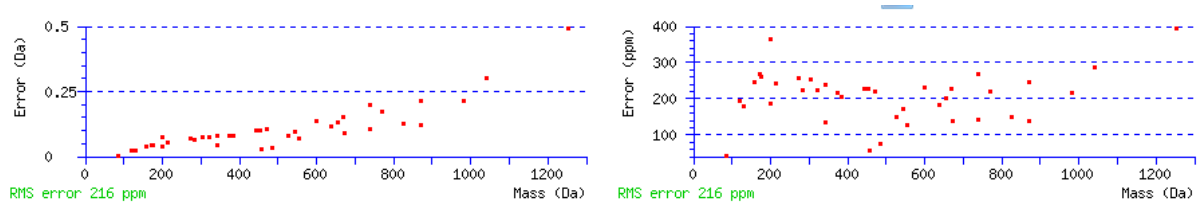
Figure 46: Root-mean-square deviation graph of obtained fragment ions; The left graph shows the Error in Dalton and the right graph shows the error in ppm.
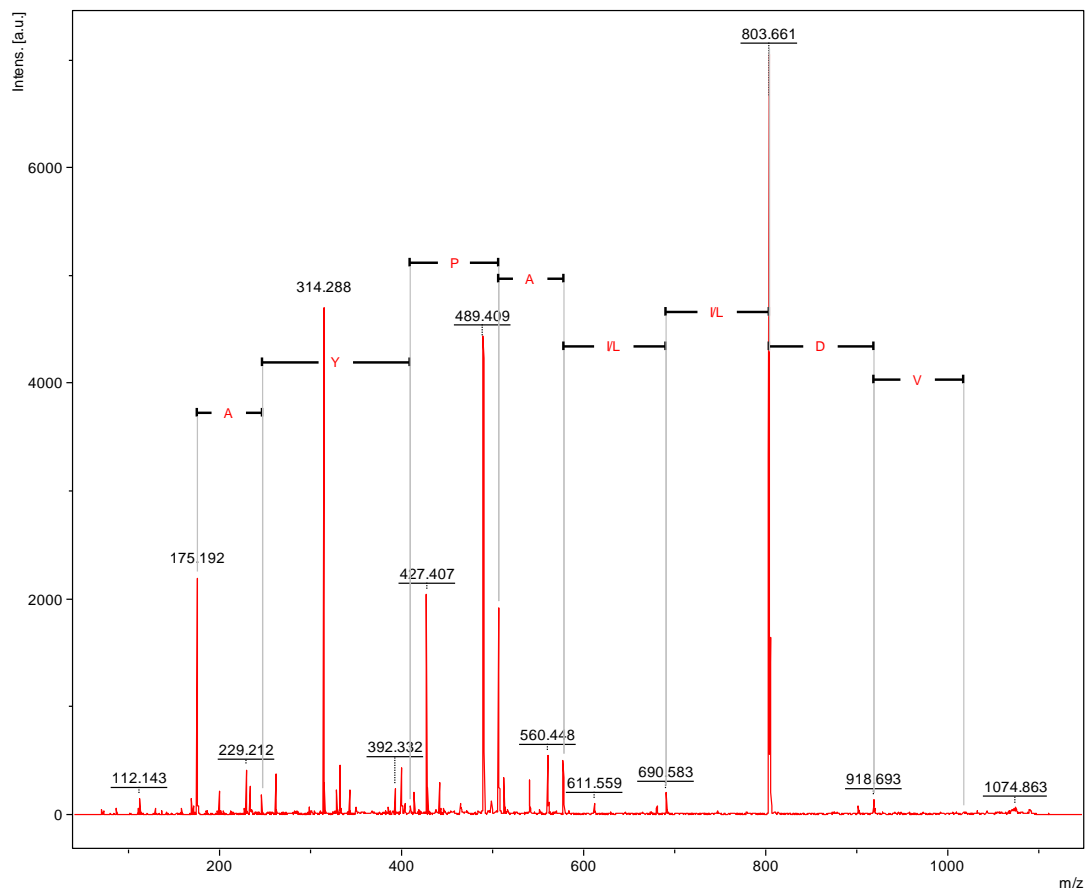

Figure 47: MS/MS spectrum of precursor with m/z 1423.80 Da of spot 11

101

Spot 11: Precursor ion with m/z 1675.95

For database search settings outlined in Chapter 2.8.2 were used.

Search results:

2. gi|119182499   **Mass:** 55808   **Score: 108**

ATP synthase beta chain, mitochondrial [*Coccidioides immitis RS*]
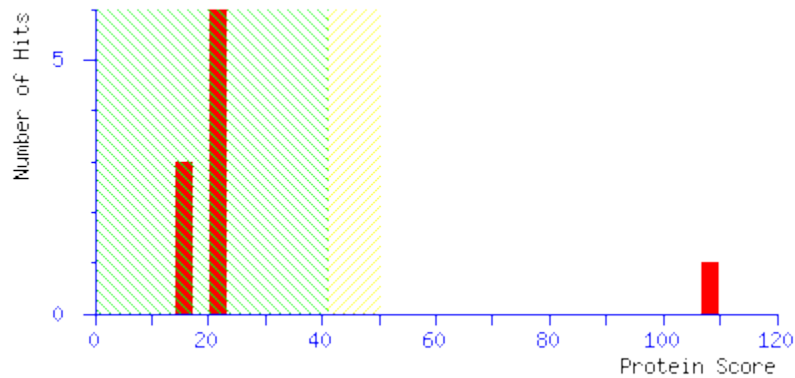
Detailed results:

Taxonomy: *Coccidioides immitis RS*

Score: 108

Expect: 7.9e-08

Nominal Mass: 55808

Calculated pI: 5.23

Database search of the part of the sequence RVVNEGLH of the spectrum shown on Figure 49 resulted in the identification of the protein ATP synthase beta chain, mitochondrial of the species *Coccidioides immitis.* As the species *Coccidioides immitis* belongs to the class Eurotiomycetes as well as *Exophiala dermatitidis* belongs to this class, these organisms can be regarded as related. The identified protein is therefore relevant for the species *Exophiala dermatitidis.*

A detailed list of all fragment ions of the identified sequence RVVNEGLHQAVELVL is shown on Table 21.

Table 21: List of fragment ions of the identified sequence RVVNEGLHQAVELVL. Matches are marked in red: 58/254 fragment ions using 58 most intense peaks

| #	Immon.	a	a*	a⁰	b	b*	b⁰	d	Seq.	v	w	y	y*	y⁰	#
1	86.0964	86.0964			114.0913			44.0495	L						15
2	72.0808	185.1648			213.1598			171.1492	V	1518.8023	1531.8227	1562.8649	1545.8384	1544.8544	14
3	86.0964	298.2489			326.2438			256.2020	L	1405.7183	1404.7230	1463.7965	1446.7700	1445.7859	13
4	102.0550	427.2915		409.2809	455.2864		437.2758	369.2860	E	1276.6757	1275.6804	1350.7124	1333.6859	1332.7019	12
5	72.0808	526.3599		508.3493	554.3548		536.3443	512.3443	V	1177.6072	1190.6276	1221.6698	1204.6433	1203.6593	11
6	44.0495	597.3970		579.3865	625.3919		607.3814		A	1106.5701		1122.6014	1105.5749	1104.5909	10
7	101.0709	725.4556	708.4291	707.4450	753.4505	736.4240	735.4400	668.4341	Q	978.5116	977.5163	1051.5643	1034.5378	1033.5538	9
8	110.0713	862.5145	845.4880	844.5039	890.5094	873.4829	872.4989		H	841.4526		923.5057	906.4792	905.4952	8
9	86.0964	975.5986	958.5720	957.5880	1003.5935	986.5669	985.5829	933.5516	L	728.3686	727.3733	786.4468	769.4203	768.4363	7
10	30.0338	1032.6200	1015.5935	1014.6095	1060.6150	1043.5884	1042.6044		G			673.3628	656.3362	655.3522	6
11	102.0550	1161.6626	1144.6361	1143.6521	1189.6576	1172.6310	1171.6470	1103.6572	E	542.3045	541.3093	616.3413	599.3148	598.3307	5
12	87.0553	1275.7056	1258.6790	1257.6950	1303.7005	1286.6739	1285.6899	1232.6997	N	428.2616	427.2663	487.2987	470.2722		4
13	72.0808	1374.7740	1357.7474	1356.7634	1402.7689	1385.7423	1384.7583	1360.7583	V	329.1932	342.2136	373.2558	356.2292		3
14	72.0808	1473.8424	1456.8158	1455.8318	1501.8373	1484.8108	1483.8267	1459.8267	V	230.1248	243.1452	274.1874	257.1608		2
15	129.1135								R	74.0237	73.0284	175.1190	158.0924		1

Figure 48: Root-mean-square deviation graph of obtained fragment ions; The left graph shows the Error in Dalton and the right graph shows the error in ppm.
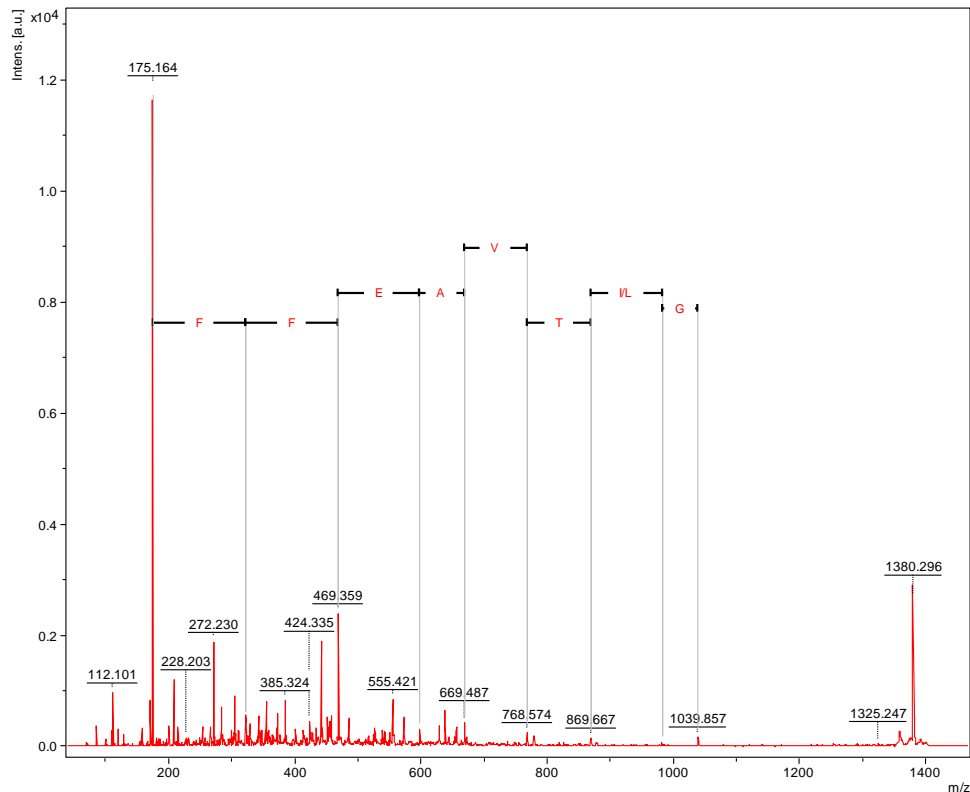

Figure 49: MS/MS spectrum of precursor with m/z 1675.95 Da of spot 11

Spot 11: Precursor ion with m/z 1779.97

For database search settings outlined in Chapter 2.8.2 were used.

Search results:

1. gi|378728418   **Mass:** 55935   **Score: 74**

    ATP synthase subunit beta, mitochondrial [*Exophiala dermatitidis NIH/UT8656*]
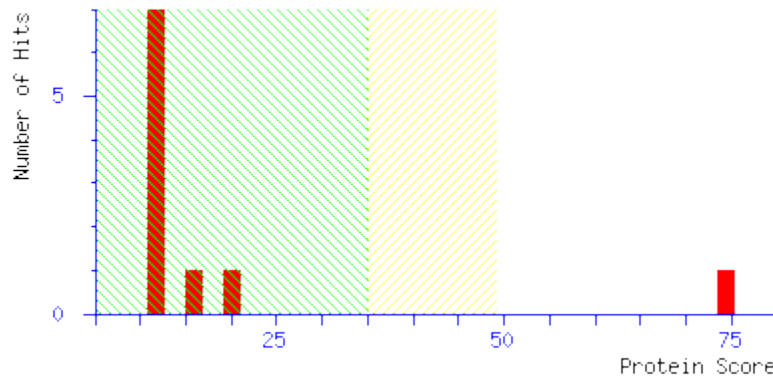
Detailed results:

Taxonomy: *Exophiala dermatitidis NIH/UT8656*

Score: 74

Expect: 0.00018

Nominal Mass: 55935

Calculated pI: 5.29

The database search of the part of the part sequence RGLT of the spectrum shown on Figure 51 resulted in the same identification as the previous analyzed sequence RFFEAVTLG showed the same protein identification, ATP synthase subunit beta, mitochondrial of the species *Exophiala dermatitidis.* Therefore this obtained result submits the previous protein identification.

A detailed list of all fragment ions of the identified sequence RGLTGPGVPISIPAGTDTA is shown on Table 22.

Table 22: List of fragment ions of the identified sequence RGLTGPGVPISIPAGTDTA. Matches are marked in red: 46/356 fragment ions using 53 most intense peaks

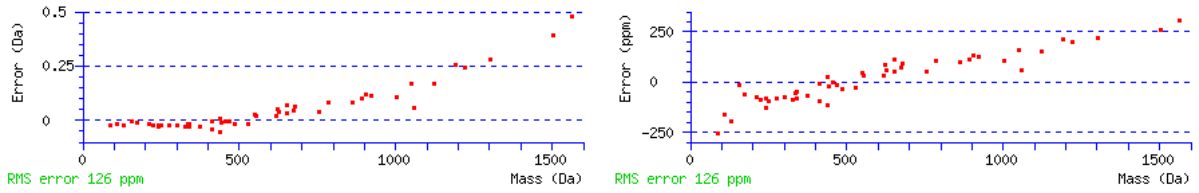| #	Immon.	a	a⁰	b	b⁰	d	d'	Seq.	v	w	w'	y	y*	y⁰	#
1	44.0495	44.0495		72.0444		44.0495		A							19
2	74.0600	145.0972	127.0866	173.0921	155.0815	129.1022	131.0815	T	1662.8810	1675.9014	1677.8806	1708.9228	1691.8963	1690.9123	18
3	88.0393	260.1241	242.1135	288.1190	270.1084	216.1343		D	1547.8540	1546.8588		1607.8751	1590.8486	1589.8646	17
4	74.0600	361.1718	343.1612	389.1667	371.1561	345.1769	347.1561	T	1446.8063	1459.8267	1461.8060	1492.8482	1475.8217	1474.8376	16
5	30.0338	418.1932	400.1827	446.1882	428.1776			G				1391.8005	1374.7740	1373.7900	15
6	44.0495	489.2304	471.2198	517.2253	499.2147			A	1318.7478			1334.7791	1317.7525	1316.7685	14
7	70.0651	586.2831	568.2726	614.2780	596.2675	560.2675		P	1221.6950	1220.6997		1263.7419	1246.7154	1245.7314	13
8	86.0964	699.3672	681.3566	727.3621	709.3515	671.3359	685.3515	I	1108.6109	1121.6313	1135.6470	1166.6892	1149.6626	1148.6786	12
9	60.0444	786.3992	768.3886	814.3941	796.3836	770.4043		S	1021.5789	1020.5837		1053.6051	1036.5786	1035.5946	11
10	86.0964	899.4833	881.4727	927.4782	909.4676	871.4520	885.4676	I	908.4948	921.5152	935.5309	966.5731	949.5465	948.5625	10
11	70.0651	996.5360	978.5255	1024.5310	1006.5204	970.5204		P	811.4421	810.4468		853.4890	836.4625	835.4785	9
12	72.0808	1095.6045	1077.5939	1123.5994	1105.5888	1081.5888		V	712.3737	725.3941		756.4363	739.4097	738.4257	8
13	30.0338	1152.6259	1134.6154	1180.6208	1162.6103			G				657.3679	640.3413	639.3573	7
14	70.0651	1249.6787	1231.6681	1277.6736	1259.6630	1223.6630		P	558.2994	557.3042		600.3464	583.3198	582.3358	6
15	30.0338	1306.7001	1288.6896	1334.6951	1316.6845			G				503.2936	486.2671	485.2831	5
16	74.0600	1407.7478	1389.7373	1435.7427	1417.7322	1391.7529	1393.7322	T	400.2303	413.2507	415.2300	446.2722	429.2456	428.2616	4
17	86.0964	1520.8319	1502.8213	1548.8268	1530.8162	1478.7849		L	287.1462	286.1510		345.2245	328.1979		3
18	30.0338	1577.8534	1559.8428	1605.8483	1587.8377			G				232.1404	215.1139		2
19	129.1135							R	74.0237	73.0284		175.1190	158.0924		1
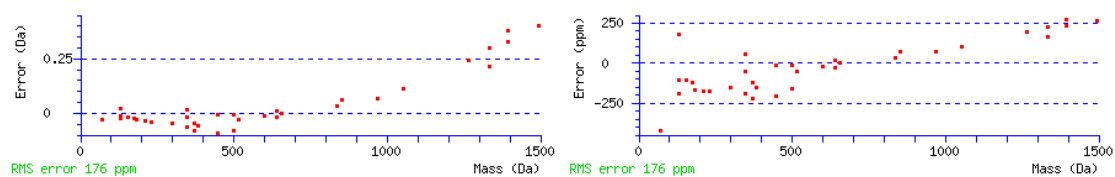
Figure 50: Root-mean-square deviation graph of obtained fragment ions; The left graph shows the Error in Dalton and the right graph shows the error in ppm.
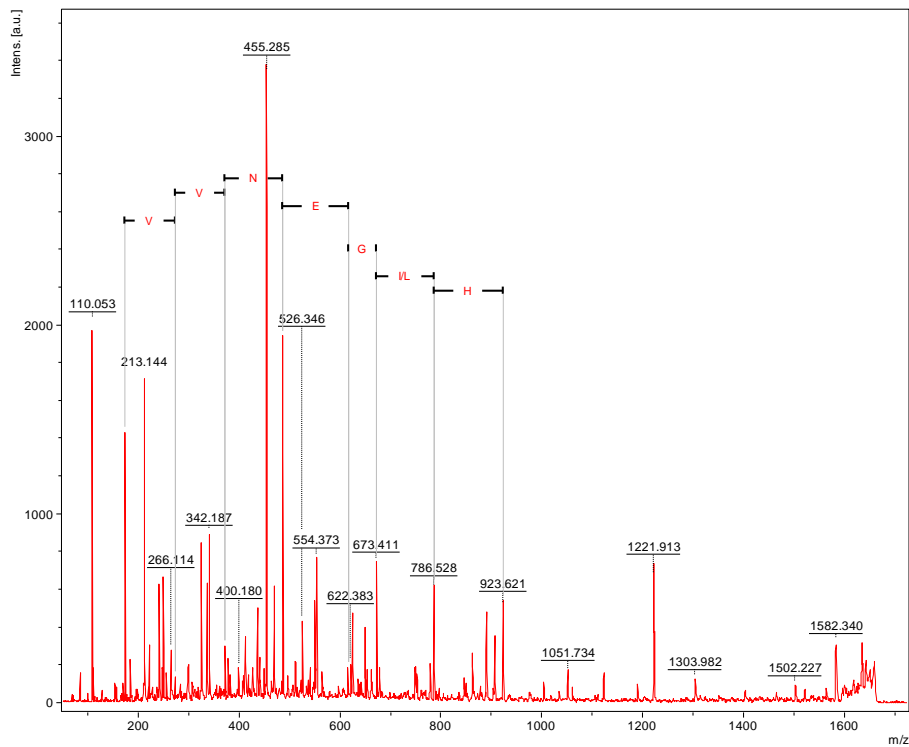

Figure 51: MS/MS spectrum of precursor with m/z 1779.97 Da of spot 11

105

Spot 11: Precursor ion with m/z 2602.18

For database search settings outlined in Chapter 2.8.2 were used.

Search results:

1. gi|378728418   **Mass:** 55935   **Score: 164**

   ATP synthase subunit beta, mitochondrial [*Exophiala dermatitidis NIH/UT8656*]
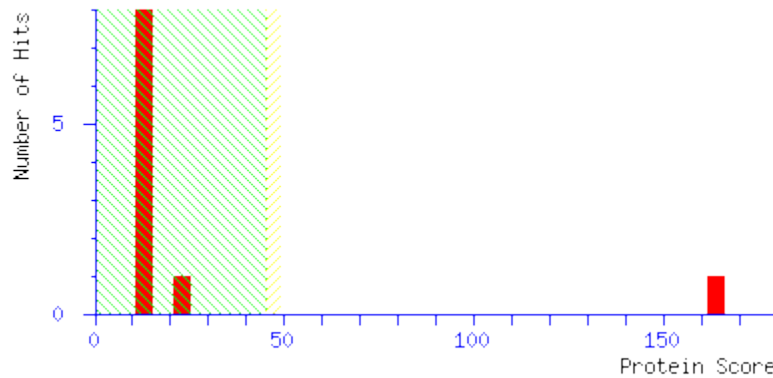
Detailed results:

Taxonomy: *Exophiala dermatitidis NIH/UT8656*

Score: 164

Expect: 1.8e-13

Nominal Mass: 55935

Calculated pI: 5.29

The database search of the sequence RASEFDGV of spectrum shown on Figure 53 resulted in the identification of the protein ATP synthase subunit beta, mitochondrial of the species *Exophiala dermatitidis.* Previously obtained results of the identification of the protein ATP synthase subunit beta, mitochondrial can therefore be submitted.

A detailed list of all fragment ions of the identified sequence RASEFDGVMYFAGEPLDDGEGNII is shown on Table 23.

Table 23: List of fragment ions of the identified sequence RASEFDGVMYFAGEPLDDGEGNII. Matches are marked in red: 30/464 fragment ions using 36 most intense peaks

| #	Immon.	a	a*	a⁰	b	b*	b⁰	d	d'	Seq.	v	w	w'	y	y*	y⁰	#
1	86.0964	86.0964			114.0913			44.0495		I							24
2	86.0964	199.1805			227.1754			171.1492	185.1648	I	2431.0143	2444.0347	2458.0503	2489.0925	2472.0660	2471.0820	23
3	87.0553	313.2234	296.1969		341.2183	324.1918		270.2176		N	2316.9714	2315.9761		2376.0085	2358.9819	2357.9979	22
4	30.0338	370.2449	353.2183		398.2398	381.2132				G				2261.9656	2244.9390	2243.9550	21
5	102.0550	499.2875	482.2609	481.2769	527.2824	510.2558	509.2718	441.2820		E	2130.9073	2129.9121		2204.9441	2187.9175	2186.9335	20
6	30.0338	556.3089	539.2824	538.2984	584.3039	567.2773	566.2933			G				2075.9015	2058.8749	2057.8909	19
7	88.0393	671.3359	654.3093	653.3253	699.3308	682.3042	681.3202	627.3461		D	1958.8589	1957.8637		2018.8800	2001.8535	2000.8695	18
8	88.0393	786.3628	769.3363	768.3523	814.3577	797.3312	796.3472	742.3730		D	1843.8320	1842.8367		1903.8531	1886.8265	1885.8425	17
9	86.0964	899.4469	882.4203	881.4363	927.4418	910.4153	909.4312	857.3999		L	1730.7479	1729.7527		1788.8261	1771.7996	1770.8156	16
10	70.0651	996.4997	979.4731	978.4891	1024.4946	1007.4680	1006.4840	970.4840		P	1633.6951	1632.6999		1675.7421	1658.7155	1657.7315	15
11	102.0550	1125.5422	1108.5157	1107.5317	1153.5372	1136.5106	1135.5266	1067.5368		E	1504.6525	1503.6573		1578.6893	1561.6628	1560.6788	14
12	30.0338	1182.5637	1165.5372	1164.5531	1210.5586	1193.5321	1192.5481			G				1449.6467	1432.6202	1431.6362	13
13	44.0495	1253.6008	1236.5743	1235.5903	1281.5957	1264.5692	1263.5852			A	1376.5940			1392.6253	1375.5987	1374.6147	12
14	120.0808	1400.6692	1383.6427	1382.6587	1428.6642	1411.6376	1410.6536			F	1229.5256			1321.5882	1304.5616	1303.5776	11
15	136.0757	1563.7326	1546.7060	1545.7220	1591.7275	1574.7009	1573.7169			Y	1066.4622			1174.5197	1157.4932	1156.5092	10
16	104.0528	1694.7731	1677.7465	1676.7625	1722.7680	1705.7414	1704.7574	1634.7697		M	935.4217	934.4265		1011.4564	994.4299	993.4458	9
17	72.0808	1793.8415	1776.8149	1775.8309	1821.8364	1804.8098	1803.8258	1779.8258		V	836.3533	849.3737		880.4159	863.3894	862.4054	8
18	30.0338	1850.8629	1833.8364	1832.8524	1878.8578	1861.8313	1860.8473			G				781.3475	764.3210	763.3369	7
19	88.0393	1965.8899	1948.8633	1947.8793	1993.8848	1976.8582	1975.8742	1921.9000		D	664.3049	663.3097		724.3260	707.2995	706.3155	6
20	120.0808	2112.9583	2095.9317	2094.9477	2140.9532	2123.9267	2122.9426			F	517.2365			609.2991	592.2726	591.2885	5
21	102.0550	2242.0009	2224.9743	2223.9903	2269.9958	2252.9692	2251.9852	2183.9954		E	388.1939	387.1987		462.2307	445.2041	444.2201	4
22	60.0444	2329.0329	2312.0064	2311.0223	2357.0278	2340.0013	2339.0173	2313.0380		S	301.1619	300.1666		333.1881	316.1615	315.1775	3
23	44.0495	2400.0700	2383.0435	2382.0595	2428.0649	2411.0384	2410.0544			A	230.1248			246.1561	229.1295		2
24	129.1135									R	74.0237	73.0284		175.1190	158.0924		1

107

Figure 52: Root-mean-square deviation graph of obtained fragment ions; The left graph shows the Error in Dalton and the right graph shows the error in ppm.
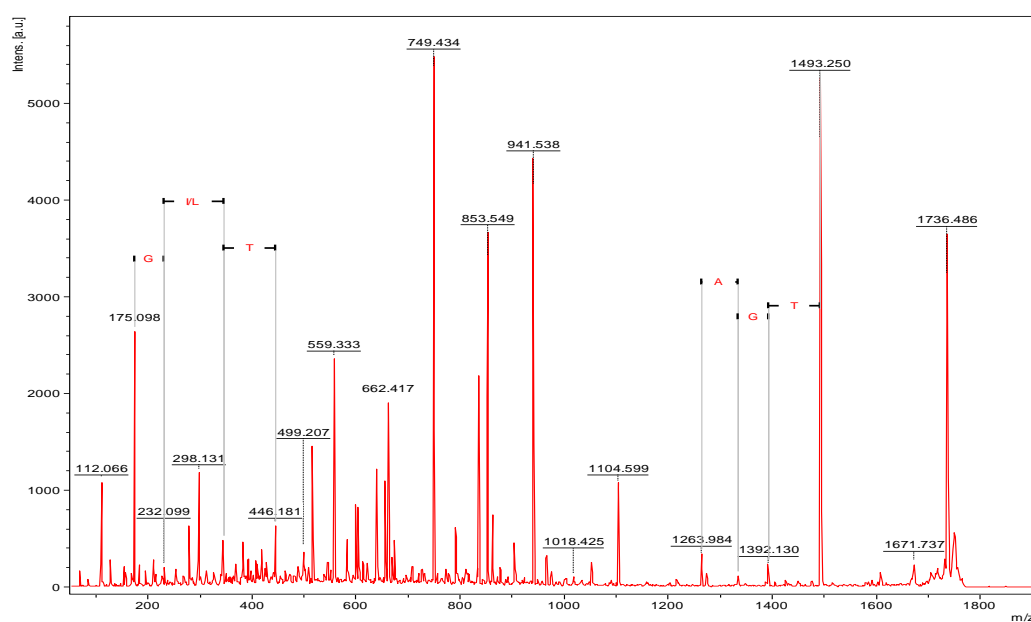

Figure 53: MS/MS spectrum of precursor with m/z 2602.18 Da of spot 11

Spot 16: Precursor ion with m/z 1614.76

For database search settings outlined in Chapter 2.8.2 were used.

Search results:

1. gi|378726950   **Mass:** 32930   **Score: 91**

    hypothetical protein HMPREF1120_01603 [*Exophiala dermatitidis NIH/UT8656*]
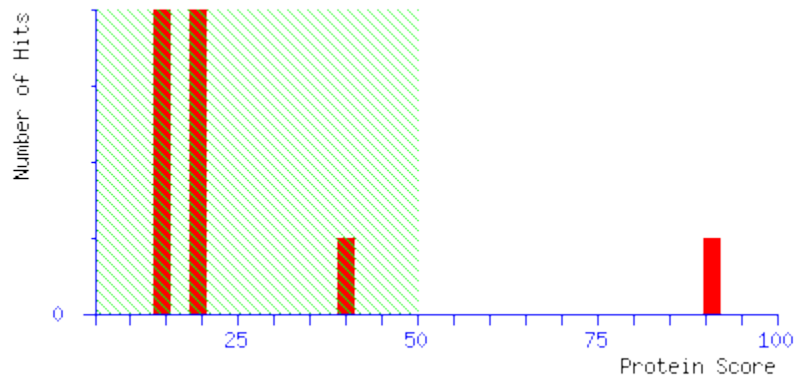
Detailed results:

Taxonomy: *Exophiala dermatitidis NIH/UT8656*

Score: 91

Expect: 4e-06

Nominal Mass: 32930

Calculated pI: 4.87

Database search of the part of the sequence RQAYPGTITEA of the spectrum shown on Figure 55 resulted in the identification of the protein hypothetical protein HMPREF1120_01603 of the species *Exophiala dermatitidis.*

A detailed list of all fragment ions of the identified sequence RQAYPGTITEASAYS is shown on Table 24.

Table 24: List of fragment ions of the identified sequence RQAYPGTITEASAYS. Matches are marked in red: 57/251 fragment ions using 82 most intense peaks

#	Immon.	a	a*	a⁰	b	b*	b⁰	d	d'	Seq.	v	w	w'	y	y*	y⁰	#
1	60.0444	60.0444		42.0338	88.0393		70.0287	44.0495		S							15
2	136.0757	223.1077		205.0972	251.1026		233.0921			Y	1419.6863			1527.7438	1510.7173	1509.7332	14
3	44.0495	294.1448		276.1343	322.1397		304.1292			A	1348.6492			1364.6805	1347.6539	1346.6699	13
4	60.0444	381.1769		363.1663	409.1718		391.1612	365.1819		S	1261.6171	1260.6219		1293.6434	1276.6168	1275.6328	12
5	44.0495	452.2140		434.2034	480.2089		462.1983			A	1190.5800			1206.6113	1189.5848	1188.6008	11
6	102.0550	581.2566		563.2460	609.2515		591.2409	523.2511		E	1061.5374	1060.5422		1135.5742	1118.5477	1117.5637	10
7	74.0600	682.3042		664.2937	710.2992		692.2886	666.3093	668.2886	T	960.4898	973.5102	975.4894	1006.5316	989.5051	988.5211	9
8	86.0964	795.3883		777.3777	823.3832		805.3727	767.3570	781.3727	I	847.4057	860.4261	874.4417	905.4839	888.4574	887.4734	8
9	74.0600	896.4360		878.4254	924.4309		906.4203	880.4411	882.4203	T	746.3580	759.3784	761.3577	792.3999	775.3733	774.3893	7
10	30.0338	953.4575		935.4469	981.4524		963.4418			G				691.3522	674.3257		6
11	70.0651	1050.5102		1032.4997	1078.5051		1060.4946	1024.4946		P	592.2838	591.2885		634.3307	617.3042		5
12	136.0757	1213.5735		1195.5630	1241.5685		1223.5579			Y	429.2205			537.2780	520.2514		4
13	44.0495	1284.6107		1266.6001	1312.6056		1294.5950			A	358.1833			374.2146	357.1881		3
14	101.0709	1412.6692	1395.6427	1394.6587	1440.6642	1423.6376	1422.6536	1355.6478		Q	230.1248	229.1295		303.1775	286.1510		2
15	129.1135									R	74.0237	73.0284		175.1190	158.0924		1

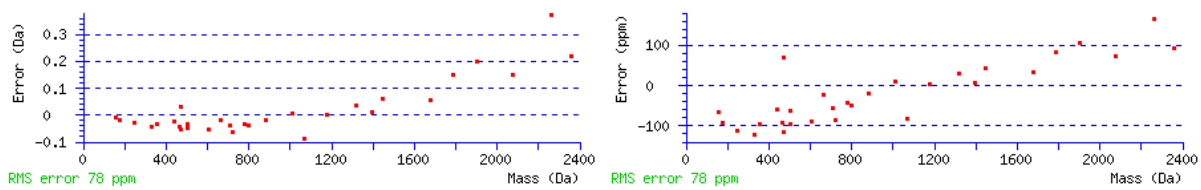
RMS error 169 ppm

RMS error 169 ppm
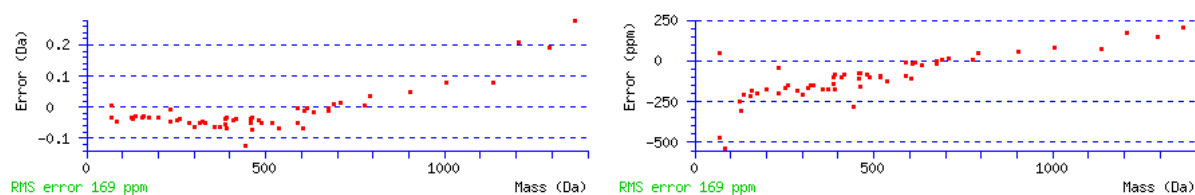
Figure 54: Root-mean-square deviation graph of obtained fragment ions; The left graph shows the Error in Dalton and the right graph shows the error in ppm.
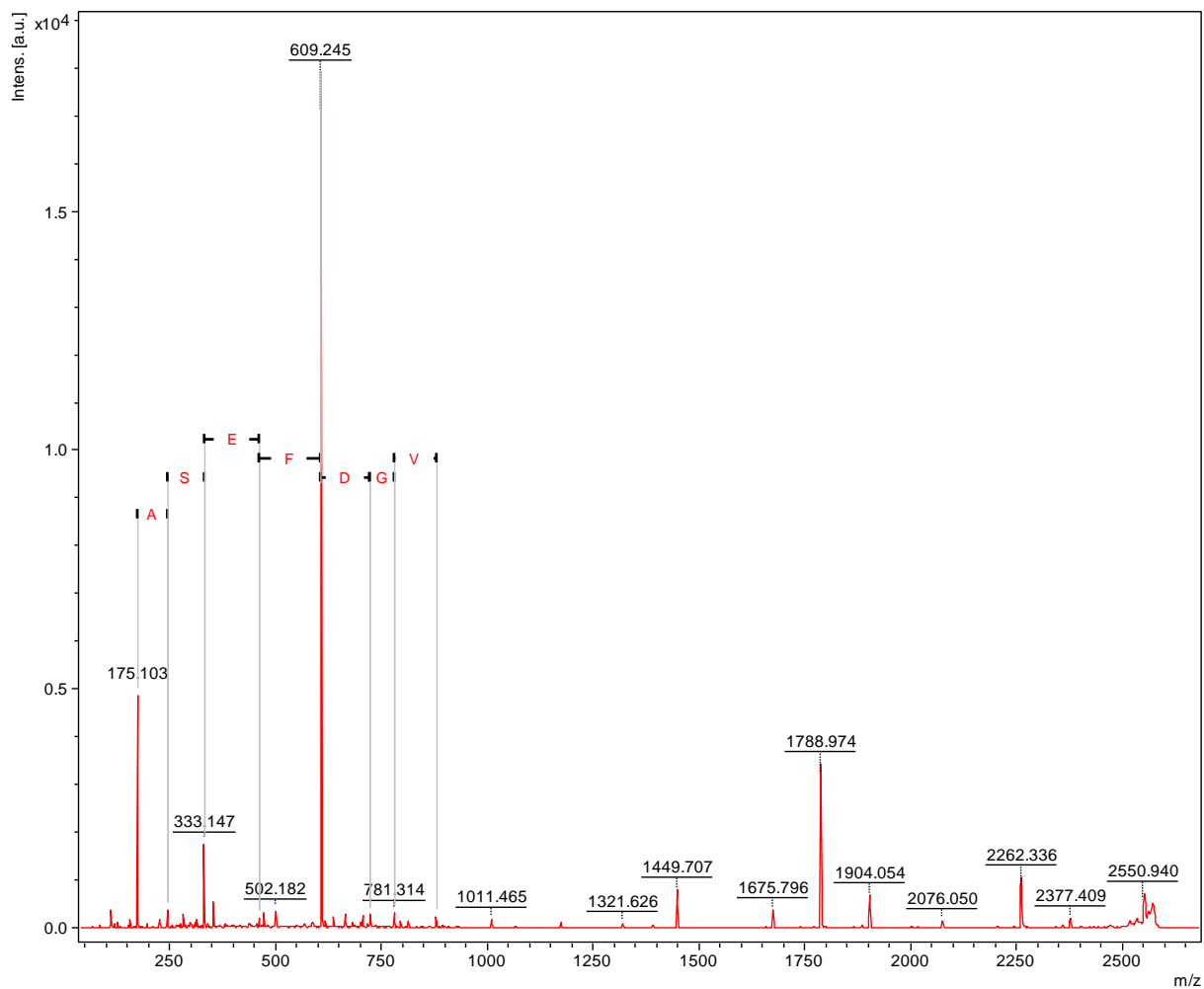
Figure 55: MS/MS spectrum of precursor with m/z 1614.76 Da of spot 16

Spot 18: Precursor ion with m/z 1516.76

For database search settings outlined in Chapter 2.8.2 were used.

Search results:

1. gi|113229   **Mass:** 42268   **Score: 63**
    RecName: Full=Actin-2 [*Absidia glauca*]
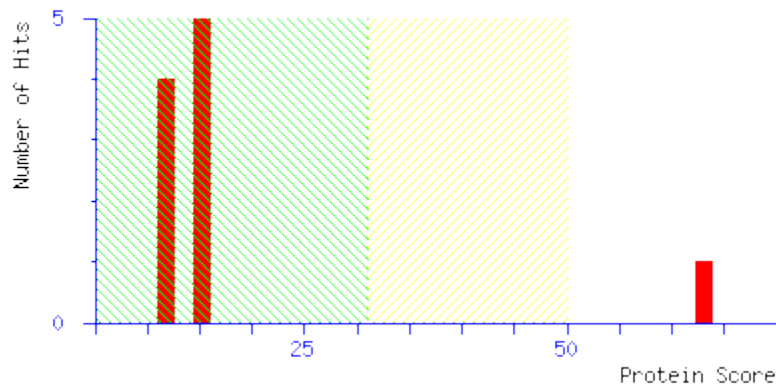
Detailed results:

Taxonomy: *Absidia glauca*

Score: 63

Expect: 0.0026

Nominal Mass: 42268

Calculated pI: 5.37

Database search of the part of the sequence RHVI of the spectrum shown on Figure 57 resulted in the identification of the protein Actin-2 of the species *Absidia glauca.* The species *Absidia glauca* belongs to the Zygomycota and is therefore not closely related to the species *Exophiala dermatitidis* which belongs to Dikarya. Nevertheless Zygomycota and Dikarya belong to the kingdom fungi and therefore the mentioned protein identification can be regarded as relevant.

A detailed list of all fragment ions of the identified sequence RHVISPGSEDYEQ is shown on Table 25.

Table 25: List of fragment ions of the identified sequence RHVISPGSEDYEQ. Matches are marked in red: 26/232 fragment ions using 34 most intense peaks

| #	Immon.	a	a*	a⁰	b	b*	b⁰	d	d'	Seq.	v	w	w'	y	y*	y⁰	#
1	101.0709	101.0709	84.0444		129.0659	112.0393		44.0495		Q							13
2	102.0550	230.1135	213.0870	212.1030	**258.1084**	241.0819	240.0979	172.1081		E	1314.6073	1313.6121		1388.6441	1371.6175	1370.6335	12
3	*136.0757*	393.1769	376.1503	375.1663	421.1718	404.1452	403.1612			Y	1151.5440			*1259.6015*	1242.5749	1241.5909	11
4	88.0393	508.2038	491.1773	490.1932	536.1987	*519.1722*	518.1882	464.2140		D	1036.5170	1035.5218		1096.5382	*1079.5116*	1078.5276	10
5	102.0550	637.2464	620.2198	619.2358	**665.2413**	*648.2148*	647.2307	579.2409		E	907.4744	906.4792		*981.5112*	964.4847	963.5007	9
6	60.0444	724.2784	707.2519	706.2679	752.2733	735.2468	734.2628	*708.2835*		S	820.4424	819.4472		*852.4686*	835.4421	834.4581	8
7	30.0338	781.2999	764.2733	763.2893	809.2948	792.2683	791.2842			G				*765.4366*	748.4100	747.4260	7
8	70.0651	878.3527	861.3261	860.3421	906.3476	889.3210	888.3370	*852.3370*		P	666.3682	665.3729		*708.4151*	691.3886	690.4046	6
9	60.0444	965.3847	948.3581	947.3741	993.3796	976.3530	975.3690	949.3898		S	579.3362	578.3409		611.3624	594.3358	593.3518	5
10	86.0964	1078.4687	1061.4422	1060.4582	1106.4637	1089.4371	1088.4531	1050.4374	1064.4531	I	466.2521	479.2725	493.2881	*524.3303*	507.3038		4
11	72.0808	1177.5372	1160.5106	1159.5266	1205.5321	1188.5055	1187.5215	1163.5215		V	367.1837	380.2041		*411.2463*	394.2197		3
12	*110.0713*	1314.5961	1297.5695	1296.5855	**1342.5910**	1325.5644	1324.5804			H	230.1248			*312.1779*	295.1513		2
13	129.1135									R	74.0237	73.0284		*175.1190*	158.0924		1

Figure 56: Root-mean-square deviation graph of obtained fragment ions; The left graph shows the Error in Dalton and the right graph shows the error in ppm.
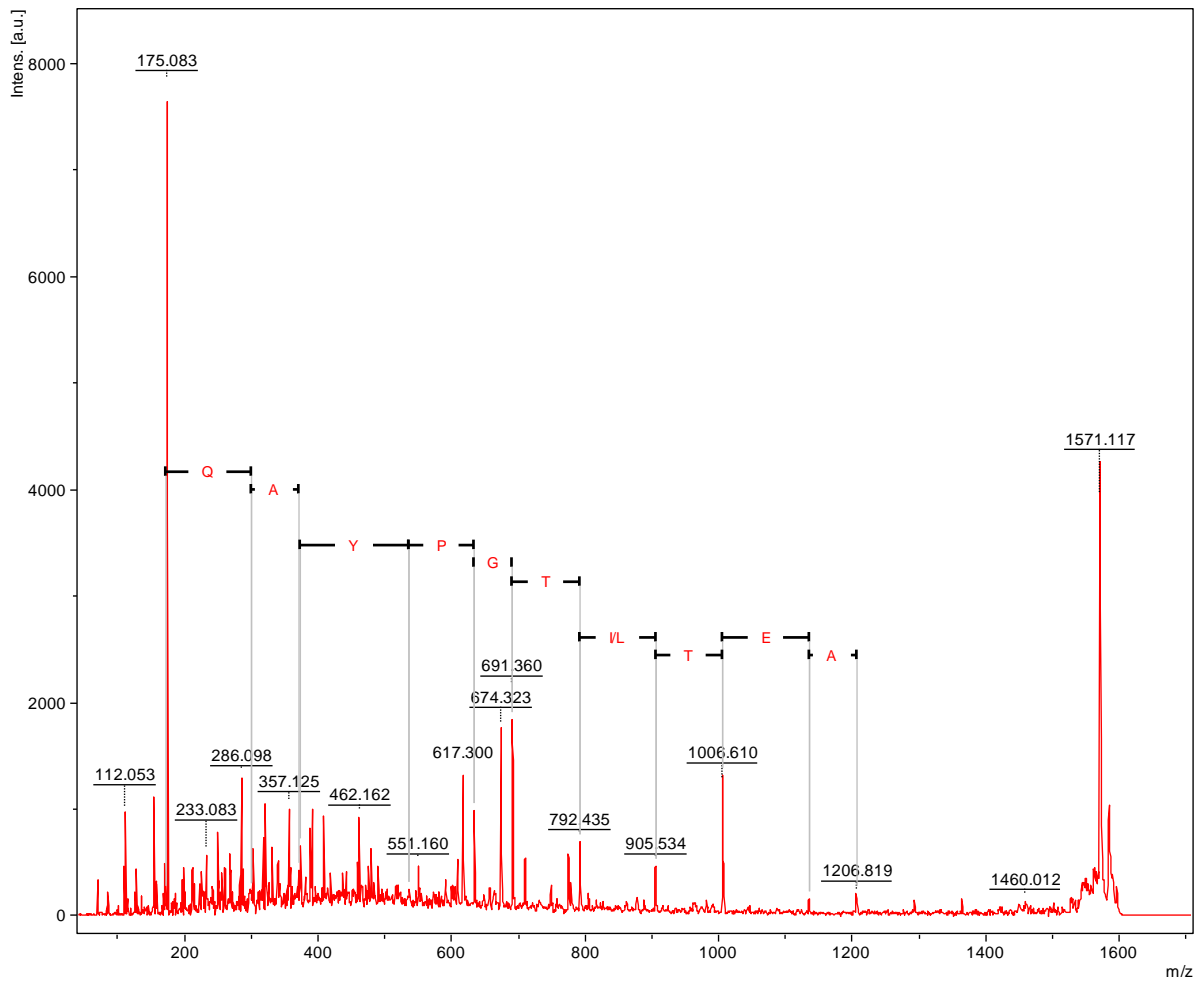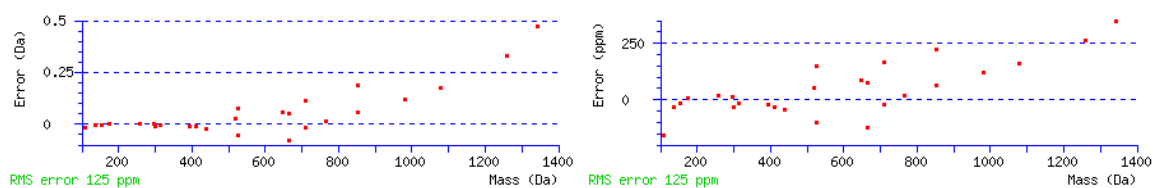

Figure 57: MS/MS spectrum of precursor with m/z 1516.76 Da of spot 18

Spot 20: Precursor ion with m/z 1756.00

For database search settings outlined in Chapter 2.8.2 were used.

Search results:

1. gi|37780013   **Mass:** 29129   **Score: 62**

    NADP-dependent mannitol dehydrogenase [*Alternaria alternata*]
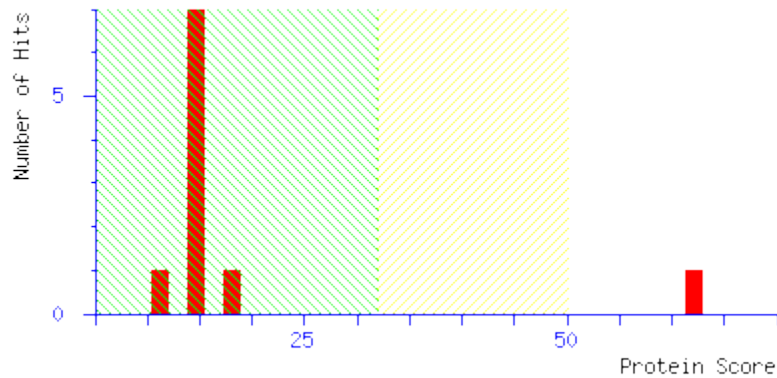
Detailed results:

Taxonomy: *Alternaria alternata*

Score: 62

Expect: 0.0032

Nominal Mass: 29129

Calculated pI: 5.86

Database search of the part of the sequence RAAE of the spectrum shown on Figure 59 resulted in the identification of the protein NADP-dependent mannitol dehydrogenase of the species *Alternaria alternata.* The species *Alternaria alternata* belongs to the order Pleosporales which belongs to Pezizomycotina and *Exophiala dermatitidis* belongs to Pezizomycotina too, these organisms, can be regarded as related.

A detailed list of all fragment ions of the identified sequence RAAETGIGTPGSAGTVIVV is shown on Table 26.

Table 26: List of fragment ions of the identified sequence RAAETGIGTPGSAGTVIVV. Matches are marked in red: 44/361 fragment ions using 54 most intense peaks

#	Immon.	a	a⁰	b	b⁰	d	d'	Seq.	v	w	w'	y	y*	y⁰	#
1	72.0808	72.0808		100.0757		44.0495		V							19

114

#								AA							#
2	72.0808	171.1492		199.1441		157.1335		V	1612.8289	1625.8493		1656.8915	1639.8650	1638.8810	18
3	86.0964	284.2333		312.2282		256.2020	270.2176	I	1499.7449	1512.7653	1526.7809	1557.8231	1540.7966	1539.8125	17
4	72.0808	383.3017		411.2966		369.2860		V	1400.6764	1413.6969		1444.7390	1427.7125	1426.7285	16
5	74.0600	484.3493	466.3388	512.3443	494.3337	468.3544	470.3337	T	1299.6288	1312.6492	1314.6284	1345.6706	1328.6441	1327.6601	15
6	30.0338	541.3708	523.3602	569.3657	551.3552			G				1244.6230	1227.5964	1226.6124	14
7	44.0495	612.4079	594.3974	640.4028	622.3923			A	1171.5702			1187.6015	1170.5749	1169.5909	13
8	60.0444	699.4400	681.4294	727.4349	709.4243	683.4450		S	1084.5382	1083.5429		1116.5644	1099.5378	1098.5538	12
9	30.0338	756.4614	738.4509	784.4563	766.4458			G				1029.5324	1012.5058	1011.5218	11
10	70.0651	853.5142	835.5036	881.5091	863.4985	827.4985		P	930.4639	929.4687		972.5109	955.4843	954.5003	10
11	74.0600	954.5619	936.5513	982.5568	964.5462	938.5669	940.5462	T	829.4163	842.4367	844.4159	875.4581	858.4316	857.4476	9
12	30.0338	1011.5833	993.5728	1039.5782	1021.5677			G				774.4104	757.3839	756.3999	8
13	86.0964	1124.6674	1106.6568	1152.6623	1134.6517	1096.6361	1110.6517	I	659.3107	672.3311	686.3468	717.3890	700.3624	699.3784	7
14	30.0338	1181.6889	1163.6783	1209.6838	1191.6732			G				604.3049	587.2784	586.2944	6
15	74.0600	1282.7365	1264.7260	1310.7314	1292.7209	1266.7416	1268.7209	T	501.2416	514.2620	516.2413	547.2835	530.2569	529.2729	5
16	102.0550	1411.7791	1393.7686	1439.7740	1421.7635	1353.7736		E	372.1990	371.2037		446.2358	429.2092	428.2252	4
17	44.0495	1482.8162	1464.8057	1510.8112	1492.8006			A	301.1619			317.1932	300.1666		3
18	44.0495	1553.8534	1535.8428	1581.8483	1563.8377			A	230.1248			246.1561	229.1295		2
19	129.1135							R	74.0237	73.0284		175.1190	158.0924		1
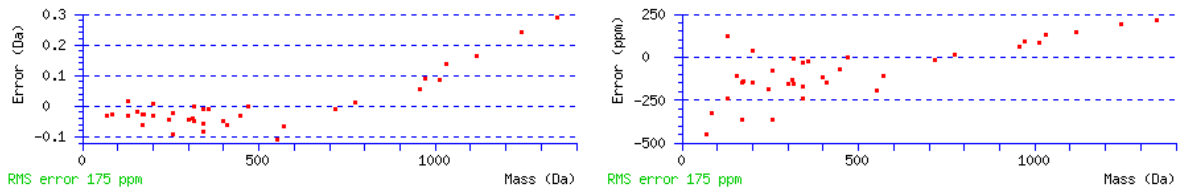
Figure 58: Root-mean-square deviation graph of obtained fragment ions; The left graph shows the Error in Dalton and the right graph shows the error in ppm.
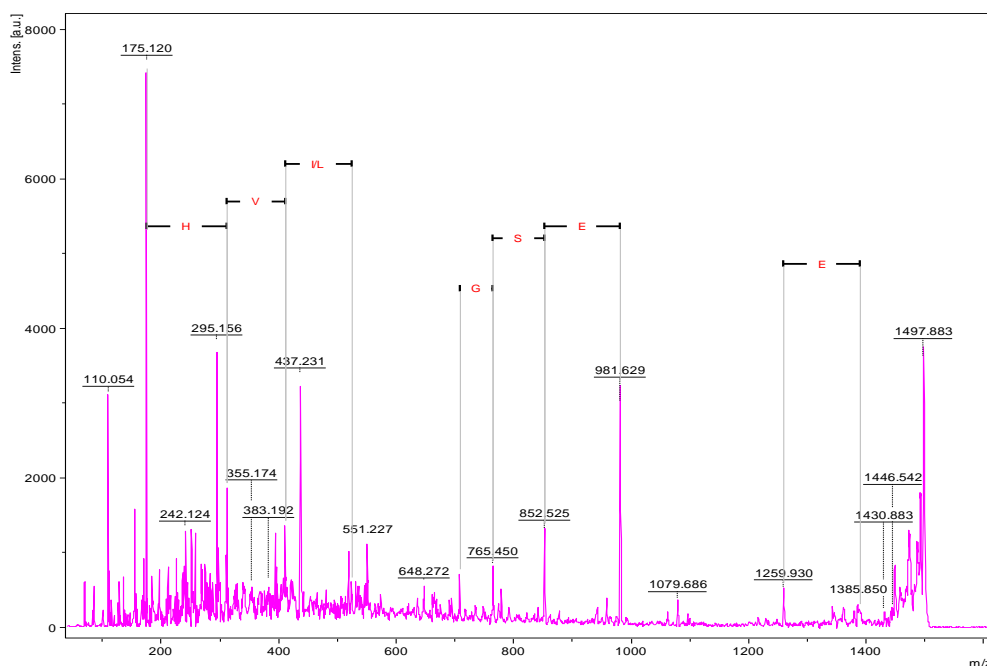

Figure 59: MS/MS spectrum of precursor with m/z 1756.00 Da of spot 20

Spot 21: Precursor ions with m/z 1172.64 and m/z 1438.72

For database search settings outlined in Chapter 2.8.2 were used.

Search results:

1. gi|378730330   **Mass:** 43283   **Score: 87**

    mannitol-1-phosphate 5-dehydrogenase [*Exophiala dermatitidis NIH/UT8656*]

Detailed results of precursor ion with m/z 1172.64:

Taxonomy: *Exophiala dermatitidis NIH/UT8656*

Score: 36

Expect: 1.6

Nominal Mass: 43283

Calculated pI: 5.13

Database search of the part of the sequence REAL of the spectrum shown on Figure 61 resulted in the identification of the protein mannitol-1-phosphate 5-dehydrogenase of the species *Exophiala dermatitidis.*

A detailed list of all fragment ions of the identified sequence REALQAAPGIF is shown on Table 27.

Table 27: List of fragment ions of the identified sequence REALQAAPGIF. Matches are marked in red: 38/160 fragment ions using 52 most intense peaks

| #	Immon.	a	a*	a⁰	b	b*	b⁰	d	d'	Seq.	v	w	w'	y	y*	y⁰	#
1	120.0808	120.0808			148.0757			44.0495		F							11
2	86.0964	233.1648			261.1598			205.1335	219.1492	I	967.4956	980.5160	994.5316	1025.5738	1008.5473	1007.5633	10
3	30.0338	290.1863			318.1812					G				912.4898	895.4632	894.4792	9
4	70.0651	387.2391			415.2340			361.2234		P	813.4213	812.4261		855.4683	838.4417	837.4577	8
5	44.0495	458.2762			486.2711					A	742.3842			758.4155	741.3890	740.4050	7
6	44.0495	529.3133			557.3082					A	671.3471			687.3784	670.3519	669.3679	6
7	101.0709	657.3719	640.3453		685.3668	668.3402		600.3504		Q	543.2885	542.2933		616.3413	599.3148	598.3307	5
8	86.0964	770.4559	753.4294		798.4509	781.4243		728.4090		L	430.2045	429.2092		488.2827	471.2562	470.2722	4
9	44.0495	841.4931	824.4665		869.4880	852.4614				A	359.1674			375.1987	358.1721	357.1881	3
10	102.0550	970.5356	953.5091	952.5251	998.5306	981.5040	980.5200	912.5302		E	230.1248	229.1295		304.1615	287.1350	286.1510	2
11	129.1135									R	74.0237	73.0284		175.1190	158.0924		1

Figure 60: Root-mean-square deviation graph of obtained fragment ions; The left graph shows the Error in Dalton and the right graph shows the error in ppm.
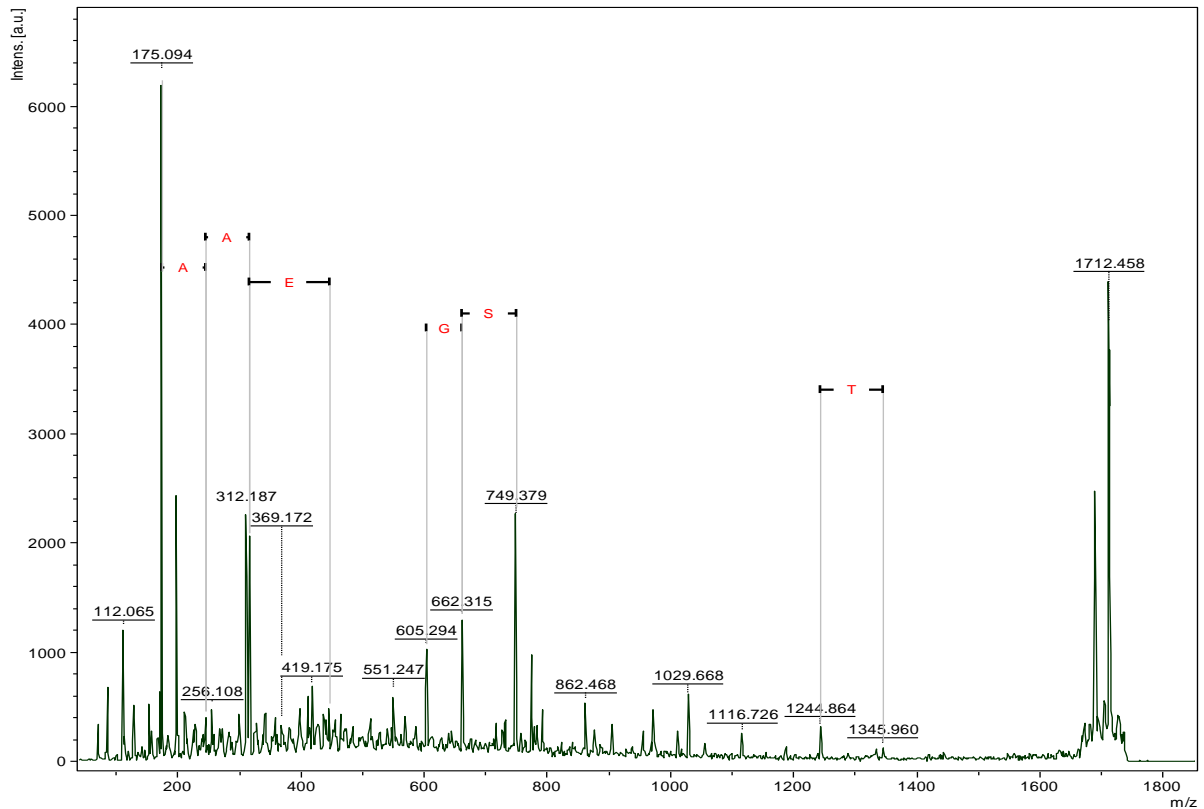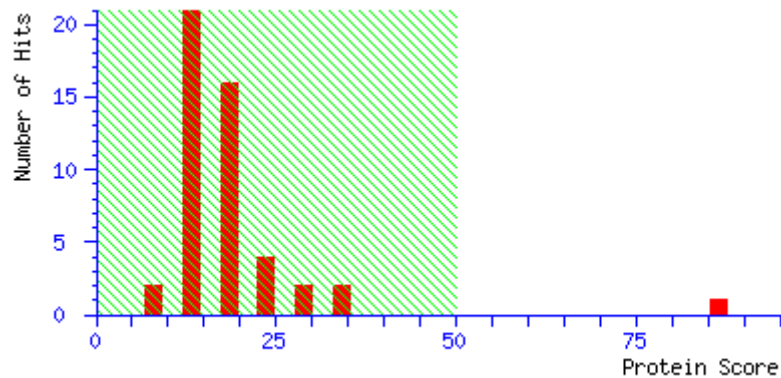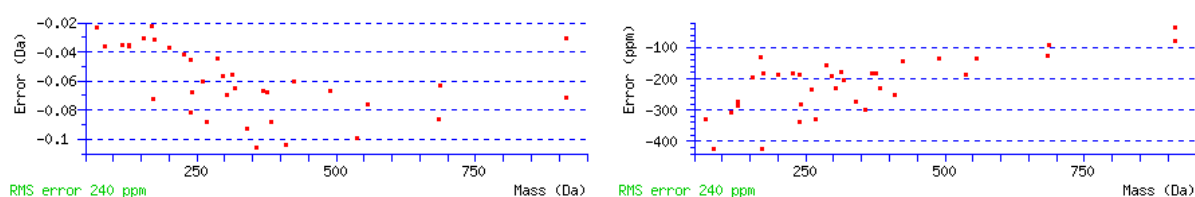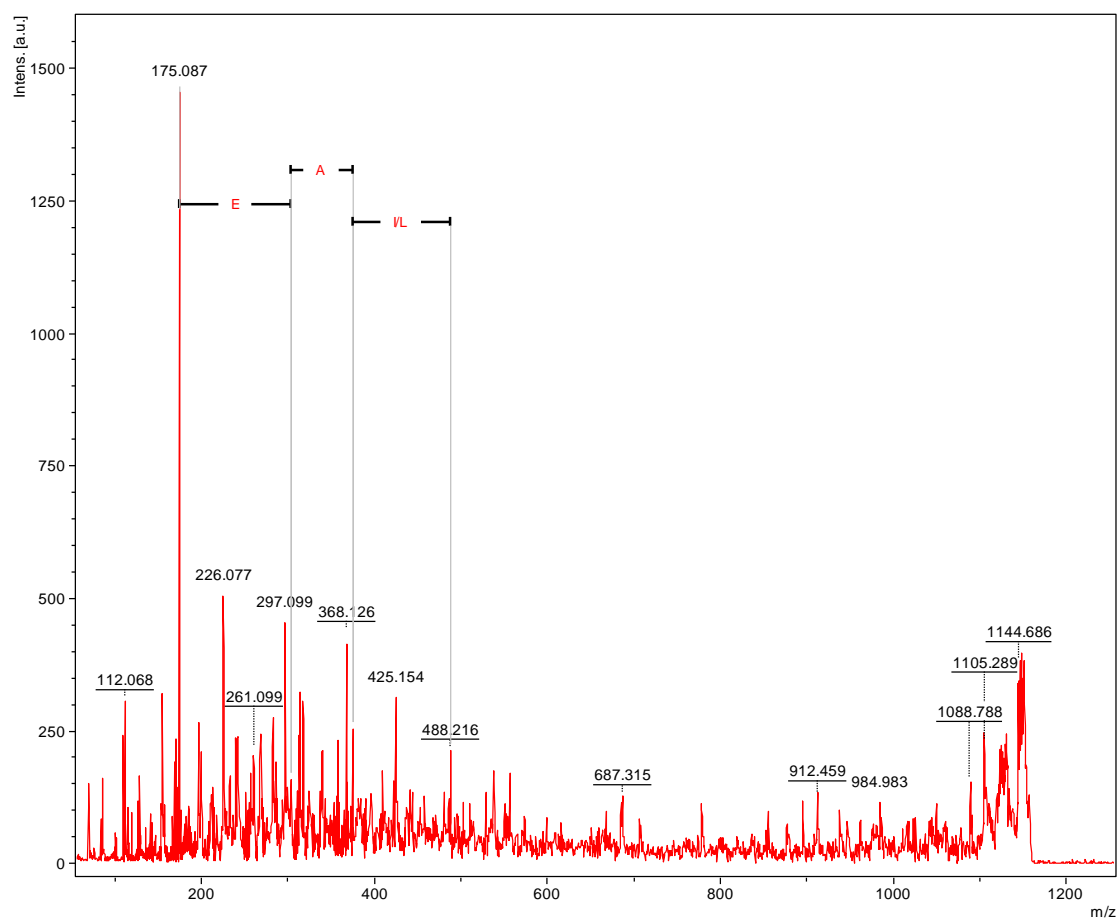

Figure 61: MS/MS spectrum of precursor with m/z 1172.64 Da of spot 21

117

Detailed results of precursor ion with m/z 1438.72:

Taxonomy: *Exophiala dermatitidis NIH/UT8656*

Score: 20

Expect: 45

Nominal Mass: 43283

Calculated pI: 5.13

Database search of the spectrum shown on Figure 63 resulted also in the identification of the protein mannitol-1-phosphate 5-dehydrogenase of the species *Exophiala dermatitidis.*

A detailed list of all fragment ions of the identified sequence RVCVDELHPNSI is shown on Table 28.

Table 28: List of fragment ions of the identified sequence RVCVDELHPNSI. Matches are marked in red: 33/198 fragment ions using 59 most intense peaks

| #	Immon.	a	a*	a⁰	b	b*	b⁰	d	Seq.	v	w	y	y*	y⁰	#
1	86.0964	*86.0964*			114.0913			44.0495	I						12
2	60.0444	173.1285		155.1179	201.1234		183.1128	157.1335	S	1293.6004	1292.6052	1325.6267	1308.6001	1307.6161	11
3	87.0553	287.1714	270.1448	269.1608	**315.1663**	298.1397	297.1557	244.1656	N	1179.5575	1178.5623	1238.5946	*1221.5681*	1220.5841	10
4	70.0651	384.2241	367.1976	366.2136	412.2191	395.1925	394.2085	358.2085	P	1082.5048	1081.5095	*1124.5517*	1107.5252	1106.5411	9
5	110.0713	*521.2831*	504.2565	503.2725	**549.2780**	532.2514	531.2674		H	945.4458		1027.4989	1010.4724	1009.4884	8
6	86.0964	*634.3671*	617.3406	616.3566	662.3620	645.3355	644.3515	592.3202	L	832.3618	831.3665	890.4400	873.4135	872.4295	7
7	102.0550	763.4097	746.3832	745.3991	**791.4046**	774.3781	773.3941	705.4042	E	703.3192	702.3239	777.3560	760.3294	759.3454	6
8	88.0393	878.4367	861.4101	860.4261	**906.4316**	889.4050	888.4210	834.4468	D	588.2922	587.2970	*648.3134*	631.2868	630.3028	5
9	72.0808	977.5051	960.4785	959.4945	1005.5000	988.4734	987.4894	963.4894	V	489.2238	502.2442	*533.2864*	516.2599		4
10	133.0430	1137.5357	1120.5092	1119.5252	1165.5306	1148.5041	1147.5201	1048.5422	C	329.1932	328.1979	*434.2180*	417.1915		3
11	72.0808	1236.6041	1219.5776	1218.5936	1264.5990	1247.5725	1246.5885	1222.5885	V	230.1248	243.1452	274.1874	257.1608		2
12	129.1135								R	74.0237	73.0284	*175.1190*	158.0924		1
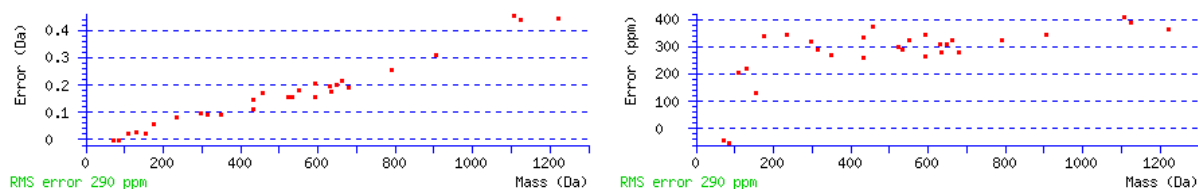
Figure 62: Root-mean-square deviation graph of obtained fragment ions; The left graph shows the Error in Dalton and the right graph shows the error in ppm.
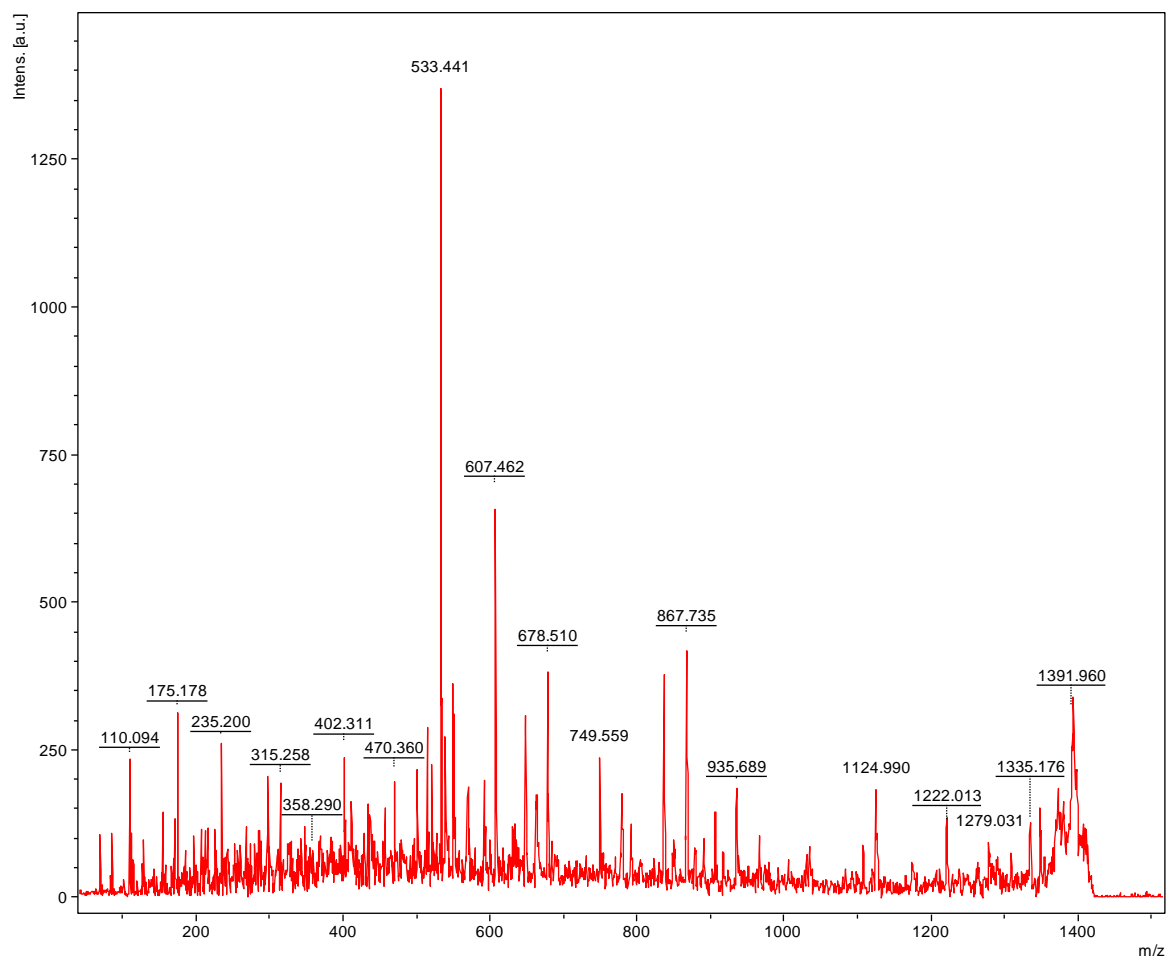
Figure 63: MS/MS spectrum of precursor with m/z 1438.72 Da of spot 21

3.4.4 Summary of identifications

Table 29: List of identified proteins

Spot	Expected Protein (according to http://world-2dpage.expasy.org/swiss-2dpage/data/gifs/swiss_2dpage/YEAST.gif)	Identified Protein	Species	Number of peptides for ID
1	Glyceraldehyde-3-phosphate dehydrogenase 3	**Glyceraldehyde-3-phosphate dehydrogenase**	Aspergillus oryzae RIB40	**1/6**
2	Glyceraldehyde-3-phosphate dehydrogenase 3	**Glyceraldehyde-3-phosphate dehydrogenase 2**	Cryphonectria parasitica	**1/3**
3	Triosephosphate isomerase	No significant result		
4	Fructose-bisphosphate aldolase	No significant result		
5	Peroxiredoxin TSA1	No significant result		
6	Glyceraldehyde-3-phosphate dehydrogenase 3	No significant result		
7	Superoxide dismutase	No significant result		
8	Adenylate kinase 1	No significant result		
9	Pyruvate decarboxylase isozyme 1	No significant result		
10	5-methyltetrahydropteroyltriglutamate--homocysteine methyltransferase	No significant result		
11	ATP synthase subunit beta, mitochondrial	**ATP synthase subunit beta, mitochondrial**	Saccharomyces cerevisiae; Exophiala dermatitidis; Coccidioides immitis	**5/8**
12	Enolase 1	No significant result		
13	Enolase 2	No significant		

		result		
14	Glucose-6-phosphate 1-dehydrogenase	No significant result		
15	Phosphoglycerate mutase 1	No significant result		
16	60S acidic ribosomal protein	**Hypothetical protein HMPREF1120_016 03**	Exophiala dermatitidis	**1/3**
17	Heat shock protein STI1	No significant result		
18	Pyruvate decarboxylase isozyme 1	**RecName: Full=Actin**	Absidia glauca	**1/4**
19	Phosphoserine aminotransferase	No significant result		
20	Triose-phosphate Dehydrogenase 2	**NADP-dependent mannitol dehydrogenase**	Alternaria alternata	**1/2**
21	Hexokinase-2	**Mannitol-1-phosphate 5-dehydrogenase**	Exophiala dermatitidis	**2/5**
22	Heat shock protein SSB1	No significant result		
23	Enolase 2	No significant result		
24	Ubiquitin-60S ribosomal protein L40 fusion protein	No significant result		
25	Triose-phosphate Dehydrogenase 1	No significant result		

4   Conclusion

As black fungi have been isolated from hypersaline waters [2], acidic environments [3], radioactive areas [4], as human pathogens or opportunists [5] and as a dominant part of the epi- and endolithic microbial communities [6] [7] [8] [9] [10] [11], this organism needs either permanently existing or exceptionally fast adaptive cellular or metabolic responses to survive these harsh conditions [13]. To gain knowledge on proteome changes of black fungi, a relative quantitation method on the basis of iTRAQ (isobaric Tags for Relative and Absolute Protein Quantitation) has been established. The analytical workflow was developed using BSA as standard protein. The measurement of the iTRAQ labeled peptides was carried out using matrix-assisted laser desorption/ionization reflectron time-of-flight mass spectrometry (MALDI-RTOF-MS).

Substances that may interfere with the trypsin digestion, the labeling of the samples or the subsequent MS analysis had to be removed which led to the implementation of multiple clean-up steps and every single clean-up steps was checked for reproducibility and efficiency. A cation exchange chromatography clean-up step and a HyperSep™ C18 solid phase extraction clean-up step have been evaluated. However, cation exchange chromatography revealed a high loss of peptides. The final sample preparation now includes a HyperSep™ C18 solid phase extraction clean-up step prior to the iTRAQ labeling step to get rid of substances that may interfere with the labeling and a second HyperSep™ C18 solid phase extraction clean-up step prior to MALDI analysis to remove substances from the labeling step that may interfere with the MALDI analysis. In addition to these two clean-up steps, a dilution step prior to trypsin digestion had to be introduced to reduce disturbing buffer components to an appropriate amount.

For statistical evaluation of the established method using BSA the **peptides with m/z 1072, 1624 and 1713** were used because these peptides could be detected in all independent experiments**. The labeling step,** the **cleaning step** (HyperSep™ C18 solid phase extraction) and the **whole digestion procedure** (including the labeling and the cleaning step) were separately evaluated.

For the **labeling step** evaluation BSA concentration ratios of 1:1, 1:2 and 2:1 were used. For the 1:1 ratio an average measured value of 1.04 with a standard deviation of 0.19 could be obtained. For the 1:2 ratio the average measured value was 1.93 with a standard deviation of 0.32 and for the 2:1 ratio the average measured value was 0.45 with a standard deviation of 0.03.

For the **cleaning step** (HyperSep™ C18 solid phase extraction) using 4 µg protein as well as 60 µg protein a ratio of 1:1 was used. For the 4 µg protein analysis the average measured value was 0.98

with a standard deviation of 0.05 and for the 60 µg analysis the average measured value was 1.10 with a standard deviation of 0.05.

For the **whole digestion procedure** (including the labeling and the cleaning step) BSA concentration ratios of 1:1, 1:2 and 2:1 were used. For the 1:1 ratio the average measured value was 1.20 with a standard deviation of 0.21, for the 1:2 ratio the average measured value was 2.54 with a standard deviation of 0.33 and for the 2:1 ratio the average measured value was 0.42 with a standard deviation of 0.05.

The average measured value of the 1:1 ratio of all executed experiments was 1.04 with a standard deviation of 0.12, the average measured value of the 1:2 ratio 2.35 with a standard deviation of 0.28 and the average measured value of the 2:1 ratio 0.42 with a standard deviation of 0.04. In general, the findings of the method evaluation showed strong evidence of a good working iTRAQ labeling protocol.

After optimizing every sample preparation step the method was used for *Exophiala dermatitidis* **protein extracts.** The rigid cell wall and the high melanin content pose major challenges in sample preparation prior to analysis [18]. Therefore to develop a proper method for *Exophiala dermatitidis* samples the standard iTRAQ protocol had to be adapted to this fungus.

Unfortunately protein identification for *Exophiala dermatitidis* was not very successful and low signal intensities of reporter ions of the labeling group led to only a very limited number of data which could be evaluated in respect to technical and biological variation.

For the detection of the **biological reproducibility** by means of the received labeling ratios peptides with m/z 1657, 1077, 1274, 1705, 1711 and 1763 could be used for statistical evaluation. Peptides with m/z 1657 and m/z 1705 showed similar up-and down regulation patterns. Peptides with m/z 1711 and m/z 1763 showed also similar pattern. The problem of these findings was that the mentioned peptides could not be significantly identified. Results could only be regarded as a hypothesis of a possible up- or down regulation of proteins.

The evaluation of technical reproducibility by means of the received labeling ratios showed was also very difficult due to low signal intensities of reporter ions. Only the peptide with m/z 1274 could be used for statistical evaluation. As no significant identification of this peptide could be obtained, the up- or down regulation pattern could only be regarded as a hypothesis. In summary, it can be stated that findings of quantitative protein analysis of *Exophiala dermatitidis* samples proved to be difficult to interpret as obtained peptides could not be significantly identified.

As not only the mass spectrometry-based protein quantification was of interest but also the general identification of proteins present in *Exophiala dermatitidis* 25 spots of a 2D electrophoresis gel of an extract of *Exophiala dermatitidis* were cut out, digested and measured by MALDI mass spectrometry. In this way some proteins of the 2D electrophoresis gel of an extract of *Exophiala dermatitidis* could be identified. Using the Mascot database search the proteins Glyceraldehyde-3-phosphate dehydrogenase, Glyceraldehyde-3-phosphate dehydrogenase 2, ATP synthase subunit beta (mitochondrial), Hypothetical protein HMPREF1120_01603, RecName Full=Actin, NADP-dependent mannitol dehydrogenase and Mannitol-1-phosphate 5-dehydrogenase could be identified.

To sum up it can be said, that the established BSA based iTRAQ protein quantitation method can be used as a basis for further protein quantitation of black fungi which proteomes change under different growing conditions. Initial findings of black fungi of the strain *Exophiala dermatitidis* showed a regulation pattern of some peptides however without any significance. These results indicated that for these fungal samples the developed method needs to be further modified. An implementation of a liquid chromatography (LC) separation step might lead to better signals of MALDI spectra. Nevertheless the established method has potential to determine possible peptide regulations of *Exophiala dermatitidis* samples under different environmental conditions.

5 Outlook

As the extreme stress tolerance of black micro-colonial fungi is a yet unexplored field of research, only some facts about these fungi like their phenotypes, a slow growth rate and a complex structural composition are known. Their enormous stress tolerance against solar radiation, radioactivity, desiccation and oligotrophic conditions make this fungus an organism of special interest for many studies. Features of black fungi like the rigid cell wall and the high melanin content, pose major challenges in sample preparation prior to analysis which is going far beyond the routine efforts. Therefore the establishment of a proper relative protein quantitation method for *Exophiala dermatitidis* samples proved to be difficult. Nevertheless, on the basis of the established method further experiments can be performed in order to find the optimal sample preparation technique for black samples for subsequent relative quantitation measurements using iTRAQ. Gathered knowledge may then allow genetic engineering for targeted applications. In the future the knowledge can help to develop tools useful for waste management and to understand biological data collected during space programs.

6   References

1.   Harutyunyan, S., L. Muggia, and M. Grube, *Black fungi in lichens from seasonally arid habitats.* Stud Mycol, 2008. **61**: p. 83-90.
2.   Gunde-Cimerman, N., et al., *Hypersaline waters in salterns - Natural ecological niches for halophilic black yeasts.* FEMS Microbiology Ecology, 2000. **32**(3): p. 235-240.
3.   Baker, B.J., et al., *Metabolically active eukaryotic communities in extremely acidic mine drainage.* Applied and Environmental Microbiology, 2004. **70**(10): p. 6264-6271.
4.   Dadachova, E., et al., *Ionizing radiation changes the electronic properties of melanin and enhances the growth of melanized fungi.* PLoS One, 2007. **2**(5): p. e457.
5.   Matos, T., et al., *High prevalence of the neurotrope Exophiala dermatitidis and related oligotrophic black yeasts in sauna facilities.* Mycoses, 2002. **45**(9-10): p. 373-377.
6.   Friedmann, E.I., *Endolithic microorganisms in the Antarctic cold desert.* Science, 1982. **215**(4536): p. 1045-1053.
7.   Sterflinger, K., *Fungi as geologic agents.* Geomicrobiology Journal, 2000. **17**(2): p. 97-124.
8.   Burford, E.P., M. Kierans, and G.M. GADD, *Geomycology: fungi in mineral substrata.* Mycologist, 2003. **17**(3): p. 98-107.
9.   Ruibal, C., G. Platas, and G. Bills, *Isolation and characterization of melanized fungi from limestone formations in Mallorca.* Mycological Progress, 2005. **4**(1): p. 23-38.
10.   Sert, H.B., H. Sumbul, and K. Sterflinger, *Microcolonial fungi from antique marbles in Perge/Side/Termessos (Antalya/Turkey).* Antonie Van Leeuwenhoek, 2007. **91**(3): p. 217-27.
11.   Selbmann, L., et al., *Drought meets acid: three new genera in a dothidealean clade of extremotolerant fungi.* Studies in mycology, 2008. **61**(1): p. 1-20.
12.   Sterflinger, K., G. De Hoog, and G. Haase, *Phylogeny and ecology of meristematic ascomycetes.* Studies in mycology, 1999: p. 5-22.
13.   Vember, V.V. and N.N. Zhdanova, *Peculiarities of linear growth of the melanin-containing fungi Cladosporium sphaerospermum Penz. and Alternaria alternata (Fr.) Keissler.* Osobennosti lineinogo rosta melaninsoderzhashchikh gribov Cladosporium sphaerospermum Penz. i Alternaria alternata (Fr.) Keissler., 2001. **63**(3): p. 3-12.
14.   Tesei, D., et al., *Alteration of protein patterns in black rock inhabiting fungi as a response to different temperatures.* Fungal Biol, 2012. **116**(8): p. 932-40.
15.   Marzban, G., D. Tesei, and K. Sterflinger, *A Review beyond the borders: Proteomics of microclonial black fungi and black yeasts.* 2013.
16.   Sterflinger, K., Marzban, G., Marchetti-Deschmann, M., *System Biology and Ecology of Microcolonial Fungi and Their Adaptation to Extreme Environments*. BOKU University Vienna, Vienna University of Technology.
17.   de Oliveira, J.M. and L.H. de Graaff, *Proteomics of industrial fungi: trends and insights for biotechnology.* Appl Microbiol Biotechnol, 2011. **89**(2): p. 225-37.
18.   Lottspeich, F. and J.W. Engels, *Bioanalytik*. 2006: Elsevier, Spektrum Akad. Verlag.
19.   Domon, B. and R. Aebersold, *Mass Spectrometry and Protein Analysis.* Science, 2006. **312**(5771): p. 212-217.
20.   Wu, W.W., et al., *Comparative study of three proteomic quantitative methods, DIGE, cICAT, and iTRAQ, using 2D gel- or LC-MALDI TOF/TOF.* J Proteome Res, 2006. **5**(3): p. 651-8.
21.   Elliott, M.H., et al., *Current trends in quantitative proteomics.* J Mass Spectrom, 2009. **44**(12): p. 1637-60.
22.   Aebersold, R. and M. Mann, *Mass spectrometry-based proteomics.* Nature, 2003. **422**(6928): p. 198-207.
23.   de Hoffmann, E. and V. Stroobant, *Mass Spectrometry: Principles and Applications*. 2013: Wiley.
24.   Mann, M. and G. Talbo, *Developments in matrix-assisted laser desorption/ionization peptide mass spectrometry.* Curr Opin Biotechnol, 1996. **7**(1): p. 11-9.

25. Hillenkamp, F. and J. Peter-Katalinic, *MALDI MS*. 2007: Wiley. com.

26. Kemptner, J., et al., *Evaluation of matrix-assisted laser desorption/ionization (MALDI) preparation techniques for surface characterization of intact Fusarium spores by MALDI linear time-of-flight mass spectrometry.* Rapid Communications in Mass Spectrometry, 2009. **23**(6): p. 877-884.

27. Vorm, O., P. Roepstorff, and M. Mann, *Improved Resolution and Very High Sensitivity in MALDI TOF of Matrix Surfaces Made by Fast Evaporation.* Analytical Chemistry, 1994. **66**(19): p. 3281-3287.

28. Noble, D., *MALDI-TOFMS Pulses Ahead.* Analytical Chemistry, 1995. **67**(15): p. 497A-501A.

29. Karas, M. and F. Hillenkamp, *Laser desorption ionization of proteins with molecular masses exceeding 10,000 daltons.* Analytical chemistry, 1988. **60**(20): p. 2299-2301.

30. Spengler, B. and R.J. Cotter, *Ultraviolet laser desorption/ionization mass spectrometry of proteins above 100,000 daltons by pulsed ion extraction time-of-flight analysis.* Analytical chemistry, 1990. **62**(8): p. 793-796.

31. Boyle, J.G. and C.M. Whitehouse, *Time-of-flight mass spectrometry with an electrospray ion beam.* Analytical Chemistry, 1992. **64**(18): p. 2084-2089.

32. Cotter, R.J., *Time-of-flight mass spectrometry for the structural analysis of biological molecules.* Analytical chemistry, 1992. **64**(21): p. 1027A-1039A.

33. Weickhardt, C., F. Moritz, and J. Grotemeyer, *Time-of-flight mass spectrometry: State-of the-art in chemical analysis and molecular science.* Mass Spectrometry Reviews, 1996. **15**(3): p. 139-162.

34. Wollnik, H., *Time-of-flight mass analyzers.* Mass Spectrometry Reviews, 1993. **12**(2): p. 89-114.

35. Mamyrin, B.A., et al., *Mass reflection: a new nonmagnetic time-of-flight high resolution mass- spectrometer.* Journal Name: Zh. Eksp. Teor. Fiz. 64: No. 1, 82-89(Jan 1973).; Other Information: Orig. Receipt Date: 30-JUN-73, 1973: p. Medium: X.

36. Mamyrin, B.A., *Laser assisted reflectron time-of-flight mass spectrometry.* International Journal of Mass Spectrometry and Ion Processes, 1994. **131**(0): p. 1-19.

37. Cotter, R.J., et al., *Tandem Time-of-Flight Mass Spectrometry with a Curved Field Reflectron.* Analytical Chemistry, 2004. **76**(7): p. 1976-1981.

38. Brown, R.S., B.L. Carr, and J.J. Lennon, *Factors that influence the observed fast fragmentation of peptides in matrix-assisted laser desorption.* Journal of the American Society for Mass Spectrometry, 1996. **7**(3): p. 225-232.

39. Kaufmann, R., et al., *Post-source decay and delayed extraction in matrix-assisted laser desorption/ionization-reflectron time-of-flight mass spectrometry. Are there trade-offs?* Rapid Commun Mass Spectrom, 1996. **10**(10): p. 1199-208.

40. Kocher, T., A. Engstrom, and R.A. Zubarev, *Fragmentation of peptides in MALDI in-source decay mediated by hydrogen radicals.* Anal Chem, 2005. **77**(1): p. 172-7.

41. Juhasz, P., M.L. Vestal, and S.A. Martin, *On the initial velocity of ions generated by matrix-assisted laser desorption ionization and its effect on the calibration of delayed extraction time-of-flight mass spectra.* Journal of the American Society for Mass Spectrometry, 1997. **8**(3): p. 209-217.

42. Suckau, D., et al., *A novel MALDI LIFT-TOF/TOF mass spectrometer for proteomics.* Anal Bioanal Chem, 2003. **376**(7): p. 952-65.

43. Medzihradszky, K.F., et al., *The characteristics of peptide collision-induced dissociation using a high-performance MALDI-TOF/TOF tandem mass spectrometer.* Anal Chem, 2000. **72**(3): p. 552-8.

44. Patterson, S.D. and R. Aebersold, *Mass spectrometric approaches for the identification of gel-separated proteins.* Electrophoresis, 1995. **16**(10): p. 1791-814.

45. matrixscience.com. *Matrix Science.* [cited 2013 September].

46. Roepstorff, P. and J. Fohlman, *Proposal for a common nomenclature for sequence ions in mass spectra of peptides.* Biomed Mass Spectrom, 1984. **11**(11): p. 601.

47.   Biemann, K., *Sequencing of peptides by tandem mass spectrometry and high-energy collision-induced dissociation.* Methods Enzymol, 1990. **193**: p. 455-79.

48.   Suckau, D. and D. Cornett, *Protein sequencing by ISD and PSD MALDI-TOF MS.* Anal Mag, 1998. **26**: p. 18-21.

49.   Wilm, M. and M. Mann, *Analytical properties of the nanoelectrospray ion source.* Analytical chemistry, 1996. **68**(1): p. 1-8.

50.   Aebersold, R. and D.R. Goodlett, *Mass spectrometry in proteomics.* Chemical reviews, 2001. **101**(2): p. 269-296.

51.   Righetti, P.G., et al., *Critical survey of quantitative proteomics in two-dimensional electrophoretic approaches.* J Chromatogr A, 2004. **1051**(1-2): p. 3-17.

52.   O'Farrell, P.H., *High resolution two-dimensional electrophoresis of proteins.* J Biol Chem, 1975. **250**(10): p. 4007-21.

53.   Patton, W.F., *Detection technologies in proteome analysis.* J Chromatogr B Analyt Technol Biomed Life Sci, 2002. **771**(1-2): p. 3-31.

54.   Shi, Y., et al., *The role of liquid chromatography in proteomics.* J Chromatogr A, 2004. **1053**(1-2): p. 27-36.

55.   Gygi, S.P., et al., *Quantitative analysis of complex protein mixtures using isotope-coded affinity tags.* Nat Biotechnol, 1999. **17**(10): p. 994-9.

56.   Oda, Y., et al., *Accurate quantitation of protein expression and site-specific phosphorylation.* Proc Natl Acad Sci U S A, 1999. **96**(12): p. 6591-6.

57.   Paša-Tolić, L., et al., *High Throughput Proteome-Wide Precision Measurements of Protein Expression Using Mass Spectrometry.* Journal of the American Chemical Society, 1999. **121**(34): p. 7949-7950.

58.   Bantscheff, M., et al., *Quantitative mass spectrometry in proteomics: a critical review.* Anal Bioanal Chem, 2007. **389**(4): p. 1017-31.

59.   Ong, S. and M. Mann, *A practical recipe for stable isotope labeling by amino acids in cell culture (SILAC).* Nat Protoc, 2006. **1**(6): p. 2650 - 2660.

60.   Harsha, H.C., H. Molina, and A. Pandey, *Quantitative proteomics using stable isotope labeling with amino acids in cell culture.* Nat Protoc, 2008. **3**(3): p. 505-16.

61.   Ong, S.E. and M. Mann, *Mass spectrometry-based proteomics turns quantitative.* Nat Chem Biol, 2005. **1**(5): p. 252-62.

62.   Gevaert, K., et al., *Stable isotopic labeling in proteomics.* Proteomics, 2008. **8**(23-24): p. 4873-85.

63.   Gevaert, K. and J. Vandekerckhove, *Protein identification methods in proteomics.* Electrophoresis, 2000. **21**(6): p. 1145-54.

64.   Reynolds, K.J., X. Yao, and C. Fenselau, *Proteolytic 18O labeling for comparative proteomics: evaluation of endoprotease Glu-C as the catalytic agent.* J Proteome Res, 2002. **1**(1): p. 27-33.

65.   Wiese, S., et al., *Protein labeling by iTRAQ: a new tool for quantitative mass spectrometry in proteome research.* Proteomics, 2007. **7**(3): p. 340-50.

66.   Casado-Vela, J., et al., *iTRAQ-based quantitative analysis of protein mixtures with large fold change and dynamic range.* Proteomics, 2010. **10**(2): p. 343-7.

67.   Abdallah, C., et al., *Optimization of iTRAQ labelling coupled to OFFGEL fractionation as a proteomic workflow to the analysis of microsomal proteins of Medicago truncatula roots.* Proteome Science, 2012. **10**(1): p. 37.

68.   Pichler, P., et al., *Peptide labeling with isobaric tags yields higher identification rates using iTRAQ 4-plex compared to TMT 6-plex and iTRAQ 8-plex on LTQ Orbitrap.* Anal Chem, 2010. **82**(15): p. 6549-58.

69.   Pottiez, G., et al., *Comparison of 4-plex to 8-plex iTRAQ quantitative measurements of proteins in human plasma samples.* J Proteome Res, 2012. **11**(7): p. 3774-81.

70.   DeSouza, L.V., et al., *Endometrial carcinoma biomarker discovery and verification using differentially tagged clinical samples with multidimensional liquid chromatography and tandem mass spectrometry.* Mol Cell Proteomics, 2007. **6**(7): p. 1170-82.

71. DeSouza, L.V., et al., *Absolute quantification of potential cancer markers in clinical tissue homogenates using multiple reaction monitoring on a hybrid triple quadrupole/linear ion trap tandem mass spectrometer.* Anal Chem, 2009. **81**(9): p. 3462-70.

72. Ow, S.Y., et al., *iTRAQ underestimation in simple and complex mixtures: "the good, the bad and the ugly".* J Proteome Res, 2009. **8**(11): p. 5347-55.

73. DeSouza, L.V., et al., *Multiple reaction monitoring of mTRAQ-labeled peptides enables absolute quantification of endogenous levels of a potential cancer marker in cancerous and normal endometrial tissues.* J Proteome Res, 2008. **7**(8): p. 3525-34.

74. Zieske, L.R., *A perspective on the use of iTRAQ reagent technology for protein complex and profiling studies.* J Exp Bot, 2006. **57**(7): p. 1501-8.

75. cta.tuwien.ac.at. *Homepage of the Institute of Chemical Technologies and Analytics*. [cited 2013 September].

76. Holle, A., et al., *Optimizing UV laser focus profiles for improved MALDI performance.* Journal of Mass Spectrometry, 2006. **41**(6): p. 705-716.

77. Shevchenko, A., et al., *Mass spectrometric sequencing of proteins silver-stained polyacrylamide gels.* Anal Chem, 1996. **68**(5): p. 850-8.

78. Lan, P., et al., *iTRAQ protein profile analysis of Arabidopsis roots reveals new aspects critical for iron homeostasis.* Plant Physiol, 2011. **155**(2): p. 821-34.

79. Keller, B.O., et al., *Interferences and contaminants encountered in modern mass spectrometry.* Anal Chim Acta, 2008. **627**(1): p. 71-81.

80. Liska, A.J. and A. Shevchenko, *Expanding the organismal scope of proteomics: Cross-species protein identification by mass spectrometry and its implications.* PROTEOMICS, 2003. **3**(1): p. 19-28.

7   Appendix

Supplemental material is provided on a DVD-ROM:

- Mass spectra

- MASCOT search results

- MS Excel sheets of calculations

- Protein extraction information sheets

- Presentation in MS Powerpoint